FINAL REPORT ON SEDS EXPERIMENT DESIGN DEFINITION CONTRACT NAS8-37380

Joseph A. Carroll
Charles M. Alexander
John C. Oldson
Energy Science Laboratories, Inc.
P.O. Box 85608
San Diego, CA 92138-5608

February 1990

Summary

This report summarizes work done under NASA Contract NAS8-37380 between NASA Marshall Space Flight Center and Energy Science Laboratories (ESL). This contract was a follow-on to SBIR contract NAS8-35256, under which the Small Expendable-tether Deployment System (SEDS) was developed. The overall project objective for SEDS is to design, build, integrate, fly, and safely deploy and release an expendable tether. The purpose of this contract was to develop and document a suitable concept for an on-orbit test of SEDS. The contract had 6 tasks. Each is represented by one chapter in this report:

1. Define experiment objectives and requirements
2. Define experiment concepts to reach those objectives
3. Support NASA in experiment concept selection and definition
4. Perform analyses and tests of SEDS hardware
5. Refine the selected SEDS experiment concept
6. Support interactive SEDS system definition process

Key ESL project personnel and their responsibilities were: Joe Carroll, principal investigator; Charles Alexander, senior engineer (hardware design, fabrication, and testing); and John Oldson, Experiment Requirements Document. Kevin Cross, Matt Nilsen, and George Henschke assisted Alexander with tether fabrication and testing.

Most of the work on the first three tasks and the analyses under task 4 were completed during the first few months of the contract. This left considerable time for fabrication and test work under task 4, which ended up constituting about half the total work on this contract. That test work included designing, fabricating, assembling, and testing a full-scale flight-like SEDS deployer with 20 km tether. Because of the level of effort in these areas, they are given their own chapters of this report: chapter 7 for design refinement and fabrication, chapter 8 for testing and data analysis, and Appendix A for plots of test data from the final deployment test. Thus chapter 4 covers just the remainder of task 4: analyses other than test data analysis and experiment concept refinement.

During the first half of the contract, the emphasis was on a STS-based flight experiment. During the refinement effort (task 5), at MSFC direction, the focus on the first SEDS flight experiment shifted to a Delta-based experiment. That work has continued under a follow-on contract (NAS8-37885) to design, fabricate, and test SEDS hardware for a Delta experiment. Chapter 7 notes briefly the hardware design refinements that have resulted from the follow-on flight-hardware contract.

Besides the Delta experiment, SEDS is also manifested for a STS flight experiment some time after the planned Delta experiment. As a result, MSFC directed us to fill out the ERD (Experiment Requirements Document, under task 6) for an STS experiment, not for the Delta experiment. This ERD is included as Appendix B. The remainder of the report covers both STS and Delta experiment options, and notes key differences between them. The recommendations focus on eventual STS-based experiments, because the Delta experiment has already been developed well beyond the level reached during this contract.

i

Table of Contents

Acronyms and Abbreviations

atm	atmosphere (pressure)
APC	Auxiliary Payload Carrier (for small STS payloads)
Cd	Coefficient of drag
D&PS	Design and Performance Specification
ERD	Experiment Requirements Document
ESL	Energy Science Laboratories, Inc.
GAS	Get-Away Special (STS small payload program)
HP	Hewlett-Packard
Hz	Hertz (times per second)
IRED	Infra-Red Emitting Diode
K	degrees Kelvin
L/D	Ratio of lift to drag force
m	meter
MSFC	Marshall Space Flight Center
ppi	picks per inch (measure of braid tightness)
PTN	Phototransistor
RCS	Reaction Control System (or its propellant)
SBIR	Small Business Innovation Research Program
sec	second
SEDS	Small Expendable-tether Deployment System
STS	Space Transportation System
TSS	Tethered Satellite System

1. Define Experiment Objectives and Requirements

The purpose of the first flight test of the Small Expendable-Tether Deployment System is to prove out the SEDS concept in space by carrying out an actual deployment and release of a small payload at the end of a 20 km tether.

1.1 Experiment Objectives

Our overall objective is to fly a successful and useful expendable tether experiment at low cost. This is the key objective, because the SEDS program groundrule is that the program itself is expendable: if SEDS gets too expensive, the key issue is resolved in the negative, and the "experiment" is terminated before flight. The more detailed objectives are to:

1. Deploy the full tether length properly
2. Release the payload into the proper trajectory
3. Collect data to check tether simulation programs

The simplicity of the SEDS system limits the number of potential failure modes, but most potential SEDS users still prefer to be the second user rather than the first. Hence there is value to a well-controlled test to determine whether the full tether length can be deployed and the payload released into the planned trajectory. In addition, collecting tether dynamics data allows tests of tether simulation programs. This should increase the confidence of mission planners considering using SEDS or other tether systems.

The main potential hang-ups in deployment are:
inadequate separation velocity
high energy absorption in tie-down breakage
high tether friction on guides
tether trapping between package and baseplate
tether snagging on deployer or host vehicle components

Proper payload ejection system design can ensure any desired separation velocity. Energy absorption by tie-down breakage is expected to be <1% of the separation energy. Guide friction should be acceptably low if the tether guides are clean. (This requires a shield in a Delta-based experiment, to protect the guides from alumina in the exhaust of the upper stage motor.) Tether trapping between the bottom of the tether package and the baseplate is possible in the "universal" part of the tether winding. Proper winding geometry can prevent this, and this can be demonstrated on the ground.

Tether snagging is particularly a concern with the shuttle, because of possibly serious implications if a fouled tether is able to interfere with stowage of the manipulator arm or the Ku-band radar, or with operation of the airlock door or payload bay doors. Risks can be minimized by configuring the arm and radar in the stowed position during the SEDS experiment. In the case of a Delta experiment, the consequences are far less serious, particularly if the SEDS experiment is performed after the Delta depletion burn.

1

For most SEDS applications studied to date, deploying the payload into the proper trajectory essentially requires that a full or nearly-full deployment be made in approximately the right time (within about 10%) and at roughly the right angle (within about 10 degrees), and that the tether be cut within about 10 degrees of the vertical. This is enough for payload boosting or circularization, and for trash dumping into a large target zone. For reentry capsule applications, recovering the capsule economically requires a small recovery zone. This requires considerably tighter control of SEDS deployment. We suggest that an attempt be made to demonstrate trajectory control capabilities suitable for reentry capsules, but that this be regarded as a secondary objective rather than a primary one.

The final objective is to obtain data of a type and quality suitable for checking the various tether simulation programs used by tether analysts. The intent is to help determine which programs might be used by mission planners considering using tethers in the future. This objective is not limited to SEDS applications, but applies also to TSS, space station, and other applications whose dynamics have enough similarities to a SEDS operation that SEDS data will provide a useful check. It is not easy to specify a priori the types, precision, and absolute accuracy required for such data to be useful. But it is clearly desirable that the data be accurate enough to select between programs whose predictions are different enough to be of practical concern to mission planners.

1.2 Data Requirements

The recommended baseline data requirements are:

Baseline data-collection by on-board instruments:

1. Deployed length and rate versus time
2. Time brake-enabling sensor triggered (indicating 1 km left)
3. Tether tension (deployer or payload end): >200 Hz, summed to 10-30 Hz
4. Temperatures: core, top of canister, brake, and possibly controller

The deployment data should be collected asynchronously in the form of the elapsed times at which each of two optical turn-counters has its beam interrupted by the deploying tether. About 105,000 times need to be recorded, each with sub-millisecond time resolution: two for each turn, plus a 10-15% allowance for spurious counts induced by tether vibrations. The brake-enabling sensor indicates when braking should begin. It also starts a count-down timer that determines when the tether should be cut.

Tension data can be collected in the form of tensiometer output voltage. This data can either be capacitively averaged and digitized at a rate of 10-30 Hz, or digitized at a higher rate and averaged numerically. Our preference is to collect data at several times the tensiometer natural frequency, sum readings, and store the sum as a two byte value, coded to indicate whether the data is in a high-tension or low-tension range.

2

Temperature data will be collected from thermistors at a lower rate (about 1 Hz). Thermistors will be mounted in the electronics box; on the deployer core, canister, and brake; and possibly at other locations.

Besides the recommended baseline data, several additional types of data are suggested as "targets of opportunity," if they turn out to be feasible and affordable. They are:

Optional data-collection by on-board instruments:

1. High-frequency tension data at either or both ends after tether is "jerked" by deployment of short weighted sections of tether. Store data at >200 Hz for at least 30 seconds after each "jerk."

2. High-frequency tension measurements at payload end after tether is cut, to determine tensile relaxation waveform. Store data at >200 Hz for 10 sec.

3. Payload attitude spin-up and oscillations: use magnetometers or gyros.

4. Torques on host vehicle: derivable from guidance or RCS firing data.

Optional data-collection by ground-based instrumentation:

1. Radar observability: use ground-based radar to determine observability of dipole arrays embedded in the tether. Useful in future if tethers are left in orbit or used frequently.

2. Optical observability: use low-light TVs (such as the Cohu camera used on the STS) to image the tether in twilight, especially near apogee.

3. Tether dynamics: use radar or low-light TV to determine tether shape during deployment, swing, release and recoil, slack period, and reentry. Imagery would be most useful if the experiment is timed so that the recoil towards the payload and subsequent slack-tether behavior can be viewed.

4. Payload attitude oscillation and spin: determine radar or optical scintillation rates. Rates can calibrate tensiometer if payload moments of inertia and tether attachment location on payload are accurately known.

5. Tether impact damage assessment. Spectra weakens and radically shortens as it approaches its melting point. The tether should start to disintegrate at 100-120 km altitude. It should fail first at locations with significantly reduced cross section. Video imagery of tether breakup should be feasible if breakup occurs on the night side of the orbit. This could indicate the locations and approximate severity of any non-fatal impacts with micrometeoroids.

2. Define Experiment Concepts to Reach Experiment Objectives

This chapter describes the main options considered for different aspects of the experiment during this contract. Many of the issues were clear-cut enough to allow prompt selection of one option, and the rationales are given below. In other cases, the options were held open for further study, which is described in chapter 3. The main areas of concern were:

> payload size, mass, and complexity
> upward versus downward deployment
> means of initiating deployment
> tether length and diameter
> integrated versus separate component mounting
> mounting locations on the STS and Delta
> dedicated versus host-vehicle datalogging

Hardware and integration costs should be lowest, and integration opportunities best, if the payload is as light and as possible. However if it is small, it is hard to see; and if it is light, it must be ejected at a higher velocity for its momentum to carry it out far enough for gravity gradients to overcome tether drag and continue deployment. At the beginning of the contract, a payload near 50 kg was assumed. MSFC personnel asked us whether a lighter payload was possible. This is discussed in 3.1. The size issue was easier to resolve: the payload should be as large as is compatible with whatever mounting location is selected.

If the payload is simple, there is no reason to boost it into a long-lived orbit. And downward deployment simplifies prompt de-orbit of the tether. This keeps the tether from contributing to orbital debris. Hence we selected a downward deployment.

As originally conceived, SEDS used STS maneuvers to start and stop deployment. RCS propellant use was high, mainly for braking, so we added a tether brake to SEDS. With large payloads such as an External Tank, RCS is still attractive to start deployment. But for smaller payloads, a spring ejection system has far lower mass. There may be a safety advantage in using an RCS maneuver instead of (or along with) a spring ejection: the range rate can be very low initially, to allow time for a measured response to tether jamming and payload recoil. RCS maneuvers can increase the rate later, when the payload is far enough away that a jam will not lead to payload recontact with the orbiter. In the case of the Delta, spring ejection is clearly preferable. In follow-on experiments, brief burns of the Delta 2nd stage main engine could provide enough range rate (5-10 m/sec) to deploy even very heavy and stiff tethers, such as would be needed for electrodynamics experiments.

We considered various tether lengths and tentatively settled on 20 km as being about the shortest tether that should be able to accurately de-orbit an endmass from a typical shuttle altitude of 300 km. This length is also adequate for a 200x700 km Delta orbit.

Pages 9-11 of the SEDS SBIR Phase II final report discussed micrometeoroid risks and tradeoffs, and concluded that for early STS-based experiments with payloads much under a ton, the key tradeoff would be micrometeoroid risks versus tether mass, and that the

optimum diameter for short-lived experiments would be near 0.7 mm. We re-investigated that trade and concluded that a 0.7 mm diameter was still reasonable on the STS. For Delta-based experiments, safety issues are less and the diameter can be 0.3-0.5 mm. However it turns out that a 0.7 mm diameter is suitable for full-scale operational use on the Delta, even with a 5 ton primary payload. This is because the empty Delta second stage itself weighs just under a ton. Thus we decided to keep the same 0.7 mm tether diameter as with the STS and make the first Delta SEDS deployer and tether "full scale."

The SEDS deployer, brake, computer, and payload with ejection system can be mounted separately or structurally integrated into one package. Structural integration reduces installation costs at the Cape, but it may make load paths awkward and may make the equipment envelope exceed that available in some otherwise feasible mounting locations. (This issue was not resolved for the Delta experiment until halfway through the follow-on contract. It still has not been resolved for an STS-based experiment.)

The original SEDS concept used a GAS-can-sized deployer. It clearly makes sense to use a GAS canister for a deployer that large. But a combination of 20 km length and 0.7 mm diameter shrinks the tether deployer to about half the linear dimensions of a GAS canister. This opens the possibility of mounting the deployer, payload, and ejection system all together in a single GAS canister with motorized opening lid. (This variant on the GAS canister was demonstrated with deployment of the NUSAT--Northern Utah Satellite--in 1985.) The canister can be mounted on the payload bay sill, or on a bridge structure developed at MSFC. Another mounting arrangement uses an Auxiliary Payload Carrier or one of its derivatives. These are lightweight mounting plates developed by Rockwell to hold minor hardware items along the sill of the orbiter payload bay.

A quite distinct mounting arrangement and experiment concept is to mount SEDS on a Spartan free-flyer, deploy the Spartan from the shuttle, deploy SEDS from the Spartan, and then retrieve the Spartan. A final STS option which eliminates most safety issues is to eject a combined mother-daughter assembly from the shuttle, move a safe distance away, perform the SEDS experiment using the mother and daughter, and leave the mother in orbit without retrieving it by shuttle. This concept requires autonomous data collection and telemetry, but may be necessary if real or perceived safety issues make other options too cumbersome. However such a concept is of limited value if SEDS can be tested on the Delta first.

For the Delta, there are three mounting locations in the annulus between the 5 foot diameter second stage and the 8 foot payload fairing:

    nested between two mini-skirt struts
    attached to the outside of the electronics bay skin
    attached to the spin-table support cone (3-stage missions only)

Datalogging options include various degrees of SEDS autonomy, from dedicated control, datalogging, and telemetry; to dedicated datalogging and control with host-vehicle telemetry; to host-vehicle control, datalogging and telemetry. In each case it seems reasonable to do control and datalogging together, since control requires datacollection and processing, and the datalogger needs access to controller decisions.

3. Support NASA in Experiment Concept Selection and Definition

This task involved our study under NASA direction of the issues listed in chapter 2 which did not lend themselves to prompt resolution. The key issues requiring study were:

> payload mass and deployment method
> payload instrumentation
> integrated vs separate component mounting
> mounting locations on the STS and Delta
> dedicated vs host-vehicle datalogging

3.1 Payload Mass and Deployment Method

The smaller the payload mass, the higher the ejection velocity required to prevent tether tension from bringing deployment to a premature stop. We were asked to study the implications of a lighter payload than the 50 kg that was being considered at the start of this contract. It turns out that for payloads above 10 kg, the required ejection impulse is nearly fixed; below 10 kg, the rising velocity-squared component of tether tension increases the required impulse. Halving the payload mass from 50 to 25 kg requires doubling the ejection velocity from 0.7 to 1.4 m/sec. This doubles the required spring mass. It also increases the kinetic energy of a recoiling payload if the tether suddenly snags. On the shuttle, this increases hazards, and the higher velocities require quicker crew response. We recommend using relatively large (and preferably "soft") payloads for a shuttle-based experiment. If this is not enough, small springs should be used, and RCS burns made to sustain deployment when tether tension begins to slow deployment down. But a 1 m/sec RCS maneuver uses about 30 kg of RCS propellant. Thus additional payload mass may be more efficient than RCS use as a way of reducing required ejection rates.

Besides the ejection impulse constraint, there is a more direct constraint on minimum payload mass. Most operational applications of SEDS that have been considered to date have payloads large compared to the tether mass, and most of them benefit from wide libration after deployment. We made parametric studies of minimum-tension deployments using BEADSIM. (BEADSIM is a tether dynamics simulation program written during the SBIR Phase II contract. It is documented in section 6.3 of the Phase II final report. Refinements made to the program during this contract are described in section 5.5 of this report.) The BEADSIM runs indicate that the payload mass must be a minimum of about 3 times the tether mass for deployment to end far enough from the vertical to result in a wide libration. A 20 km x .7 mm tether weighs over 6 kg, so the minimum payload mass required for a widely librating deployment is close to 20 kg. During discussions with Delta personnel, we learned that NASA Goddard had two surplus Marman clamps qualified for 50 lb (22.7 kg) secondary payloads on the Delta, so we suggested that this payload mass be used for Delta-based experiments.

3.2 Payload Instrumentation

Tension measurements at the payload end, which is the fixed end of the tether, can be more accurate than those at the deployer and host vehicle end. In addition, the response to tether severance at the deployer end would be useful to measure. It would also be worth looking at the response to jerks imposed intentionally or unintentionally at the deployer end during deployment. But payload attitude oscillations may be large enough to require gyros or a 3-axis force sensor to derive tether tension data. This plus a datalogging and storage system increase payload complexity and cost. In addition, either telemetry is required or the instrumentation system must be recovered intact after the experiment. In all, an active payload does not seem easy to justify, particularly if radar or optical scintillation rate data (STS or ground-based) allow absolute calibration of the tension data collected at the deployer end.

On the other hand, if a payload instrumentation system is desired for other reasons, such as collecting data on the upper atmosphere until reentry and burn-up, then using this instrumentation system to also collect data useful to SEDS seems far easier to justify. Accelerometers and attitude sensors intended for atmospheric study can document tether-induced payload attitude oscillations and spin-up more accurately than scintillation rate data can, and a 3-axis force sensor in itself is not very expensive to fabricate or integrate.

Hence our recommendation is to baseline a passive payload but design it so that interested parties outside the SEDS project can add instrumentation capabilities. That requires:
  designing a lightweight payload to which either ballast or electronics can be added;
  leaving room for useful amounts of instrumentation and batteries; and
  providing a thermal environment suitable for datalogging and telemetry hardware.

3.3 Integrated vs Separate Sub-system Mounting

Physically, SEDS hardware consists of four distinct sub-systems which may be mounted either together or separately:

1. Endmass w/ejection system: 25 kg
2. Tether deployer with tether: 9 kg
3. Brake/cutter/tensiometer: 1 kg
4. Datalogger/controller: 3 kg

The masses given above do not include mounting brackets and cabling. Their masses will vary with the specific mounting arrangement.

For the mounting geometry finally selected as baseline for the Delta-based experiment option, mounting the brake on the controller moves it the right distance outboard from the Delta to eliminate a need for a structural spacer. The same would be true for a side-supported SEDS experiment on the shuttle, as would be likely if the Adaptive Payload Carrier is used. Mounting the brake and controller together also allows the final brake-to-

controller cabling connection to be made and tested out before installation on the vehicle, if that is of value. The brake assembly is light enough that mounting it on the controller should not complicate installation of the controller on the Delta or cause structural problems for the controller during launch. And worst-case tether loads are also too small to overload the controller, even if the loads reach the tether breaking strength.

Keeping the larger assemblies separate and installing them separately on the launch vehicle makes the overall SEDS equipment envelope more flexible. This allows more potential mounting locations to be used. In addition, cantilevering a heavy payload from a light deployer is inefficient and increases structural integrity verification requirements. Decoupling the payload from the deployer relaxes these requirements. This allows MSFC or industry personnel experienced with typical secondary payload support and ejection systems to work payload structural problems without constraints due to the SEDS deployer. This also simplifies the design of follow-on experiments, since changes in payload mass or center of gravity do not force re-analysis or redesign of deployer structure.

3.4 Mounting Locations on the STS or Delta

It seems feasible to mount SEDS in a GAS canister with motorized opening lid. An analogous payload, Jim McCoy's PMG (Plasma Motor-Generator), has been approved for a Hitchhiker-G experiment in a GAS canister. The first flight opportunity for the PMG is on the TSS-1 mission. This makes the tether and deployed mass superfluous, so McCoy has recommended that only the non-deployed hollow cathode device be flown. McCoy has also shifted his focus for follow-on experiments to the Delta. Hence although his experiment has already been approved for deployment from a GAS canister, we will probably not be able to point to an actual flight as a precedent for deploying SEDS from a GAS canister.

There are 3 options for mounting SEDS and a SEDS payload together in a GAS canister:

1. hollow payload surrounding top of vertical deployer
2. solid payload on top of sideways-mounted deployer
3. crescent-shaped payload side-by-side with vertical deployer

The side-by-side option should allow the most payload volume. In addition, by allowing the SEDS exit guide to be placed very near the top of the canister, the side-by-side option should minimize the likelihood that the tether can foul on the canister. Also, the side-by-side option allows access to the tether. This may be necessary if a prompt jam results in a partly-ejected payload preventing GAS lid closure. This could cause problems if the tether is not accessible for cutting by a crewman or by the remote manipulator arm.

If deployment jams in the first few meters, side-by-side mounting does cause higher payload tumble rates than the others, because the exit guide cannot be lined up with the path of the payload's center of mass. However, section 5.1 recommends the use of ripstitching on STS-based SEDS experiments. Besides cutting rebound rates, ripstitching will reduce and smear out a jam-caused impulse on the payload. Both effects will reduce tumble rates.

8

An alternative to a GAS canister is the Adaptive Payload Carrier (APC) or one of its derivatives. The APC has been developed by Rockwell to hold miscellaneous small items in the payload bay. It weighs only a small fraction of the 100+ lbs of an empty GAS canister plus mounts. The APC also takes up less room and can be mounted in more places. Further, separate mounting of the deployer and payload on one or more APCs should be more representative of most operational SEDS applications with large payloads. Such payloads would generally be mounted separate from but near the SEDS deployer.

The relative practicality of GAS vs APC mounting will probably be driven by programmatic issues. The safety implications and crew monitoring required for SEDS are clearly beyond the scope of the GAS program, and may be beyond the scope of the Hitchhiker-G program as well. On the other hand, it is not clear in advance what organizations are responsible nor what paperwork necessary for an APC-based experiment, whereas with a GAS-based Hitchhiker-G experiment, there are clear organizational responsibilities and established documentation requirements. At this point, we recommend that NASA study programmatic issues for both GAS-based Hitchhiker-G and APC-based experiment options.

For an STS-launched SEDS experiment, the Spartan free-flying spacecraft appeared at first to offer significant safety advantages. However a closer study revealed some problems. The Spartan does not have telemetry back to the orbiter. As a result, it is not necessarily easy to decide whether it is safe for the orbiter to re-approach the Spartan for recovery at the end of the shuttle mission.

On the one hand, the small orbit change induced by a successful SEDS experiment can be used as a definitive indicator of successful payload deployment, swing, and release. But this is also compatible with a meteoroid-induced tether severance late in the experiment that could result in tether fouling on the Spartan. This could create safety and operational problems during Spartan recovery similar to those that Spartan-basing is intended to avoid. On the other hand, absence of the expected orbit change is compatible with either a fouled tether (and problems during recovery), or with an early cessation of deployment followed by successful severance at the normal end-of-experiment time (which is compatible with normal recovery of the Spartan). Hence although a Spartan-based experiment may reduce risks, it does not eliminate them. And it may force a hard choice between attempting a potentially problematic recovery or losing the Spartan.

In addition, basing SEDS on the Spartan requires waiting until Spartan is scheduled to fly, and that may delay SEDS undesirably. Given these drawbacks, it seems preferable to focus mostly on other experiment concepts and return to Spartan if they prove impractical.

A free-flying mother-daughter experiment provides most of the advantages of a Spartan-based experiment (except for recovery of SEDS hardware after the experiment), but does not suffer from Spartan's disadvantages. On the other hand, a free-flyer-based experiment does require telemetry to return data to the ground. In addition, attitude oscillations on the mother (deployer) end become an issue if they are large enough to allow the deploying tether to foul on mother appendages such as antennas.

A Delta-based experiment has all of the advantages of a mother-daughter experiment, plus a reduction in paperwork requirements, scheduling uncertainty, and probable overall cost. And the Delta can provide the telemetry and attitude control functions required of the "mother" in a mother-daughter experiment.

The most attractive deployer mounting location on the Delta is outside the 2nd stage electronics bay, in the annulus between the 60" diameter bay and the 96" diameter fairing. There are four large access doors around the periphery of the bay. Two of the four spaces between those doors have obstructions, but two are clear. And conveniently, one of those locations faces nearly straight up and one faces nearly straight down when the Delta is in its normal attitude, with its telemetry antenna facing nadir.

Mounting SEDS on the conical spin-table on top of the electronics bay would allow more room for the payload. But this puts the tether close to the spin-up rockets, which increases contamination problems. It also makes it easier for the tether to foul on the spin rockets. Nesting the deployer between two mini-skirt struts is also possible, but this requires a more complicated bracket, and is likely to raise SEDS vibration loads.

Overall, the arguments seem to point toward a Delta-based experiment if that option is available. In addition, we recommend study of the programmatic issues associated with GAS-based and APC-based STS SEDS experiment options, in case the Delta option runs into problems, and for follow-on missions (most of whose development work should occur after TSS-1 flies). That allows the generic tether safety issues to be addressed and resolved by TSS-1, whose final flight safety review is now scheduled for August 1990.

3.5 Dedicated vs Host-Vehicle Datalogging and Control

As noted in chapter 2, deployer datalogging options include various degrees of SEDS autonomy. For safety reasons, we recommend that the host vehicle directly control payload ejection and have a backup tether cutting capability. But to minimize integration costs, we recommend dedicated datalogging and control, for both Delta and STS-based experiments.

On the Delta, we recommend using host vehicle telemetry. This appears cheaper than having an independent system. On the STS, there is no experiment-based requirement for telemetry, because the SEDS computer will return to earth at the end of the mission with the flight data. Hence there need be no datalinks to or through the orbiter for the sake of the experiment itself. However, STS flight safety issues may result in pressure to provide the crew SEDS data in real-time. Such a decision could require as a consequence that the entire SEDS electronics system (sensors, computer, and wiring) be 2-fault tolerant. Hence it seems preferable to focus on direct visual verification of safe experiment conditions if at all possible. If the techniques recommended in 5.1 and 5.2 are used, the crew can wait for unmistakable visual indications of payload rebound, or tether failure and recoil, before they need to initiate contingency actions.

10

4. Perform Analyses and Tests of SEDS Hardware

Task 4 involved both analyses and tests. Most of the analyses were done to resolve issues identified by MSFC, Teledyne Brown, or ourselves. Other analyses refined SEDS hardware design or testing procedures. The testing ended up involving fabrication of a flight-like SEDS tether and deployer for vibration testing at MSFC, followed by functional testing at ESL. Task 4 was then amended on April 20, 1988, to include improving the tether tie-down technique, reviewing data system functional requirements, and assisting in a MSFC-led development and test effort on a suitable electronic system.

The results of the data system functional requirements analyses have been incorporated into section 1.2. Analyses made to select key SEDS experiment parameters have been described in chapter 2 and 3. The tether and deployer design refinement, fabrication, and testing efforts were extensive enough to merit their own chapters (7 and 8). Hence this chapter will cover only miscellaneous analyses not covered elsewhere.

4.1 Orbit and Experiment Timing Constraints

In the case of a circular orbit, variations in the start time of an experiment simply shift the location of all experiment events, including reentry, an equal amount. This means that the start time can be adjusted as desired for on-orbit lighting, ground-tracking, or other reasons, with no significant change in experiment time-lines.

In the case of the eccentric orbit available on the Delta experiment (roughly 200 x 700 km), the phasing of the experiment with respect to apogee has two added effects. First, it affects the extent and duration of ground visibility, which is greatest at apogee. Second, it determines whether the orbital eccentricity assists or hinders the deorbit maneuver. Releasing something downward at perigee reduces apogee far more than perigee altitude. This can leave the payload and tether in orbit. Fortunately the Delta perigee is low enough that even worst-case phasing (release at perigee) results in a tether-plus-payload orbit life of only a few hours. But it is still preferable to release the payload in the upper half of the orbit: key events near the beginning and end of the experiment can be seen better from the ground, and reentry dispersions are more representative of typical applications.

4.2 Tether Cutter Actuation Logic

Neither the SEDS controller nor the Delta will have direct knowledge of when the post-deployment tether libration reaches the vertical, so surrogate indicators must be used to make this decision, whether the cutter is fired by SEDS or by the Delta. We did sensitivity studies using BEADSIM to determine what to base this decision on. To do this, we added routines to BEADSIM that calculate payload post-release trajectory, reentry location, and flight path angle at reentry interface (which affects reentry dispersions). These routines are discussed in more detail in section 5.5.

11

If cutter timing is simply based on elapsed time from start of deployment, then variations in deployment time can cause large differences in final libration state, and can even affect whether reentry is achieved at all on the first perigee pass after release. Sensing the end of deployment and starting a timer then is an improvement, but this is too dependent on details of brake-phase duration. In the worst case, if braking brings deployment to a stop before the end of the tether is reached, the cutter timing clock never starts.

This led us to consider some sort of "mostly deployed" sensor that would be triggered before braking began. Such a sensor might even be used to enable braking. The sensor might be simpler and potentially more reliable than enabling braking based on dual turn-counters plus software that rejects spurious turncounts. Simulations of braking strategies led us to decide to initiate braking when 95% of the tether had been deployed. This is well into the parallel-wind part of the tether package. Thus a sensor mounted inside the core seemed most suitable. An optical version of such a "brake-enabling sensor" was developed and tested during the follow-on hardware contract and is baselined for initiating both braking and cutter delay timing. It uses an IRED (infra-red emitting diode) and a PTN (phototransistor) that look through two small holes that intersect at the outside of the core. The PTN current depends on whether the tether winding covers the hole or not.

The baseline logic recommended is to cut the tether a fixed time after 95% of the tether has been deployed. For an STS experiment in a 240-300 km circular orbit, the best delay is about 1000 seconds. Near the apogee of a 200x700 km Delta orbit, 1060 seconds gives better results. We recommend that after the mission and orbit are finalized, there be consideration of including a linear or nonlinear combination of deployment time and "95% time," tuned to the specific mission orbit. For example, most of the eccentricity of the post-release orbit in the case of a Delta mission is due to the initial Delta orbit, not the tether operation. Thus the range sensitivities with respect to deployment dispersions will be different for Delta and shuttle (nearly circular) orbits.

There must also be a capability to cut the tether under anomalous conditions. In the case of the orbiter, the crew needs to be able to cut the tether at any time--even during a successful deployment, if an unrelated problem arises. Thus we recommend an "or" pyro circuit that allows either the SEDS controller or the crew to actuate the tether cutter.

In the case of the Delta, crew safety issues disappear, but another complication arises. The Delta has no command uplink capability after launch. Hence ground data analysis cannot be used for a cut decision: all anomaly detection, evaluation, and response capabilities must be on-board. The primary anomaly to which a safety-related response of cutting the tether is called for is a cessation of deployment with <95% of the tether deployed. This leaves the payload and tether attached to the Delta for the remainder of the Delta orbit life, and raises impact hazards to other spacecraft in LEO. To prevent this, we suggest that the Delta flight computer automatically fire the cutter 6300-6600 seconds after the experiment begins. This timing is late enough to avoid interfering with a normal deployment and release, but early enough to ensure that the payload and tether deorbit promptly if the deployment is normal but the SEDS controller fails to cut the tether at the proper time.

4.3 Tether Frictional Heat Dissipation

High tension early in deployment leads to a faster deployment and to higher total frictional heating. For tensions at the high end of the expected range, the total tether friction heat dissipation requirement is 6,600 joules. About 72% of this is actually due to friction during the first 19 km of deployment, before braking proper begins. Most of the tether guides that experience significant frictional heating can be fairly well heat-sunk to surrounding more massive components. An exception is the tensiometer guide. This of necessity spring-mounted and hence thermally poorly coupled to other components. Based on wrap angles and guide friction coefficients suitable for the flight hardware, the tensiometer guide may experience up to 10% of the total heat load.

If frictional heating heats the guide up beyond the melting point of Spectra, the small time that a moving tether is in contact with the guide prevents more than superficial damage to the tether. But if the guide remains hot when deployment comes to an end (or jams), then the tether can melt through and fail. Hence the peak guide temperature is of concern.

If a guide is light enough and small enough, it can neither absorb nor radiate much heat, and so it will rise to an adiabatic equilibrium temperature at which all heat generated at the interface is conducted into the tether as it moves by. This limit is worth considering. As noted on page 54 of the SEDS SBIR Phase II Final Report, at a typical tether/guide contact time of 1 millisecond, the heat penetration depth into polyethylene is only about 10 microns. Hence interface frictional heat dissipation can only be done into 1-2% of the tether mass. At a braking tension of 3 newtons with a 3375 denier tether (the last km has a ninth strand in it), an adiabatic guide that absorbs 10% of a 3 joules/meter brake heat load into 1-2% of its 0.375 grams/meter mass requires a temperature rise of 18-36K. Hence even an ideally light guide should not heat up enough to damage the tether.

For operational payloads much larger than the 23 kg of the initial payload, guide heating is larger, but by a ratio much smaller than the mass. This is mainly because deployment can be further from the vertical, and this decreases heating by the square of the cosine. Besides this, braking can be spread over twice the duration, and the moderately lower tether velocities result in longer contact times and hence better heat removal. Still, however, heat loads on the tensiometer guide need to be taken into account. It is best to have enough radiating area to get rid of heat deposited early in deployment, so the guide is cool at the beginning of braking, plus enough thermal mass to absorb the braking heat pulse. The final tensiometer guide used in the flight hardware is intended to be suitable for ambitious SEDS follow-on flights: it should allow peak and total heat loads at least 5 times higher than the maximum expected in the first experiment, without melting the tether.

4.4 Air Drag During Tether Deployment in Vacuum Chamber

During a deployment test done in August, the higher temperatures in the laboratory kept the vacuum system from reaching vacuums as low as during previous tests. We wondered if this affected tether aerodynamic drag inside the deployer. This led to the analysis below.

According to Hoerner, Fluid Dynamic Drag, pg. 3-9, Cd for a circular cylinder in cross-flow is roughly constant near 1.2 in the range 50 < Re < 300,000. From 50 to 1, it increases ten-fold. Below 1, it is:

$$Cd = 10.9/Re(0.87\text{-}Log(Re))$$

In the range 0.001 < Re < 0.1, drag varies only with the 0.11 to 0.23 power of Re. At a pressure of 84 microns, the mean free path equals the tether diameter. Below 84 microns, as the regime shifts from viscous to free molecular flow, drag should begin to drop nearly linearly with pressure.

During one deployment test, the chamber pressure was 158 microns. If V=2.0 m/sec, d=0.0008 m, and M/l=0.00033 kg/m, then Re=0.02, Cd=212, and the drag is 0.5 * Sqr(2) * 212 * 158/760000 * 1.225 * 0.0008, or 0.09 millinewtons/meter. By comparison, gravity is 0.00033 * 9.8, or 3.2 millinew/m, and centrifugal force equals 0.00033 * Sqr(2) / 0.125, or 10.6 millinew/m. At higher speed, low-Re drag goes up roughly with velocity, and centrifugal force with the second power, so the ratio of drag to centrifugal force decreases. Drag/gravity remains <1 up to 40 m/sec.

In tabular form, at 2 speeds, forces on 3000 denier Spectra tether are:

Force (millinew/m)	2 m/sec	6 m/sec
Centrifugal	10.6	95.0
Gravity	2.9	2.9
Drag (1 atm)	2.4	21.2
" (1 Torr)	0.13	0.52
" (0.1 Torr)	0.08	0.29

Based on the above, we concluded that getting the pressure below 1 Torr (1000 microns) should be entirely adequate for drag reduction.

Another area of possible concern, vacuum-induced friction changes, was studied in some detail during the SBIR Phase II work (see Phase II report, pp. 22-24). That work indicated that the friction coefficient of Spectra in contact with itself or miscellaneous guide materials (metal and ceramic) did not vary significantly when the surrounding environment was changed from normal room air to dry nitrogen or vacuum. This is compatible with NASA SP-277, **Friction, Wear, and Lubrication in Vacuum.** SP-277 says that although the friction coefficients of metal, graphite, and ceramics can change radically when water vapor, oxygen, and/or inert gases are removed, polymer friction coefficients change little.

14

5. Refine the Selected SEDS Experiment Concept

This chapter covers refinement of deployment schemes, dynamics experiments, simulation models, and brake control laws. Other aspects of task 5 are covered in more detail elsewhere: data reduction and analysis of test results in chapter 8, and the ERD in Appendix B. Under this task we also had the responsibility of supporting NASA in preparing a Design and Performance Specification for baselining. That effort took the form of a critical review of a NASA-generated draft, followed by a telecon presenting our suggestions for revisions. NASA personnel then revised the D&PS.

5.1 Recommended STS Initial Deployment Scheme

For an STS-based experiment, the primary hazards are recontact by the payload early in deployment (covered in this section), or by the tether, later in deployment (covered in the next section). Payload recontact would be caused by the tether suddenly jamming early in deployment, so that the payload stretches the tether and then rebounds toward the orbiter. The worst case would be dragless deployment followed by a sudden jam and a perfectly elastic rebound: then the time from jam to recontact would equal the time from ejection to jam. In real cases, tether drag and energy absorption in jamming and rebound will increase the rebound time. Thus the time criticality for crew response is greatest in the first few seconds after payload ejection, and decreases continuously thereafter.

We recommend using a "ripstitched" section of tether next to the payload to absorb deployment energy inelastically. The ripstitching can be designed to tear only at a much higher tension, say between 25 and 35 newtons, than the 5 newtons expected in a normal deployment. For redundancy, the tether can be ripstitched in several places adjacent to each other. Then even if one does not rip, the others can absorb the energy. Ripstitching is used in critical applications in parachuting, and the rip tension can apparently be controlled within about 10%. Preliminary experimental work was done on this during the SBIR Phase II contract and is described on page 29 of the Phase II final report.

If the payload mass is 23 kg and the payload is ejected at 1.5 m/sec from the orbiter, 26 joules must be absorbed. A ripstitch tension of 25-35 newtons requires a "stroke" of 0.7-1.0 meter, plus redundancy allowance. Analyses and BEADSIM simulations with the baseline tether and a 23 kg payload both indicate that the residual rebound velocity of the payload should be about $0.0014 * \mathrm{Sqrt}(L) * \mathrm{RipTension}$. At 1 m deployed length and 35 newtons tension, this works out to 0.05 m/sec; at 10 meters, 0.15 m/sec. These velocities give radically more time for response (35 sec vs 0.7 sec; 71 sec vs 7 sec) compared to elastic rebound, and radically reduce the potential for recontact-induced damage to the orbiter.

If such ripstitching is not deemed adequate by STS safety and operations personnel, then we recommend that payload ejection be done slowly, and STS RCS propellant be reserved for a "back-away" evasive maneuver in event of an early jam. Once the range reaches about 20 meters, transverse evasive maneuvers begin to require less propellant than back-away

maneuvers. Then most of the RCS propellant reserved for an evasive maneuver can gradually be used to increase range rate. This concept allows springs to provide half the required 1.5 m/s range rate, and RCS the rest. RCS use is comparable to the payload mass (23 kg). If safety requires nearly all of the 1.5 m/s to be provided by RCS, RCS use is doubled. In this case, it makes sense to increase the payload mass to at least 30 kg. This reduces the required separation velocity and hence the RCS requirement.

5.2 Recommended Balance-of-Deployment Scheme on STS

After about 5 minutes of deployment, orbital dynamics become important enough that even an undamped payload rebound will definitely miss the orbiter. This remains true for the rest of the deployment. However if the deployer does jam, the tether will go slack during the rebound. Possible fouling on some part of the orbiter is of concern, particularly due to loads that may be imposed on the fouled component when the tether goes taut again.

A related concern is that if the tether fails under load due to micrometeoroid-induced damage, it will recoil towards and perhaps foul on the orbiter. There will not be a subsequent strong yank as would occur if the payload were still attached, but a fouled tether may still pose risks to the STS. The highest recoil velocities will occur if the tether breaks at the peak tension occurring after a jam. We ran BEADSIM simulations of sudden jams 0.5, 2, 4, 6, 10, 12, 15, and 18 km into deployment. From 0.5 to 4 km the peak tension is <35 newtons, and ripstitching does not come into play. Later in deployment, the velocity grows enough larger than the initial 1.5 m/s that 1 meter of 35 newton ripstitching has only a small effect. Simulations of the later jams indicate that the worst case is a jam at 15 km, which causes a peak tension of 77 newtons. Based on recoil test data on page 28 of our Phase II report, the recoil velocity at 77 newtons tension and a temperature near 200K, with a 15% more massive tether than used there, should be about 21 m/s.

Preliminary work done during Phase II indicated that if the geometry is favorable, the STS RCS thrusters may be able to "blow away" a SEDS tether recoiling at a velocity of up to 40 m/sec. We understand that the Smithsonian Astrophysical Observatory is studying this concept in more detail. The Rendezvous and Proximity Operations Handbook (JSC-10589, May 1988, pg 7-31) also mentions this as a way to deal with a recoiling tether.

This scheme is most effective if the tether passes more or less transversely through an RCS plume, close to the thruster. This orientation is not necessary during the first half hour, because ripstitching would limit the peak tension after a jam to 35 newtons. After the first half hour, the deployment angle leads the vertical by 45-65 degrees. This makes the usual STS attitude (nose-forward, payload-bay-toward-earth) nearly optimal for blowing the tether away with the nose RCS jets. Once the swing begins, the orbiter should probably pitch its nose slowly toward earth (with help from the rising SEDS tension), to keep the tether squarely in the nose RCS plume until the tether is cut. The jets that impinge on the tether should be inhibited from firing inadvertently by selecting the "low-Z" attitude control mode. But the crew must be able to fire those jets manually (and with little delay), if it is necessary to blow the tether away.

16

5.3 Recommended Delta Deployment Scheme

For a Delta-based experiment, we propose using the same downward deployment, payload mass, and initial ejection velocity as for an STS-based experiment. The safety implications of payload or tether recontact are radically less, so spring-ejection is feasible and rip-stitching is unnecessary. But we do recommend that the Delta pitch down during the swing, to reduce attitude-hold cold-gas usage. Our more detailed recommendations are below.

The Delta should complete its primary mission before beginning the SEDS experiment. This includes orbit injection, deployment of and separation from the primary payload, and an engine firing to deplete residual Delta second-stage propellants (but the attitude-control nitrogen propellant should not be depleted). This keeps SEDS from being able to affect the depletion burn vector, which could complicate post-mission performance evaluation.

The Delta second stage should then roll about 50 degrees from its normal attitude, so the payload faces nadir (and 5 degrees backward, due to the conical shape of the electronics bay). Then the Delta provides power to the SEDS electronics box and closes the pyro circuits to fire the bolt cutters, allowing 4 springs to eject the SEDS payload from the Marman clamp at 1.5 m/sec. As the payload moves away from the Delta, it pulls on the tether and breaks the two tether tie-downs inside the SEDS deployer. The two jerks on the tether induce an attitude rate of several degrees/sec on the payload. This causes the payload to oscillate about the equilibrium attitude thereafter. The Delta then rolls back much of the way towards its usual attitude, until the SEDS deployer faces nadir. No brake is applied, so the tether tension after tie-down breakage is only 3-4 grams. Over the next 20 minutes this tension gradually reduces the range rate from 1.5 to under 1 m/sec.

After 20 minutes, orbital effects become dominant, and the deployment rate gradually increases. After 78 minutes, 19 km of tether have been deployed, inertial and geometric effects have increased the tension by a factor of 20, and the rapidly increasing tension has begun to passively brake deployment from its peak rate of 11 m/sec. Then active braking is applied, 3 brake turns at 1 turn per minute. This further increases tension to 3 newtons and decreases range rate to <0.5 m/sec by the time the end of the tether is reached, to minimize the amount of tether stretch and rebound when the end is reached. During the braking phase, the tethered "dumbbell" (Delta-tether-endmass) begins to swing toward the vertical. About 14 minutes after the end of deployment (and 1060 seconds after 95% of the tether has been deployed), the tether is cut at the Delta end, just before the dumbbell reaches the vertical. This "slings" the endmass and attached tether backward into a lower energy trajectory. The endmass enters the earth's atmosphere about 1/3 orbit later, dragging the tether with it, and they burn up. The Delta's orbit is raised several km.

Deployment rate and tension data are collected and processed by the SEDS electronics system as specified in section 1.2 of this report, and then formatted and sent to the Delta telemetry system for broadcast to the ground. In addition, the optional data requirements listed in 1.2 (both vehicle-based and ground-based) appear feasible and are recommended for use. Items which affect flight hardware design have already been incorporated into the SEDS hardware design, and the other items (radar and optical imagery) require only a fairly short lead time before the experiment is flown.

17

5.4 Dynamics Experiments

The deployment schemes described above, together with the tether and deployer designs described in chapter 7, allow a number of complementary dynamics experiments to be done. These are described briefly below.

First, we have found that although our tensiometer is quite stable in scale factor, it is subject to zero shifts and drifts up to 1% of full-scale, due to such items as momentary overload during tie-down breakage. In order to calibrate the returned tension data, we need an independent means of determining absolute tension periodically during the experiment. Average absolute tension over periods of a few minutes can be derived from payload mass properties and attitude oscillation periods. The oscillation period data can in turn be collected from instrumentation on-board the payload, or (with lower but perhaps adequate accuracy) by taking a Fourier transform of the deployment rate to find the frequency of the rate variation caused by payload oscillation. A third option which is intermittently available is to use ground-based radar to determine radar scintillation rates.

Parts of the Fourier transform of deployment rates should also be useful for two other reasons. The high frequency portion helps determine how much the tether damps high-frequency variations associated with deploying a universal wind. The low-frequency portion shows the period and relative amplitude of various transverse modes, providing a test of computer models capable of simulating SEDS deployments.

Payload attitude oscillations should decay over time, partly due to the secularly rising tension, and partly due to oscillation-caused changes in deployment rate and hence tension. Oscillation decay is best measured on the payload but may be deducible from deployment rate variations.

Tension data, its Fourier transform, and payload attitude oscillation data should indicate to potential users whether SEDS can provide a stable and smooth enough ride that flimsy appendages such as solar arrays might be deployed before payload boosting by SEDS.

As the experiment proceeds, imperfect torque balancing in the braided tether will gradually induce payload spin-up around the tether axis. Preliminary tests and calculations indicate that the final rate should be of order 2 rpm. Measuring the actual rate should be useful to potential operational users of SEDS. Some users may actually prefer non-zero spin, if it can be guaranteed. For example, slow spin about a vertical axis at release provides a good initial attitude for a ballistic capsule that reenters 1/4 to 1/3 orbit after release.

About four minutes before the braking phase begins, the winding shifts from universal to parallel. This greatly reduces deployer-caused high-frequency tension variations, while tension is still low. Vibration energy already injected into the tether is gradually damped, both by inherent tether damping and by the now large velocity-squared component of tether tension. This decay further characterizes tether and deployer properties.

We have incorporated three short high-mass sections in the last 2.5 km of parallel-wound part of the tether. These sections are 400 meters apart and will deploy at about 36 second

intervals. Each will cause a momentary jump in deployment tension. A tensile wave will then propagate down the tether, reflect off the payload, and return to the deployer. Deployment rate and tension data during this period will provide yet another window on the dynamic response of tether and deployer. It would be particularly useful to have high-frequency tension data at the payload end to determine wavefront smearing.

Near the end of braking, as the unwinding rate falls below 15 turns/sec, dynamics inside the deployer shift from a "sling" mode (which makes tension vary with velocity squared) to a less desirable slip-stick scrubbing mode. To delay this mode transition, we have embedded a heavy insert inside the final 100 m of tether. Tension measurements during this phase will help us evaluate the effectiveness of this method of delaying transition.

Radar imagery of the endmasses will provide an independent determination of the libration angle at several times during deployment. In addition, we have embedded a uniformly-spaced 100-element radar dipole array in the middle of the tether. The times at which the array glints provide attitude information on the middle of the tether. This can provide an independent determination of some aspects of transverse tether dynamics, to provide more confidence that simulation models are indeed predicting tether behavior accurately.

Optical imaging of the tether at twilight by low-light TV cameras located on the ground or on aircraft may provide the best data on transverse tether dynamics, and the most vivid and easily interpretable data of all. The resolution (after image enhancement) should be comparable to that shown on most computer graphics of tether simulations, and the images could be directly compared with BEADSIM or other tether simulation programs. The frame-blanking and frame-transfer techniques used in CCD-type TV cameras guarantee that each frame represents a coherent snapshot in time. Camera jiggle could be cancelled out using stars in each image for reference. Post-processing might be fairly expensive, but it need not be done unless the imagery collected and the potential benefits justify it.

5.5 BEADSIM Refinement

The main simulation model used during the contract was BEADSIM, a program developed during the SEDS SBIR Phase II contract and documented in the Phase II final report, pages 115-129. During this contract significant refinements were made to BEADSIM.

The most important one was to model tension gradients along the tether. We considered this necessary because in the initial SEDS experiment the tether is 30% as massive as the payload. Thus tension gradients along the tether (and increased tension during braking, to decelerate the tether) are non-trivial. We were able to include tension gradients while retaining large-timestep stability by keeping track of the gradient and damping transient changes in the gradient, while not damping overall tension changes. This effectively damps acoustic modes (which is what limits timesteps in most detailed tether simulation models) while not damping the fundamental sprung-mass mode. We verified the modal separation by a series of runs: the sprung-mass mode damped out quickly if the viscous damping tether parameter was set high, but very slowly if that term was set to zero.

19

Another refinement was to incorporate the effects of exit guide friction on deployment tension. This varies with the tether wrap angle around the exit guide, which varies with the tether exit angle relative to the vertical.

A third change was to allow the exosphere temperature to be specified as a program input, rather than assuming a fixed 1000K exosphere atmosphere. In addition, the drag model was improved so that libration-induced horizontal velocity properly affected the dynamic pressure.

Another change was to allow the run to be stopped at a fixed time after 95% of the tether had been deployed. This was added to test our suspicion that such a cutter timing logic might be adequate for flight. We found that cutting the tether 1000-1060 seconds after 95% is deployed actually reduces range dispersions compared to release at the vertical. This was encouraging, because in a Delta-based experiment it might be quite expensive to determine on-board in real time when the tether reaches the vertical.

We also refined the program outputs. The graphics were improved, and additional "bottom line" data were computed. For example, the final states of the endmasses and tether are used to compute subsequent orbital parameters and expected orbital life for the Delta, payload, tether, Delta plus tether, and payload plus tether. The orbit life calculation uses the empirical correlation on page 145 of the NASA Tether Handbook (2nd edition, done under contract NASW-4341).

If it is clear an object would reenter by the next perigee, probable range at impact and entry angle (which affects footprint size) are computed instead of orbit life. Range at impact is based on the results of a program which tracks lifting reentry trajectories. We found that the mean of extreme impact ranges for objects having L/D of -0.4 to +0.4 (the L/D values used for External Tank debris impact footprint studies) was close to that for an L/D of +0.2. We then developed a rough empirical correlation that predicts impact range for objects with an L/D of +0.2. This is based on a ballistic-coefficient-specific "reentry altitude" at which the object sees 0.1 gee deceleration, plus the vertical velocity at that altitude.

During the follow-on flight hardware contract, additional significant changes were made. They will be described in more detail in the final report for that contract but should be mentioned here. The main ones were: changing the calculations from an LVLH (local-vertical, local horizontal) reference frame to an inertial frame, and eliminating linearization of the gravity gradient. These changes allowed far better treatment of eccentric orbits, whose dynamic effects and periodic aerodynamic drag effects are both significant. The deployment tension algorithm was also refined to better fit the test data in Appendix A: the velocity-squared component of tension now varies with the inverse 1.6 power of remaining package diameter, rather than the inverse square. Finally, the reentry range correlation was improved by shifting to a reentry altitude at which deceleration is one gee.

20

5.6 SEDS Brake Control Law

Based on BEADSIM simulations, braking at a fixed motor rate near the end of deployment provides a smooth tension profile and keeps residual transverse tether oscillations small. The questions are: when to begin, and whether to vary the rate based on turn-counter data.

In LEO, braking that takes place longer than 11 minutes before the end of deployment is counterproductive: orbital mechanics makes a deceleration impulse have a delayed effect of accelerating deployment after 11 minutes. And even at times less than 11 minutes, the effectiveness has a nearly quadratic drop-off in efficiency: roughly $1-Sqr(T/11)$ for an impulse T minutes before the end of the tether is reached. Thus braking should last significantly less than 11 minutes. For large masses deployed at high tension, the key trade is that a short brake phase raises peak loads while a longer braking phase raises total heat loads. Such high-tension deployments have little curve in the tether at the beginning of braking, and the transverse period is shorter. Thus brake tension can ramp up fairly quickly without "twanging" the tether. Preliminary analyses indicate that the optimum brake duration with heavy payloads is probably about 6-8 minutes, including a 2-3 minute ramp. This implies that braking should begin when about 10% of the tether is left.

For lighter payloads such as in the first experiment, a significantly shorter braking time increases braking tensions, making them representative of heavier payloads and providing a better test of the brake. On the other hand, very short braking times and the resulting high tensions are more likely to result in payload rebound and a slack tether at the end of braking. Based on these two issues, we have chosen a braking time of 3-4 minutes for the first experiment. This implies beginning when about 5% of the tether (1 km) is left.

If the brake friction coefficient is less than expected, deceleration will be less than expected and the end of deployment will be reached with fewer turns of brake and at non-negligible deployment velocity. So: should we use turn-count feedback? The basic logic should probably be to use count-rate feedback within fairly narrow time-based limits. Then counter problems can only throw brake operation slightly off. In any case, the relatively modest final velocities remaining at the end of deployment (<2 m/sec) for a plausible range of friction coefficients make this issue less than critical: the tether and payload can tolerate the jerk and subsequent dynamics from a complete failure of braking (with a final velocity over 5 m/s), and off-optimum braking causes far less serious dynamics than this.

As with cutter actuation, there must be consideration of anomalous conditions. If the Delta goes into the proper orbit there is no way in which 95% deployment can be reached in less than about 4600 seconds. Thus inhibiting brake actuation for 4600 seconds, independent of the brake-enabling sensor, can limit the problems caused by a false positive in the brake-enabling sensor. There is no urgent necessity to a backup brake actuation independent of the brake-enabling sensor, because the tether and payload can tolerate a brake failure. However one can easily use the "C" turn-count channel (turn-count data processed to discount multiple counts in the A and B channels) as a backup for the brake-enabling sensor. This does rely on both A and B channels working properly, but this is better than no backup system, and it is unlikely to experience false positives that could initiate braking too early. Similar logic should be suitable for STS-based experiments.

There appears to be no need to try to adjust deployment tension or timing by using the brake early in deployment. This is because the selected payload and expected range of tether tensions result in low sensitivities of deployment time and reentry range to tension variations. In fact, the sensitivities actually change sign in the region of interest. The table below shows the effect of variations in minimum deployment tension on 95% time, final libration angle, and reentry range (in degrees relative to the location on earth over which the experiment starts). The experiment is assumed to begin at apogee, and the tether is assumed to be cut 1060 seconds after 95% of the tether length is deployed. Deployment time is mainly controlled by the tension during the first 40 minutes of deployment. The tension then typically ranges between 10 and 40% higher than the specified "MinTension," due to varying exit guide friction and inertial effects.

MinTension	95% time	Libr.Amp.	Angle at cut	Reentry range
1.0 grams	4818 sec	56 deg	-5 deg	474.35 deg
1.5	4717	54	-4	472.68
2.0	4649	53	-3	471.87
2.5	4618	52	-2	471.81
3.0	4636	50	-1	472.62
3.5	4742	49	-1	474.76

For the 3.5:1 range of "MinTensions" considered, all ranges are within 3 degrees. For the less extreme values (1.5-3.0 grams), the ranges are all within 1 degree.

5.7 Payload Design Recommendations

The baseline payload design is passive, but instrumentation and telemetry may be added for other purposes. If this is done, the following instrumentation would be useful. A tensiometer on the payload should allow more accurate tension measurement than the running-line tensiometer does at the deployer end of the tether. In addition, it allows measurement of the tensile relaxation transient when the tether is cut at the other end, and of the dynamics imposed by deployment of sections of tether having heavy inserts. This will help characterize tether properties and should assist safety assessment of STS-based tether operations. A magnetometer, gyro, or properly-located accelerometer can sense payload attitude dynamics, including the buildup of spin about the tether axis due to tether torsional set. One or more photocells could be useful for spin state determination when the payload is in the sun.

Other instruments should also be considered if they are useful for non-tether studies (such as upper atmosphere characterization) during the 2 hours between the beginning of deployment and reentry.

6. Support Interactive SEDS Systems Definition Process

Under this task we prepared an ERD and assisted NASA and Teledyne Brown Engineering in various areas. This included providing thermal properties data to Sheryl Hunt of Teledyne Brown, helping Chris Rupp of MSFC refine SEDS data collection hardware and software requirements, and reviewing and providing feedback on draft NASA documents related to SEDS. The ERD is included as Appendix B. This chapter hence just covers aspects of datacollection system development which we were involved in and which are not covered elsewhere.

During most of this contract, it was still not clear whether a tensiometer would be feasible on the first flight, so near-term data system development efforts focused on collecting turn-count data. Chris Rupp proposed connecting a resistor in the PTN circuit to a comparator, which would interrupt the microprocessor, which would in turn read and store the time of the interruption. Rupp refined this by adding two intermediate stages. The first stretched the pulse to make the circuit immune to prompt retriggering, which can be caused by tether vibrations superimposed on the mean unwinding motion. The second intermediate stage shortened the pulse seen by the microprocessor interrupt pin to an appropriate length.

We were asked to suggest an appropriate period during which the turn-counter should ignore repeated beam-interruptions. The maximum unwinding rate occurs at the beginning of the braking phase. In a normal deployment this occurs 1 km before the end. The maximum rate is about 52 turns/sec. If the brake does not work, then the unwinding rate continues to rise, even though the linear deployment velocity is already falling, due to passive braking effects. In this case the peak unwinding rate is about 68 turns/sec. Given a possible non-uniformity in unwinding rates, we recommended that the non-retriggerable period be several milliseconds, but short compared to the 15 millisecond average repeat time for valid turns at the highest expected unwinding rate of 68 turns/sec.

A non-retriggerable period of only a few milliseconds cannot eliminate all vibration-induced spurious counts at lower unwinding rates: our final deployment test under this contract had 10% spurious counts. Getting a correct count requires using two counters (A & B) a half turn apart, and using set-reset logic on their outputs to derive a logical "C" channel. The C channel disregards any A "recounts" that occur before B is triggered. Unfortunately, this logic eliminates the redundancy of having two independent counters.

We discussed this problem with Rupp. The decision was made to store and transmit data from both turn-count channels: then even if one channel fails, all data collected is still sent to the ground. As shown at the end of Appendix A, we were able to take one channel's data and plot it in a way that allowed us to see clearly which turn-counts were spurious and disregard them. But it seemed infeasible to have the SEDS computer do such editing in real time. Thus if we used A or B channels to actuate the brake, the count would include spurious turns, but if we used the C channel, we lost redundancy. This is what led us to propose a dedicated "95% deployed" sensor to enable braking. This sensor is independent of the "C" turn-counter and has fewer failure modes. In addition, it can be backed up by the C turn-counter, which is extremely unlikely to trigger braking early.

We were also asked what turn-count time resolution was needed. It seems desirable to be able to capture brief deployment speed variations of a few percent at the time of highest deployment speed, in order to capture reflections of tensile waves generated by the dynamics experiments. This requires resolution of well under a millisecond. This is too short for the required length of the major loop in the data system software (which lasts 2 milliseconds as of this report date). Rupp refined the software so that the turn-count time includes the count of a minor loop that executes about 60 times for each major loop. This gives a resolution of about 30 microseconds, or about .2% of a turn at the maximum unwinding rate.

Problems during high-speed tests of the turn-counter led us to the realization that the PTN capacitance was far higher than we expected. Inspection of spec sheets for many different PTNs showed that this was a generic characteristic. The combination of high capacitance and low current when used with low-power IREDs resulted in a time constant over 0.1 millisecond. This caused the PTN response at the maximum tether unwinding rate to be rather low. As a result, the comparator threshold has to be set accurately.

Measurements taken before and after the last deployment indicated a significant change in PTN current. The only clearly identifiable change in conditions was the removal of the tether package by deployment. This is an unavoidable change, and we worried about its effect in flight. In addition, although the temperature sensitivities of IRED and PTN have opposing effects, the canister-mounted PTNs will be exposed to far larger temperature changes than the core-mounted IREDs (and those temperature changes are not entirely in phase anyway). These changes can also move the current away from the comparator threshold. Finally, stray sunlight entering the canister can also affect the PTN current.

Based on these concerns, we recommended that the comparator circuit be modified to recognize only sudden reductions in PTN current. This was done by MSFC in 1989. In addition, we took pains when designing the flight hardware to minimize PTN sensitivity to either multiply-reflected IRED output or sunlight: the PTNs are multiply-apertured, so that they only are exposed to light from near the IRED; and the region which the PTNs do see around the IREDs (essentially, the inside of the conical flange) is both black to reduce multiple reflections, and well baffled against direct or scattered sunlight.

Note that the correlation between turn-count data and length data involves nonlinearities on at least 4 scales: package diameter, winding pattern, position within one winding axial cycle, and dynamic effects. The first three nonlinearities can be characterized during winding by recording turns versus length for that winding. Dynamic effects can only be characterized by in-lab deployment of a well-characterized winding at relevant rates, with length being monitored at high resolution along with turn-counts. While this obviously cannot be done for the final flight winding, the dynamic effects do depend on the other three parameters. As a result, the patterns of difference between length as measured by a metering wheel during laboratory deployment, and length estimates derived from winding parameters plus turn-counters, can be broken down into components which depend on the various winding properties. Those components can then be applied to windings of similar design which are deployed at similar rates.

24

7. Design and Fabricate Flight-like SEDS Hardware

Task 4 required ESL to participate in vibration tests and electronics system development tests. This required designing and fabricating a full-length flight-like tether and a more flight-like tether deployer than had been developed during the SBIR Phase II contract. This chapter describes that effort, most of which focused on refining the tether braid design and the tether winding pattern.

7.1 Tether Design and Fabrication

The first task was to select a design for a full-length 20 km tether. We re-calibrated the tensile testing machine load cell, modified the datalogger software so that tension (stress) would be logged as a function of elongation (strain) rather than of time, and prepared test samples. We investigated the following braid design variables:

1) Number and size of yarns (eg. 8 x 375 denier, 4 x 650 denier)
2) Braid pattern (with 8x braids only: under 2 & over 2, versus under 1 & over 1
3) Tension of yarn being laid into the braid
4) Pre-twist of yarn being laid into the braid
5) Picks (pattern repeats) per inch of braid
6) Size and height of braid-point guide above base plate

We made 23 test samples of 5 distinct braid designs, varying items 3), 5), and 6) above. We inspected all samples and tested 5 to failure. Based on this, we made these tentative decisions:

1) The braid should be an 8 x 375 construction, to trap yarn ends inside the braid
2) As Allied suggests, yarn tension should be kept low during braiding (about 8 oz)
3) Zero yarn pre-twist gives the most uniform and predictable braid
4) A loose braid (4 ppi) gives the highest strength and modulus
5) The braid-point guide size and position has only minor effects on the braid

The braider supply packages can hold only about 2.5 km of 375 denier yarn. Thus a 20-km tether must have splices in it. We decided to splice yarns one at a time. We start a splice by tucking the free end of the new yarn inside the braid (hence our preference for an 8-yarn braid over a 4-yarn braid, which does not fully trap the end). Then we co-braid the old and new yarns for a distance. Then we tuck the end of the old yarn inside the braid. In the follow-on flight hardware contract, we decided to splice the whole tether every 2.5 km. This replaces 56 on-line yarn splices with 7 off-line full-tether splices. It also eliminates worries about messing up a 20 km tether when braiding is nearly complete.

Based on the above parameters, we fabricated samples and conducted 60 tension tests. We plotted stress and strain, and noted ultimate strength. These tests led us to select 4.01 picks-per-inch for the prototype tether, and a standardized yarn splice involving 12 inches of overlap. We found this to preserve the full strength of the tether.

25

Next we focused on braiding a 20 km prototype tether. We completed this in late October, 1987, by which time four different people were trained in operating the braiding machine and forming the yarn splices. We consider the finished tether of good quality, even though a few minor yarn flaws and oil-stains are present. This tether has a breaking strength of 750 newtons (170 lbs) and is suitable for use with objects weighing up to at least a ton (e.g., the Delta 2nd stage). On the first SEDS experiment the expected maximum tension is <5 newtons (1 lb). For improved resistance to ascent heating, atomic oxygen, and (on the Delta) exposure to upper stage exhaust, we recommend adding a short length of heavier Nomex or Kevlar tether for the free end that is exposed before deployment begins.

7.2 Winding Development

We then focused on finding a flight-like winding design capable of surviving the expected vibration environment. On our first winding, we wound the first 3582 meters (14972 turns) in a parallel wind, and the remaining 16418 meters (32568 turns) in a progressive universal wind, with 6 turns per axial cycle. This was the first time we had wound a Spectra package this deep, and there were two unwelcome surprises.

First, there was a 161 meter discrepancy between the overall length measured during braiding and that measured during rewinding. We found that the cause was inadequate back-tension on the braider. This caused slippage on the capstan, which tightened the braid and locally reduced tether strength and modulus. Increasing the torque on the takeup reel so that it was comparable to that at the braid point kept this problem from recurring.

Second, and more troubling, we found that even though the universally-wound portion of the tether was wound with a 9-inch lead traverse, the package was not 9 inches long. It began at less than 9 inches, but as more layers were added, each compressing the underlying layers, the package began to bulge at each end. By the time we finished, the maximum length was 11.75 inches, and the ends were quite soft. We considered the large bulge and soft ends completely unacceptable for either vibration or deployment tests.

In early November, we unwound the universal portion of the winding and experimented with different winding ratios with larger lead. Windings with 4 and 5 turns per cycle caused excessive slippage at the turn-arounds. We then tried 5 turns, regressive, and found that this did not help.

This led us to try a multi-pattern winding. We started with 6 turns per cycle when the diameter was small, and switched to 5 turns, 4 turns, and 3 turns as the package diameter gradually increased. The reduced number of turns per cycle compensated for the increased circumference per turn as the package diameter increased, and kept the lead angle from decreasing so much that the outer parts of the package lost axial cohesiveness. This procedure reduced the maximum package length from 11.75 to 9.70 inches. This represents a 75% reduction in bulge or excess length. This revised winding was adequate both in length and solidity for testing and flight. It is documented in section 7.3.

We did have other winding-related problems. Deployments during the SBIR contracts had been with relatively short lengths of tether, and friction in the gland valve and a large number of other fixed tether guides helped make the takeup tension high enough to form a fairly dense takeup winding. However here we were winding a full 20 km length, and doing so at not much more than the deployment tension. The result was a very loose, "cotton-candy-like" takeup winding which filled up the takeup reel when there were still 4.5 km left to be deployed. In addition, increasing tension and/or centrifugal force as deployment progressed caused a "hernia" in the underlying low density takeup winding. The bulged mass of winding was in danger of fouling on the level wind mechanism. To allow us to complete the deployment, we stopped the test, removed the takeup reel, wrapped the winding tightly in thin polyethylene sheet and overwound it with a few turns of cord at high tension. This formed a dense and stable bed for the last 4.5 km to wind on.

We started rewinding the 20 km of tether onto the core for a second 20-km deployment in late May. The first few km wound off the supply reel (formerly takeup reel) relatively well, because it had been wound under tension onto a stable base. However after 4.5 km had been unwound and the plastic wrap removed, the remaining winding tended to jam as it unwound. Our response was to periodically unwind several dozen turns manually, rewind them under more tension, and then run the winder until those turns were exhausted and the unwinding became uneven again. After about 150 meters of this procedure, the tether suddenly broke near the metering wheel.

After some discussion, we cut out 20 meters of tether surrounding the break, for tensile tests and other diagnostics. The tensile tests proved normal, but a microscope inspection of the tether ends at the winding break was quite revealing. We had earlier noticed that when Spectra breaks at its ultimate load, the individual fibers each develop a "mushroom" or cap shape at their end, apparently as a result of recoil and intra-fiber shearing during the failure of each fiber. The fiber ends in the tensile test samples looked normal, but most of the fiber ends at the winding break had no cap: instead, they resembled fiber ends in tethers that had been cut. We then inspected the tether winding path. We found that part of one of the ceramic "pigtail" guides had broken off, perhaps as a result of a jerk earlier in the winding. The remaining part had a very sharp edge. That edge was not in the normal tether path, but it could be reached if the tether was vibrating. We think that the jerky unwinding from the supply spool caused the tether to vibrate enough to reach the sharp edge. The tether then failed at the next jerk. We covered the sharp edge with epoxy, joined the two tether ends in a non-flight-like manner, and completed the winding.

We later performed an automated diameter inspection of 1.3 km of tether upstream of this break. This convinced us that there had been no partial cuts upstream. To keep the problem from recurring as a result of the remaining full-length deployment under this contract, we imposed braking periodically during the deployment, to "clamp" the winding down before enough loose winding had accumulated to create a hernia. This also provided more data on brake characteristics than a more flight-like deployment would.

During the follow-on flight hardware contract we took additional precautions. One was to add a "squeegee" type tensioner to the takeup system. This added 100-200 grams to the takeup tension all through deployment. A second was to make HardTuf-coated ductile

aluminum guides and substitute them for the brittle ceramic guides wherever possible. A third was to add an accumulator to the winder path, with enough capacity that the winder could be stopped after a jam, before the tether tension had increased unacceptably.

7.3 As-Fabricated Specification of 20 Km Tether and Winding for Vibration Tests

The tether is braided from Spectra 1000 fiber (375 nominal denier) manufactured by Allied Fibers. The fiber was "converted" or wound onto cop tubes in preparation for braiding, by Conneault, with no yarn twist. We then braided 8 yarns together into a hollow tubular braid on a New England Butt "Maypole" type braider at ESL, with continuous monitoring of production. We set the braider at minimum tension and braided the tether using 158 picks per meter (4.01 per inch). We made yarn splices by co-braiding 2 yarns and tucking the ends inside the core of the hollow braid. The actual average denier for the tether, as weighed after fabrication and winding, was 8 x 327 denier. The overall length is 20 km plus or minus 100 m, measured at room temperature at the winding tension, during winding.

We made a winding in November 1987. This was vibration tested and deployed in March-April 1988. A second full winding was made in May, vibration tested in June, and deployed in August. (Test data from that deployment are in Appendix A.) Comparing the two windings, the number of turns with each pattern was within a few hundred of each other; the winding tensions were very similar; and the overall wound package dimensions were within 1 mm of each other. Winding data are listed below for the May 1988 winding.

Winding	Turns/Cycle	#Turns	Segment Length	Tension
Parallel		14852	3586 m	17 new
Universal	6	11034	4310 m	11 new
"	5	4152	1955 m	9 new
"	4	12658	7138 m	7 new
"	3	4413	2926 m	4 new

Package Dimensions: .214 m diameter, .246 m maximum length

Tie-downs: The free end of the winding is tied to underlying layers at the top "turn-around" with a loop of #50 mercerized cotton thread. The thread is knotted with a square knot and the free ends are trimmed about 4 mm from the knot. A second tie-down of the same design holds the last bottom turn-around in place. (This second tie-down was used only for the May 1988 winding.)

28

7.4 Deployer Design and Fabrication

During our SBIR Phase II contract we used clear plastic deployers for diagnostic purposes. The current contract required a flight-like aluminum deployer for vibration tests. We retained the basic design shown in the SBIR final report, which used separate pieces for the cone and cylinder of the canister, joined to each other via a machined ring. We had a cone spun and heat-treated. Its response to heat-treating showed it was the wrong alloy. We had another one made, this time of 6061. We modified the baseplate design by adding stiffening ribs between the central thick section of the baseplate and the periphery. In addition, we substituted flush rivets for the flush screws used in the Phase II design. We fabricated a deployer to this modified design. The tether rubbing surfaces on the inside of the cone and cylinder were sanded and beadblasted. Toward the end of the contract, we had the core HardTuf coated to reduce scrubbing friction at the very end of deployment. The deployer sensors (tensiometer, temperature sensors, and turn-counters) were all new. They are described below.

In Phase II, we measured tension using an Entran semi-conductor load cell which measured the force associated with a 180 degree reversal in tether direction. For this contract we designed a more flight-like cantilever-beam tensiometer that bent the tether only 30 degrees. It used four Omega strain gauges wired in Wheatstone bridge fashion, mounted just above the base of the beam, two on each side. We made two different beams, one 10 mils thick and one 20 mils thick. The thin one was used for most of the tests, when tensions were low. We used the thicker one for tests involving braking, when tension was much higher. In the case of overloads, the beam could "bottom out" against a support. The tether passed through a small eyelet at the top of each beam. The eyelet was made of aluminum wire. It was anodized to reduce friction and increase wear resistance. The tensiometer was mounted on top of the orbiting guide on top of the brake post, and rotated with the orbiting guide. The leads passed through the hollow brake post and were thin and flexible enough to absorb the 4 rotations needed within the length of the brake post.

During Phase II we had used a small laser for a light source, to provide enough beam brightness to use the phototransistors in room light with a clear plastic deployer. To make this deployer more "flight like," we substituted IREDs (infrared emitting diodes). We mounted them in holes in the conical top of the deployer. They pointed at and illuminated PTNs (phototransistors) mounted inside the hollow core of the deployer. Some effort was required to get good alignment. In one deployment test, the alignment was poor enough on one channel that its data was lost.

During Phase II we used platinum resistance thermometers. Here we substituted AD590 semi-conductor temperature sensors. These sensors have a fixed output of 1 microamp per degree K for any supply voltage between 4 and 30 volts. The current was converted to a voltage by a resistor in series. We used two AD590s: one on the brake motor casing, and the other on top of the orbiting guide at the top of the brake post.

Finally, our Phase II brake motor was a direct current gearmotor. For this contract we found a suitable geared stepper motor (Airpax). We drove it by using a Hewlett Packard signal generator to control several power transistors.

8. Perform Tests on SEDS Hardware and Analyze Test Data

Our test efforts were aimed at fabricating and providing a vibration test article to MSFC, and then performing a deployment test at ESL after MSFC completed the vibration test. Section 8.1 summarizes the vibration testing. Sections 8.2 to 8.4 describe the deployment test hardware, procedures, testing, and results. The discussion of the early tests focuses on "lessons learned." The final deployment was more straightforward and provided very useful data. That deployment and the results are described in 8.4. The data for that deployment are plotted in Appendix A.

8.1 Summary of Vibration Testing and Test Results

We shipped our first 20-km winding to MSFC in November 1987 for vibration testing, while the rest of the deployer was still being designed and fabricated. This and other vibration tests were done by J. Herring of MSFC. The free end of the tether was tied to the top of the package, but the last tether turn-around at the bottom was not tied down. When the winding was vibration tested, this turn-around came loose. This allowed underlying groups of turns to become loose and pile up on the baseplate in a progressive manner, one "axial cycle" at a time. In all, nearly 50 turns were dislodged by the vibration test, without the tie-down ever coming loose. This was rather embarrassing. But we quickly realized that the problem could be cured merely by tieing down the last bottom turn-around as well as the top end.

After we deployed this winding, we re-wound it in May 1988, tied it down at both ends as described in 7.3, and sent it to MSFC for another vibration test. This test was performed in late June. Nothing came loose. On this test, the fundamental lateral frequency was 200 Hz, and the fundamental frequency along the axis was 700 Hz. These frequencies are for a core mounted directly to a rigid base. Baseplate and mounting bracket flexibility could significantly reduce the frequencies.

The empty deployer was shipped to Marshall in late May for a separate vibration test. That test was done on May 31-June 1, 1988. The Airpax stepper motor (which was not flight-qualified, nor intended for flight) came apart during the high-level longitudinal vibration testing. The brake design had the motor on a short cantilevered beam, and this beam amplified the test vibration level of 19 Gees to 108 Gees (measured on the motor). This vibration intensity was enough to shear the small rivets that held the motor together, and the motor separated. The case was securely taped back on, and the test continued. No other anomalies occurred during the test.

The peak response of the empty canister to longitudinal accelerations was in the 800-1200 Hz range, except for the motor, which also responded significantly at 300 and 400 Hz. Due to the limited bending stiffness of the baseplate, the lateral response of the empty deployer had a peak at much lower frequency, 70-80 Hz, plus peaks between 400 and 600 Hz.

30

8.2 Deployment Test Hardware Changes from Phase II

During Phase II, our in-vacuum deployment tests passed the tether out through a two-stage gland valve to a takeup device in room air. We felt that doing this with a flight tether would degrade it undesirably. In addition, splices and other inserts which change the tether diameter periodically would require the use of a loose-fitting gland, thus raising residual air pressure in the vacuum chamber too much. In addition, a jam or other complication during deployment might require that we cut the tether. These issues caused us to change over to an in-vacuum takeup device.

We learned from motor suppliers that even though the brush-type motors used in most variable-speed applications have brush lives rated in the thousands of hours in room air, the brushes last only a few hours in vacuum. This and the cost of other types of suitable motors led us to mount a brush-type motor on the outside of the vacuum chamber endplate and use a Ferrofluidic rotary feedthrough to pass shaft power into the chamber. On the inside of the endplate we built a takeup system. We used a standard industrial reel 8" long, with 5" core diameter and 12" flange diameter, and a Norco ball-reverser level wind.

Some of the instrumentation system was the same as during Phase II:

> Video and audio recording equipment for documenting tests
> Tether metering wheel and mechanical length turn-counter
> HP plotters for displaying data graphically
> Miscellaneous vacuum and air-pressure gauges

The main changes were new deployer sensors (see 7.4), use of a precision HP-based datalogging system rather than the Analog Devices pre-amp and Data Translation board, and (for the last full-length deployment test only) use of a prototype of the MSFC-developed SEDS computer to collect turn-count data.

We used the HP-based datalogging system to collect tension data because the Data Translation hardware was on temporary loan to another MSFC-funded project at ESL, and that project was in a critical phase (preparing for flight on a KC-135). The HP system could collect only one channel of data at the speeds required, so temperature data were collected on a strip-chart recorder. The SEDS computer was programmed by Chris Rupp to collect optical turn-count data from two phototransistors.

The new tensiometer required that the tether deploy upward after leaving the tensiometer. This in turn required that the vacuum chamber be vertical. We built a wooden stand for the chamber, added more electrical feedthroughs on the bottom endplate for the increased instrumentation, and mounted handles on the other endplate to simplify handling.

To prepare for a test we mounted the deployer on the bottom baseplate and connected the deployer sensors, IREDS, and brake stepper motor to the feedthroughs. Then we wired the HP data-logging system, strip-chart recorder, IRED power supplies, and stepper-motor controller to the other side of the feedthroughs and checked out all systems. For the final tests we also wired in the MSFC-developed SEDS computer to keep track of turn counts.

31

Next we lifted the 175 lb acrylic vacuum chamber cylinder, tipped it over the deployer, and eased it into position on the endplate, ensuring that the gasket was positioned properly. Then we threaded the free tether end through the takeup lead control and attached it to the takeup reel, and installed the top endplate while manually turning the motor to take out slack as we moved the endplate into position. Finally we attached the vacuum pump and pumped down the system.

Other than the new instrumentation and the new preparation sequence just described, test procedures were the same as those used in Phase II (see Phase II final report, pp 68-69). Deployment speeds were set by manually adjusting the takeup motor control rheostat, which controlled motor rpm. Accurate control of deployment rate required accurate prediction of takeup package diameter as deployment progressed. We did not know this very precisely, so our estimates of deployment rate and deployed length grew less accurate as the test proceeded and the takeup package diameter increased.

8.3 Early Tests and Test Results

During this contract the following deployments were done (all in 1988):

20 km deployment in 6 tests, March 29 to April 8
2-3.5 km deployments in 3 tests, May 10-25, in clear canister
20 km deployment in 5 tests, August 24-25 (see section 8.4)

All deployments used a range of deployment speeds above and below those expected for that part of the tether during a normal deployment in space, with speed changes occurring typically at intervals of 15 to 60 seconds. The purposes of the two full 20 km deployments were similar: 1) to determine whether a full deployment would occur without snagging, at tensions in the range expected, with no unexpected deleterious phenomena; and 2) to characterize deployment tension more accurately as a function of length, speed, and brake position, to improve BEADSIM simulations. The two short deployments deployed parallel-type windings representing the last 3.5 km of tether. These deployments were done inside the clear plastic canister used in Phase II. They were made to determine the cause of an unexpected increase in tension at low speeds near the end of the first deployment.

The first deployment was broken into six tests: 1700, 500, 3000, 10200, 3500, and 1000 m. The first test modeled the early decreasing-speed part of deployment which ends when gravity gradient effects become more important than tether tension. Speeds ranged from 0.8 to 2.6 m/sec. Analysis of the data showed a change in tension waveform near 2 m/sec. We attribute this to a mode transition between gravity-dominated and centrifugal-force-dominated tether dynamics inside the deployer. We decided to concentrate remaining efforts on speeds >2 m/sec, with only an occasional drop to lower speeds for comparison.

The computer did not take data properly during the second test, so we aborted the test when we realized something was wrong. The third and fourth tests modelled a gradual increase in speed as deployment progressed.

As noted in 7.2, after the fourth test the takeup reel was nearly full, and we had to compress and wrap the loose winding to allow the deployment to be completed. The fifth test modeled the end of deployment, starting at high speed (10-12 m/sec) and gradually reducing the speed and adding brake. Vibrations in the cantilever beam and in the 1 meter of tether between the deployer and takeup reel provided a visual indication of tension and tension variations.

Several minutes into the fifth test we saw a radical reduction in the amount of vibration. This was a clear indication of the transition from universal to parallel wind. About 8 minutes into the test, at a speed near 2 m/sec, the brake orbiting guide suddenly unwound. Apparently tension inside the deployer had increased. The several turns of brake induced a much larger increase in the tension at the top of the brake, and this was enough to overcome the holding torque of the geared stepper motor. (Once a stepper starts to be back-driven, the motor "cogs" and has little average torque against continued back-driving.)

At this point about 1 km of tether remained. For the next test we added about 8 turns of brake and deployed slowly (0-2 m/sec), to determine the uniformity of the tether spiral angle, and hence the maximum number of turns of brake that could be used without adjacent turns fouling on each other. This test bottomed out the tensiometer, so we did not use the computer, but just videotaped the test. A tension spike pulled out the wire loop at the top of the tensiometer. Significant excursions in takeup motor rpm indicated there were substantial and irregular tension variations over time.

This was an unwelcome discovery. The core geometry we were using was based on experience gained during Phase II deployments, but it had not itself been tested during Phase II. To find out what was going on, we felt it necessary to do a 3.5 km deployment using the clear plastic canister that we used in Phase II. We wound an existing 3.5 km length of 4x650 Spectra onto the core to model the final 3.5 km of tether to be deployed, mounted the core inside the clear plastic deployer canister, and deployed this in vacuum. We imaged the internal deployer dynamics with a camcorder and also logged tension data.

The TV images were far more instructive than the tension data. We found a transition from a centrifugal or slinging mode, in which the tether is flung out against the canister, to a "scrubbing" or slip-stick mode, in which the tether scrubs against the conical flange at the top of the core. The transition occurred at 2-3 m/sec deployment speed. It occurred at lower speed as the deployment progressed. The transition velocities corresponded to a relatively fixed unwinding rate of about 15 turns/sec, with the following two exceptions.

First, there was hysteresis in the mode change: once a mode was triggered, a small change in conditions would not generally trigger the reverse change. This seems quite reasonable, since centrifugal force is over twice as large when the tether is slung against the 10" diameter canister as when it is scrubbing against the 4" diameter core flange.

Second, the scrubbing mode started more readily when tether was deploying from near the top and had less catenary mass to pull it outward. The scrubbing also seemed more intense then, as might be expected from the greater bend angle around the flange.

By this time we had heard of the Tiodize Corporation's HardTuf coating process. This is a low-friction Teflon-impregnated hard anodizing for aluminum. We sent the core up to Tiodize for coating. It turned out that rather than coating just the rim of the flange, it was cheaper to coat the entire core (except the base and screw holes, which were masked). When the core was sent back, we rewound the 3.5 km long 4x650 tether on it and did another deployment, on May 25. As expected, the coating had little effect on the transition between slinging and scrubbing modes, but it significantly reduced the tension and tension variations in the scrubbing mode once that mode began. This reduced the deleterious effect of the transition. Still, however, the scrubbing mode roughly doubled the tension compared to that in the slinging mode under similar conditions.

Next we inspected BEADSIM results more carefully. We realized that the mode transition would not occur until the last 100 meters of deployment, because the deployment rate would exceed 3 m/sec until then. We also realized that adding mass to the tether should delay the transition, if it did not at the same time increase the tether stiffness excessively. This led to experiments with thin strands of solder embedded in the tether. These were successful enough that we decided to embed solder in the last 100 meters of the flight tether fabricated during the follow-on contract. This and a change in winding pattern together delayed the transition to 1.5-2 m/sec, or the last 25-45 meters of tether.

8.4 Final Deployment Tests, Results, and Analyses

Our last deployment used the 20 km tether, which was wound on the core after the core was HardTuf-coated. We had problems in doing the winding, as discussed in section 7.2. These problems had no effect on the quality or characteristics of the winding, except for the knot about 4.7 km from the end of the tether. We arranged to deploy the knot slowly between two tests, to prevent damaging the wire loop in the tensiometer. The knot gave us accurate knowledge of how much tether remained at the beginning of the last test, allowing us better control of that test than during the first 20-km deployment.

To prevent recurrence of the "cotton candy" winding described in 7.2, we decided to apply braking periodically, to raise deployment tension and compress the winding. Using the brake early in deployment also allowed us to characterize the brake over a wider range of conditions. The brake increased tensions enough that we decided to use the high-range tensiometer for all of the tests. This reduced the resolution by a factor of 4 during the unbraked part of early deployment, but it made the database more uniform.

To simplify post-test analysis, we decided to use the same tension datarate in each test and to make the tests of equal duration. We broke the deployment into five tests, each about 15 minutes long. Constraints on the HP datalogger memory size led us to choose a test duration of 906 seconds and a datarate of 300 Hz. This datarate is a multiple of 60 Hz, and roughly 1.5 times the tensiometer frequency. The SEDS computer was also used for this test. It collected turn-count data with sub-millisecond time resolution. We wired the computer to the phototransistors and attached to to a terminal for control.

34

We did the five tests on August 24 and 25, 1988. Between tests, we did just enough data analysis to verify that the sensors and dataloggers were working properly. Far more thorough data reduction and analyses were done over the following month. These efforts involved writing several dozen different Pascal programs to scan, digest, and present the data in different ways. Most of the programs focused on the turn count data. Two displays from an editing program are shown at the end of Appendix A. These programs were later enhanced to analyze data from deployments done in 1989, during the flight-hardware contract. They will be further enhanced for analysis of data from the flight hardware qualification functional test, which is expected to occur in March 1990.

The data are shown in summary form in Appendix A, along with eight "snapshots" of details of particular interest. The data are stored in five floppy disks, copies of which have been provided to Chris Rupp. The main value of the data is that it allowed us to reach the conclusions discussed below. For future analyses, data from the qualification functional test of the flight hardware will be of far greater utility. But the data from the August 1988 deployment will remain of value for comparison with the flight hardware test data.

The most important conclusions concerned the turn count data. First, a properly functioning channel with a several-millisecond non-retriggerable period will record about 10% more counts than there are turns. Although 0% spurious counts is preferable, 10% is small enough that all counts can be stored and transmitted to the ground for post-flight editing. More importantly, our data reduction showed that even in the absence of a second channel, inherent patterns in the valid data allow a combination of automated plus manual editing to distinguish between turns and vibration-caused counts with high reliability (i.e., no errors in 5,000 spurious counts in this deployment). Detail 8 at the end of Appendix A shows how a single spurious count changes the pattern and hence can be identified clearly.

The data also showed that as the remaining package diameter decreased, tension ramped up slower than our rough expectation of an inverse square relationship. We do not know which of several aspects of the changing geometry cause this. But the data fit an inverse 1.6 power of package diameter fairly well, so we have modified BEADSIM appropriately.

Also, the brake has relatively more effect in amplifying very low tensions than in amplifying higher ones. We attribute this to tether stiffness, which is only prominent at the lowest deployment speeds. This will be taken into account in cases where braking is considered for use early in deployment. It does not affect braking under other conditions, other than possibly during the last 20-50 meters of deployment.

A final conclusion resulted from our adding sequential groups of five 300 Hz tension datapoints together to get rid of 60 Hz noise, and doing all subsequent work with the resulting 60 Hz database. After some puzzlement, we realized that some of the 60 Hz sums were within range, but appeared to include one or more off-scale readings. This led us to suggest that the flight software check for off-scale readings in the 500 Hz data before summing that data into 30 Hz sums for storage and transmission to the ground, and flag sums that include off-scale readings. For flagged data, it may be more useful to report the number of off-scale readings than to report a sum which includes inaccurate readings.

9. Conclusions and Recommendations

The key conclusion from this study is that the Delta-based SEDS flight experiment concept developed and refined under tasks 2-5 of this contract appears eminently feasible. The recommended experiment has already been developed significantly through the combined efforts of MSFC, ESL, and McDonnell Douglas during the follow-on flight hardware contract. Thus there is no need to repeat the recommendations made earlier in the report here. But we do have a list of recommendations for STS-based experiment options. Some of them also appear relevant to TSS and other tether experiments on the STS, so we have divided the recommendations into generic and SEDS-specific categories.

9.1 Two Recommendations for All STS-based Tether Experiments

The major generic safety issues associated with tether operations on the STS are recontact with a rebounding payload or a recoiling tether. Much of the discussion in 5.1 and 5.2 is relevant to STS-based tether experiments other than SEDS, and it is timely to begin serious consideration of their implications. Thus we make the two recommendations below:

9.1.1 Energy Absorption to Minimize Payload Rebound After Deployer Jam:

"Ripstitching" or an equivalent energy absorption mechanism provides a way to absorb tension spikes associated with deployer jamming or other malfunction. By absorbing energy rather than simply storing it, payload rebound is minimized. This appears beneficial not only to SEDS but also possibly to TSS-1 and/or TSS-2, in the event of deployer jamming or various other failure modes. We recommend that ripstitching or equivalent one-shot energy absorbers be studied by the TSS program, and that follow-on SEDS efforts directed at STS experiments plan on developing, testing, and using ripstitching to reduce rebound.

9.1.2 RCS Thruster Use to Blow away a Recoiling Tether:

STS RCS thrusters may be able to "blow away" a recoiling SEDS tether, even one recoiling at a velocity of 40 m/sec, if the geometry is favorable. We recommend that this be studied seriously as a way of dealing with a tether that has failed under load and is recoiling back toward the orbiter. If a thorough study indicates this is as effective as it now appears to be, we recommend that during STS operations with tethers, the orbiter be oriented so that the tether passes squarely through the plume of one or more RCS jets, and that those jets be inhibited from firing for attitude control but allowed to fire under manual crew control, if it is necessary to blow the tether away. We believe it is timely to consider this for the TSS, and believe that the necessary studies would be relevant to nearly any STS-based tether operation.

9.2 Recommendations Specific to STS-based SEDS Experiments

We recommend that NASA study programmatic issues and other tradeoffs between mounting SEDS in GAS/Hitchhiker-G hardware and mounting it on an Auxiliary Payload Carriers (APC). We suspect that an APC-mounted experiment will allow more flexible placement of deployer and payload, with less modifications from the SEDS hardware design developed for a Delta-based experiment. In addition, it should better resemble most operational applications of SEDS on the STS. However these two options need to be studied in more detail before one is selected.

Second, we recommend that if ripstitching is not deemed adequate by STS safety and operations personnel as a way of controlling payload rebound in the event of a deployer jam, then SEDS payload ejection be done slowly, and STS RCS propellant be reserved for a "back-away" evasive maneuver in event of an early jam. Once the range reaches about 20 meters, transverse evasive maneuvers begin to require less propellant than back-away maneuvers, and most of the RCS propellant reserved for an evasive maneuver can gradually be used to increase range rate. We suggest that the necessary maneuvers be studied along with STS/TSS contingency operations, because we think that the similarities and differences between TSS and SEDS will cross-fertilize the investigation of maneuvers for each.

Finally, given the changes in STS philosophy since Challenger, it seems appropriate to focus study of STS-based SEDS experiments on those which need the STS or greatly benefit from it. In addition, if the first SEDS/STS experiment is developed primarily after TSS and one or more SEDS/Delta experiments fly, it seems appropriate to consider experiments that actually provide useful benefits to a shuttle mission. One example is deorbiting a reentry capsule filled with materials samples, early enough in a SpaceLab or SpaceHab mission that prompt analyses on the ground can provide useful feedback for efforts later in the mission. This could be of considerable value in helping justify space-station-based materials processing. This concept is rather far afield from the original intent of this study, but it may be a reasonable focus for a first or early STS-based use of SEDS.

Appendix A. Test Data from Final Deployment

This appendix shows data from the last tether deployment under this contract, which was done August 24-25, 1988. The deployment was divided into five 906-second tests. Turn-counts were recorded with sub-millisecond time resolution, and tensiometer output voltage was measured at 300 Hz. The tension readings were summed into groups of 5 to cancel out 60 Hz noise, and all analysis was done on the resulting 60 Hz sums.

Each test is plotted on two facing pages, from top to bottom, with a slight overlap in the data covered by the two pages. Each datapoint plotted represents the average value during one second. Brake position is plotted in the left column, tension on the right column, and rate data in between. Note that the rate and tension scales change from test to test. In addition, to keep the tension data on the plot, the tension is divided by 3 to the X power, where X is the number of turns of brake in use then. Since tension goes up by roughly a factor of 3 per turn, the as-plotted tension appears to be little affected by braking.

The labels "Detail #1..8" in the plots indicate that there are detailed plots of that data at the end of Appendix A. The first 7 show 60 Hz tension data that are of particular interest. The last detail displays turn-count intervals in a way that helps identify spurious counts.
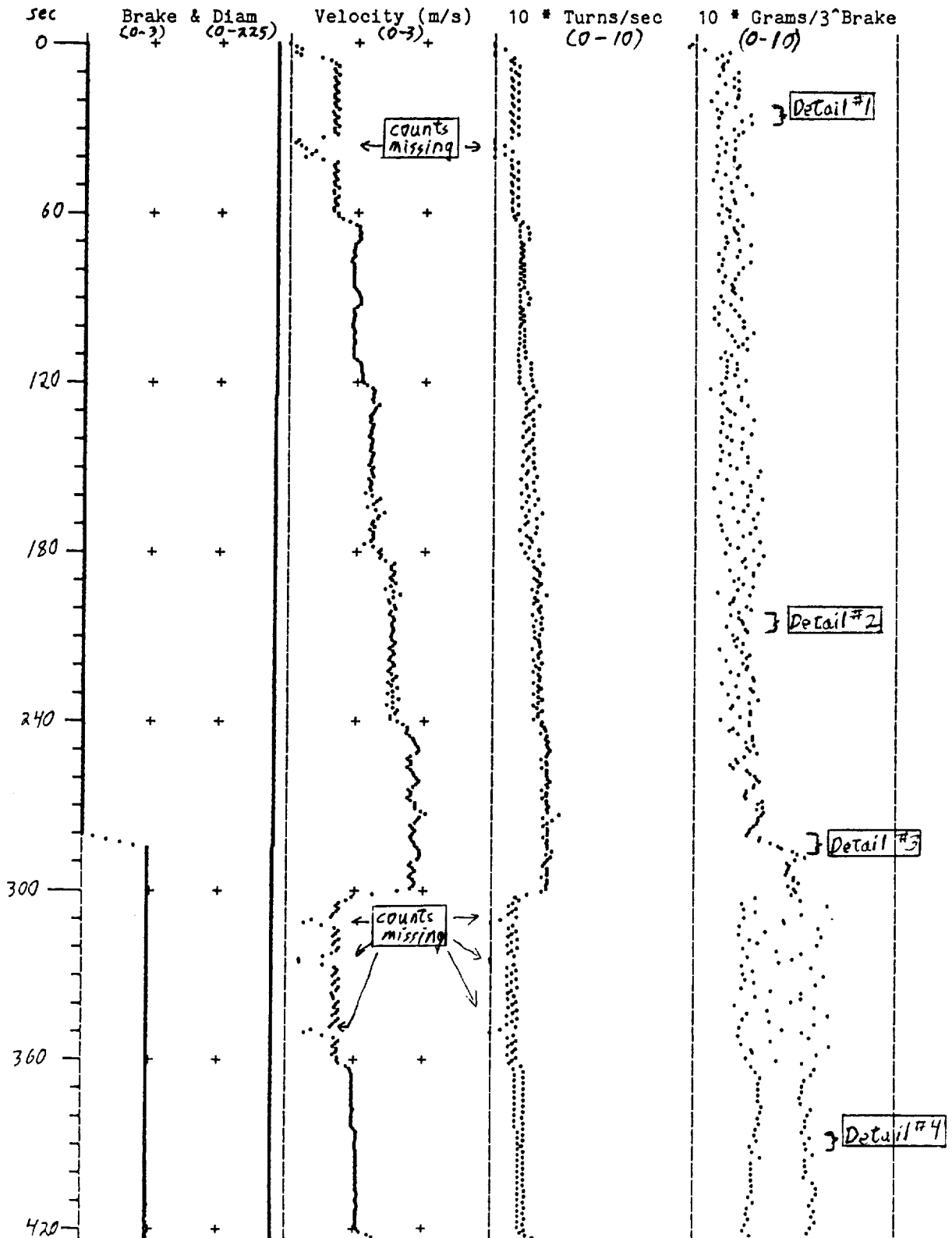
We changed the takeup motor speed shortly after the beginning of each minute during each test. We selected a pattern of takeup rates that scanned through speeds relevant to that part of deployment every 5 minutes (every 3 minutes during test #5). We added just under one turn of brake shortly before the end of each scan, at a time when the speed was stable and at its highest value for that scan.

Each test starts with zero deployment rate and zero brake, and except for tests #3 and #4, in which the takeup reel did not stop fast enough, each test ends with zero deployment rate and zero brake. This allows a check of tensiometer zero shifts during the test. (Zero rate and zero brake need not imply zero tension, but informal tests show the difference is usually <1 gram.) Zero shifts during tests #1 and #2 were <1 gram. During test #5, the shift was 3 grams. This was probably caused by occurrence of the scrubbing mode when 3 turns of brake were applied (mostly from 720 to 780 seconds). This increased the tension to over 730 grams, which bottomed out the tensiometer against a mechanical stop. The taped end of the tether peeled loose at 875 seconds; this also bottomed out the tensiometer briefly. The tie-downs probably did the same, but we accidentally broke them when we plugged the takeup motor in before test #1, so any shift they caused preceded test #1.
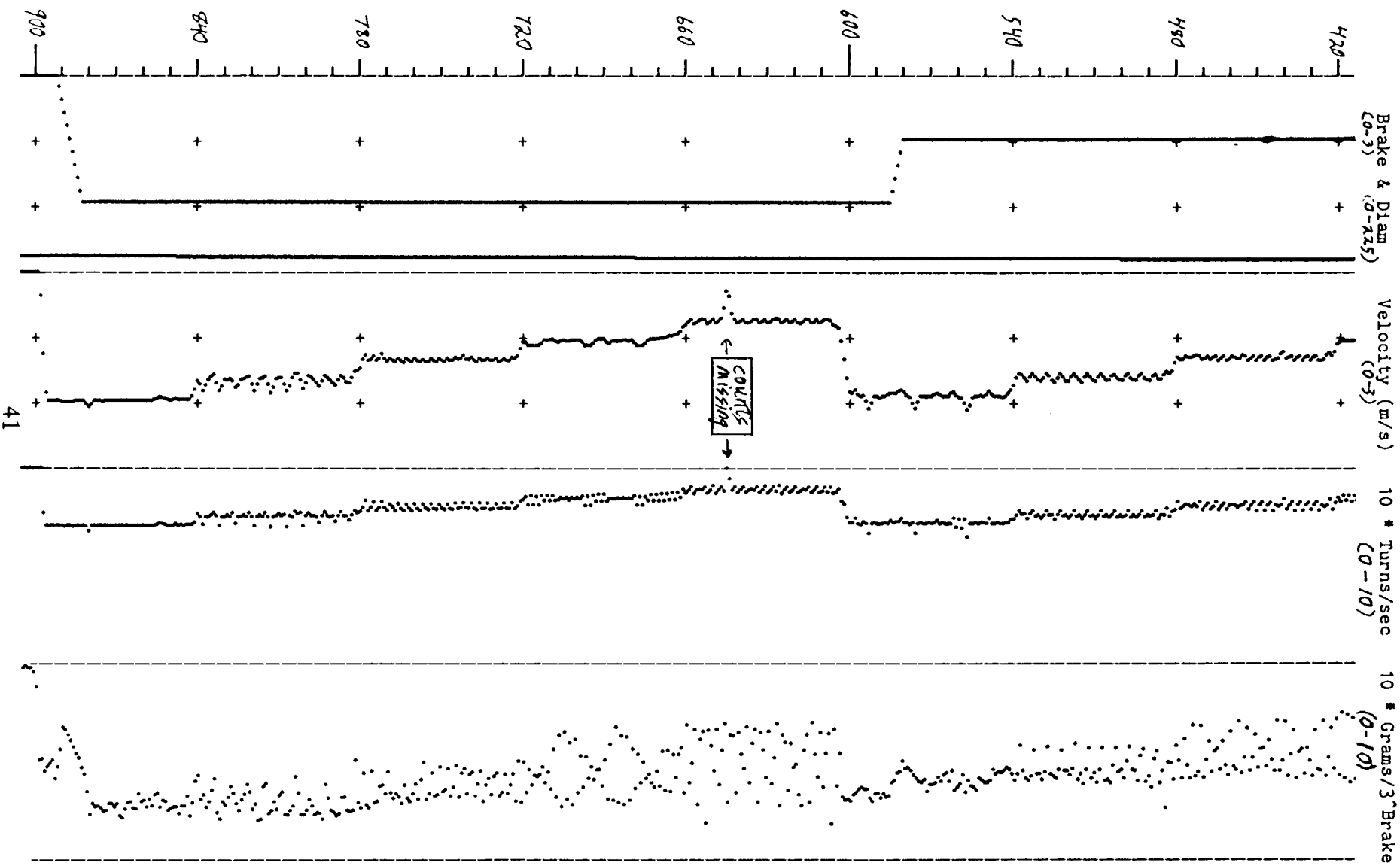
Other than the scrubbing-plus-brake and tape-peel episodes near the end of test #5, there were very few off-scale tension values. The 60 Hz data show about 10 individual off-scale values each in tests #4 and #5, about 3 each in tests #2 and #3, and none in test #1. There are a comparable number of additional 60 Hz sums in each test that were enough higher than surrounding values that they may have included one or two off-scale readings. We think these individual off-scale tensions are due to turn-arounds that are pinched between the bottom of the package and the baseplate. (Similar tension spikes in the first deployment during the flight-hardware contract have been clearly identified with this.)

Shown below are second-by-second data for a 906-sec SEDS
deployment test, one of 5 that deployed a 20 km tether.
The time scale marks 10, 60, and 300 second intervals.
Tests 1-5 started with 0, 1, 3, 8, and 15 km deployed.
Brake is 1 turn per "+" mark; pack diameter, 75 mm/+.
Velocity, Turns/sec, & Tension are in units shown per +,
and the scales differ for each test. Tension is divided
by 3 for each BrakeTurn to keep the data on the page.

900 840 780 720 660 600 540 480 420

Brake & Diam
(0-3)
(0-.225)

Velocity (m/s)
(0-3)

41

counts
missing

10 * Turns/sec
(0-10)

10 * Grams/3"Brake
(0-10)

AUGUST 1988 SEDS 20 KM VACUUM DEPLOYMENT, TEST #2

Shown below are second-by-second data for a 906-sec SEDS
deployment test, one of 5 that deployed a 20 km tether.
The time scale marks 10, 60, and 300 second intervals.
Tests 1-5 started with 0, 1, 3, 8, and 15 km deployed.
Brake is 1 turn per "+" mark; pack diameter, 75 mm/+.
Velocity, Turns/sec, & Tension are in units shown per +,
and the scales differ for each test. Tension is divided
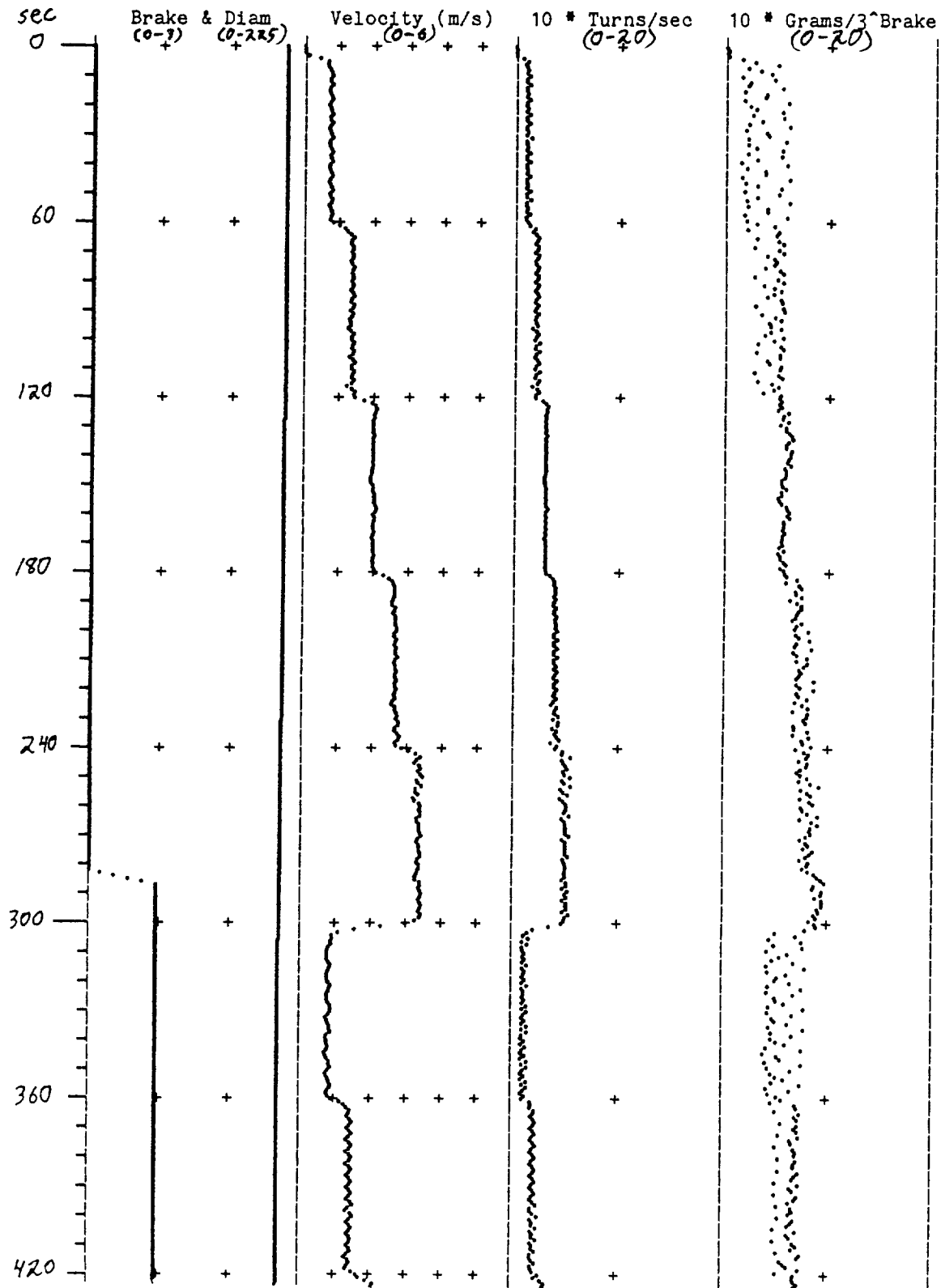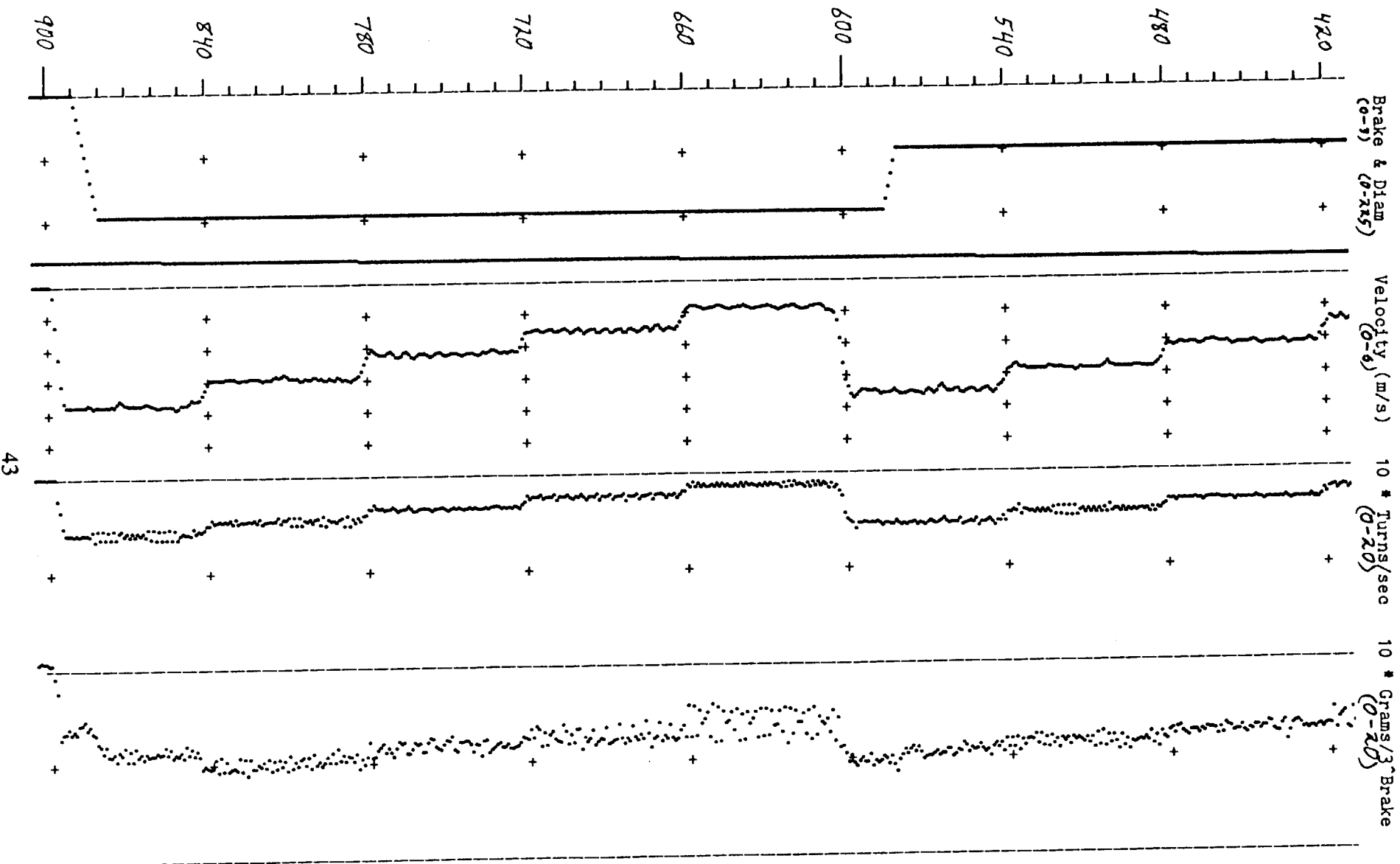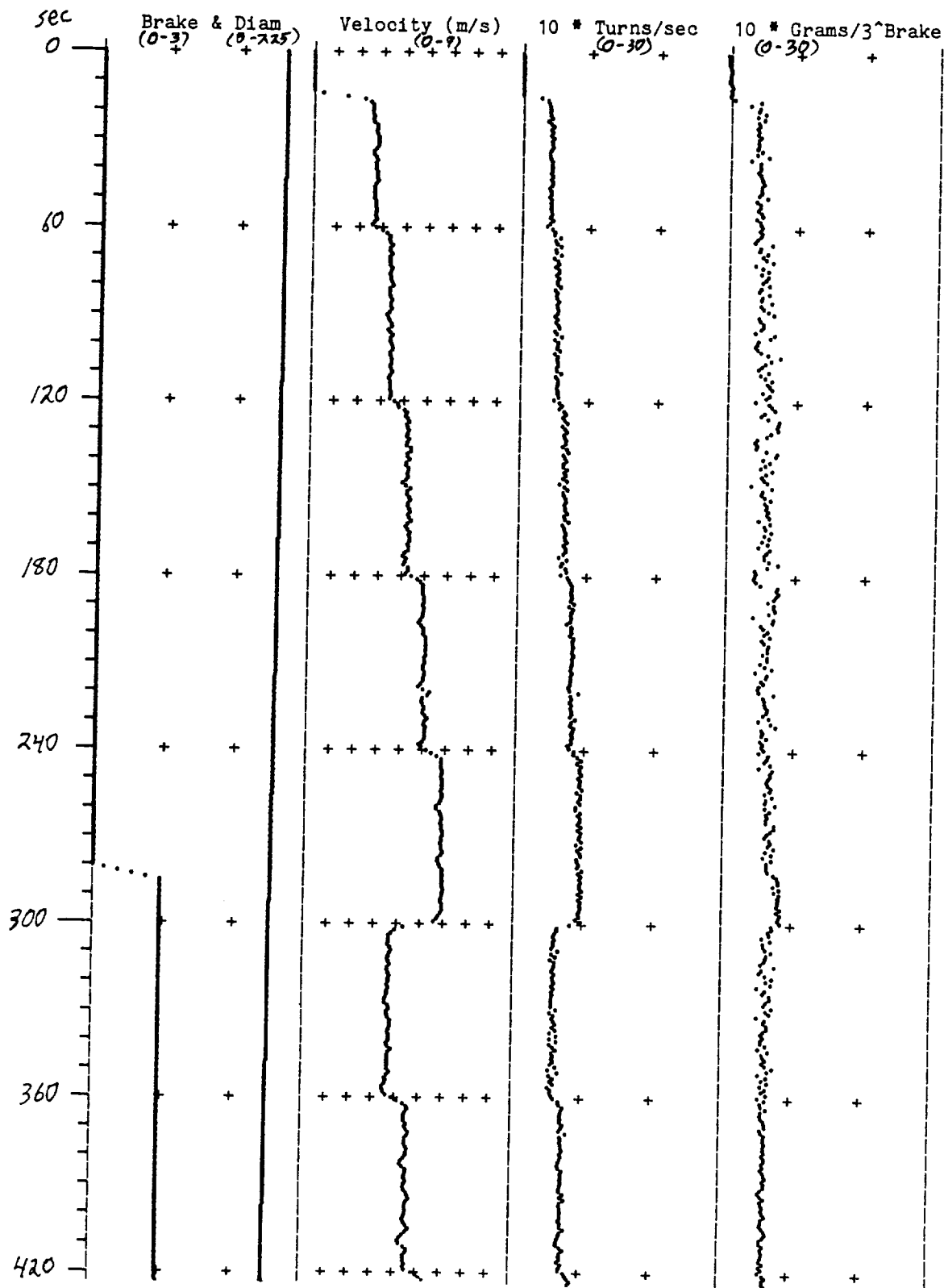by 3 for each BrakeTurn to keep the data on the page.

sec	Brake & Diam (0-9)	(0-225)	Velocity (m/s) (0-6)	10 * Turns/sec (0-20)	10 * Grams/3^Brake (0-20)
0					
60	+	+	+ + + + +	+	+
120	+	+	+ + + + +	+	+
180	+	+	+ + + + +	+	+
240	+	+	+ + + + +	+	+
300	+	+	+ + + + +	+	+
360	+	+	+ + + + +	+	+
420	+	+	+ + + + +	+	+

42

(Test #2)

Brake & Diam (0-9) (0-1x5)

Velocity (m/s) (0-6)

10 * Turns/sec (0-20)

10 * Grams/3 Brake (0-20)

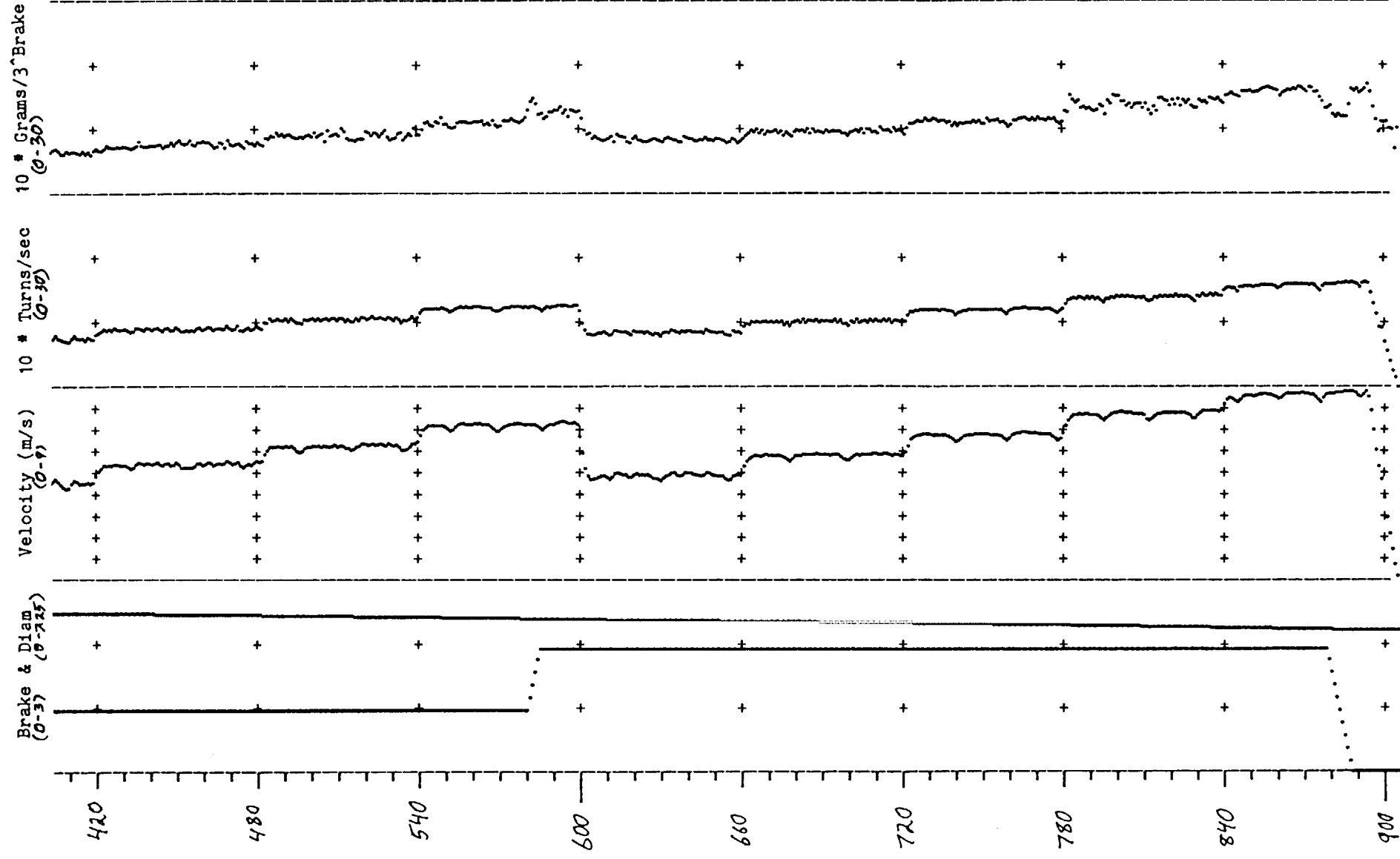43

900 840 780 720 660 600 540 480 420

AUGUST 1988 SEDS 20 KM VACUUM DEPLOYMENT, TEST #3

Shown below are second-by-second data for a 906-sec SEDS
deployment test, one of 5 that deployed a 20 km tether.
The time scale marks 10, 60, and 300 second intervals.
Tests 1-5 started with 0, 1, 3, 8, and 15 km deployed.
Brake is 1 turn per "+" mark; pack diameter, 75 mm/+.
Velocity, Turns/sec, & Tension are in units shown per +,
and the scales differ for each test. Tension is divided
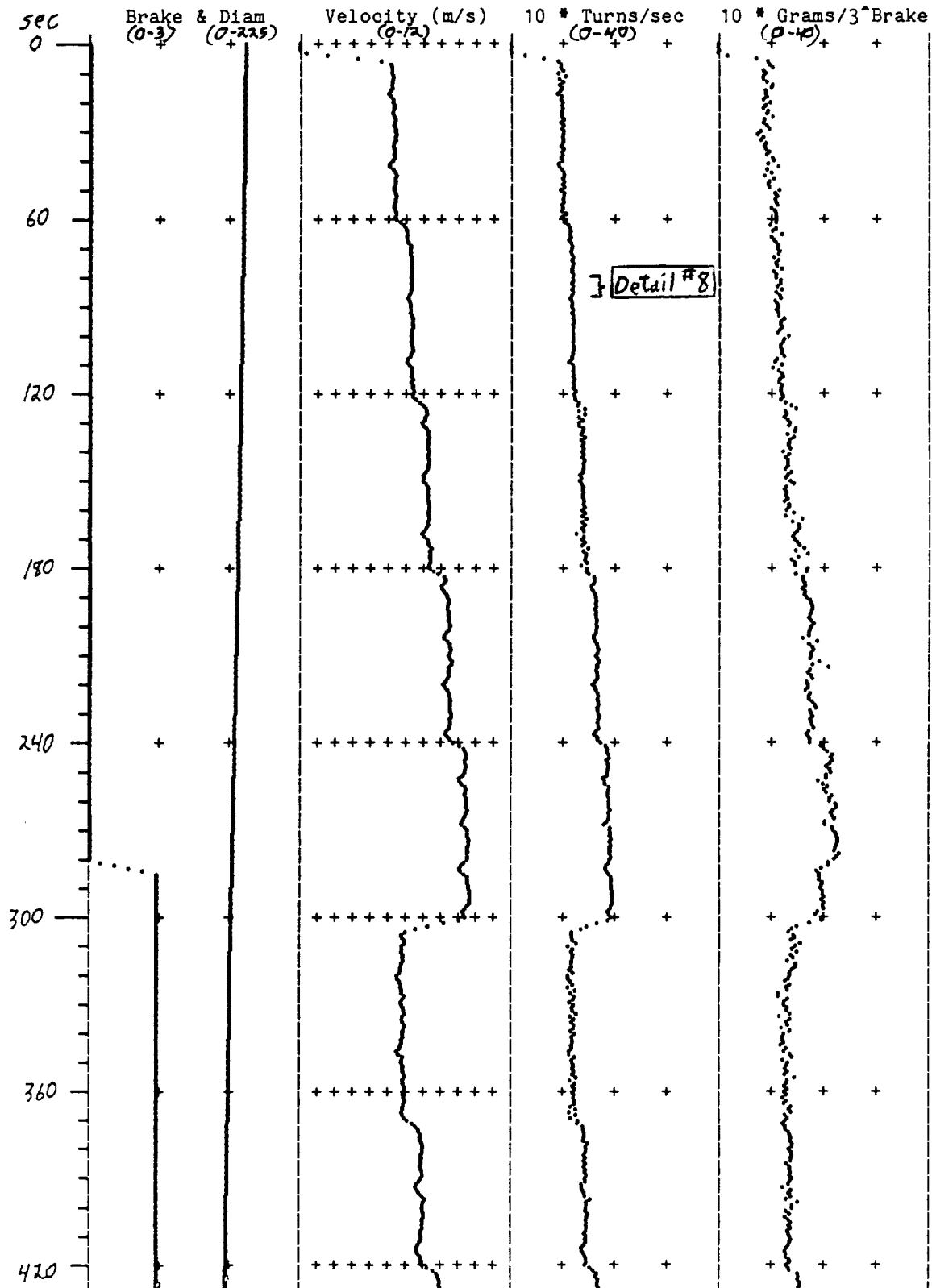by 3 for each BrakeTurn to keep the data on the page.

sec	Brake & Diam (0-3) (0-225)	Velocity (m/s) (0-9)	10 * Turns/sec (0-30)	10 * Grams/3^Brake (0-30)

44

(Test #3)

10 * Grams/3"Brake (0-30)

10 * Turns/sec (0-30)

Velocity (m/s) (0-9)

Brake & Diam (0-715)

Brake (0-3)

45

420 480 540 600 660 720 780 840 900

Shown below are second-by-second data for a 906-sec SEDS
deployment test, one of 5 that deployed a 20 km tether.
The time scale marks 10, 60, and 300 second intervals.
Tests 1-5 started with 0, 1, 3, 8, and 15 km deployed.
Brake is 1 turn per "+" mark; pack diameter, 75 mm/+.
Velocity, Turns/sec, & Tension are in units shown per +,
and the scales differ for each test. Tension is divided
by 3 for each BrakeTurn to keep the data on the page.

(Test #4)

Brake & Diam
(0-3)
(0-2.25)

Velocity (m/s)
(0-72)

10 * Turns/sec
(0-40)

10 * Grams/3"Brake
(0-40)

900
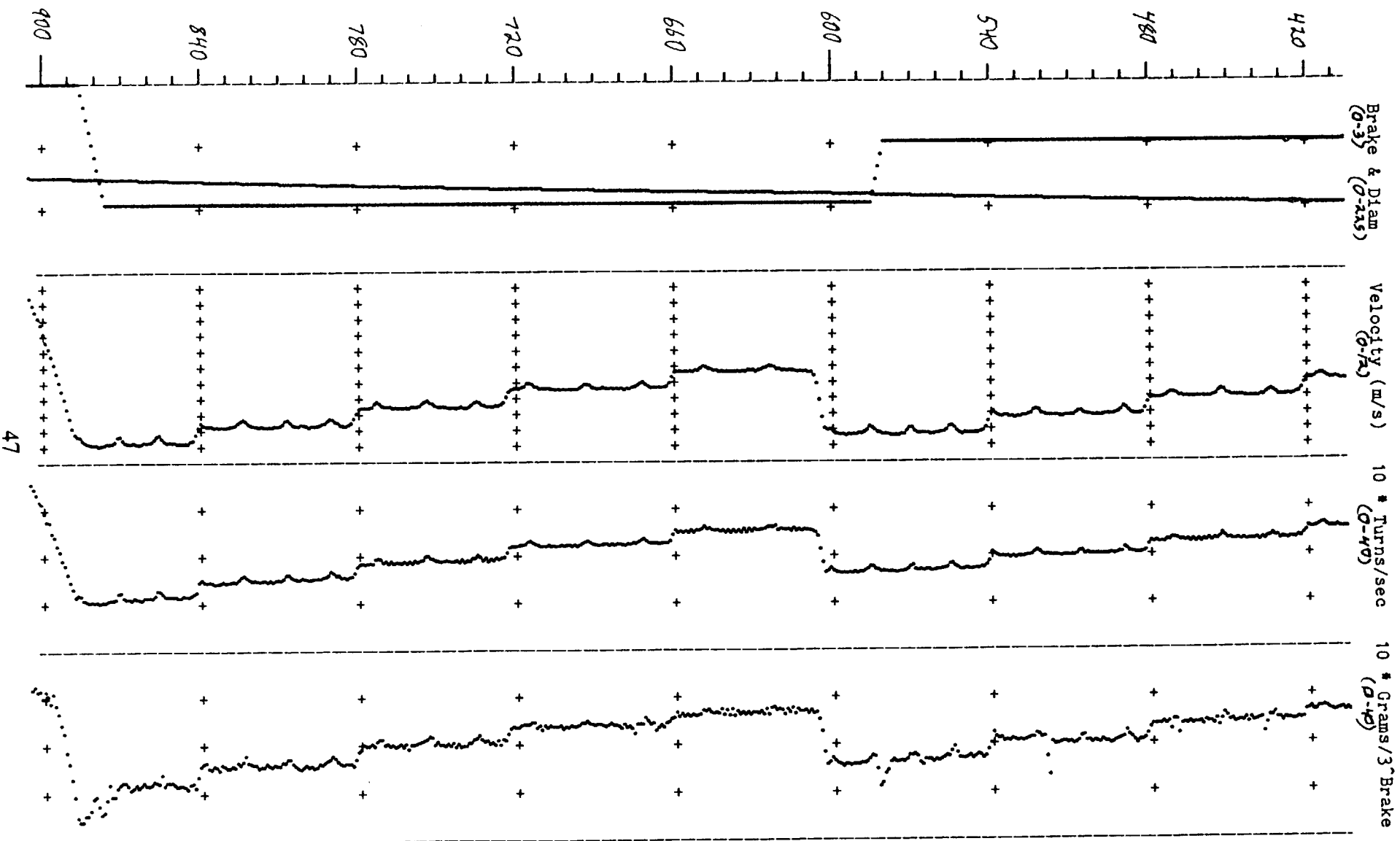
840

780

720

660

600

540

480

420

47

AUGUST 1988 SEDS 20 KM VACUUM DEPLOYMENT, TEST #5

Shown below are second-by-second data for a 906-sec SEDS
deployment test, one of 5 that deployed a 20 km tether.
The time scale marks 10, 60, and 300 second intervals.
Tests 1-5 started with 0, 1, 3, 8, and 15 km deployed.
Brake is 1 turn per "+" mark; pack diameter, 75 mm/+.
Velocity, Turns/sec, & Tension are in units shown per +,
and the scales differ for each test. Tension is divided
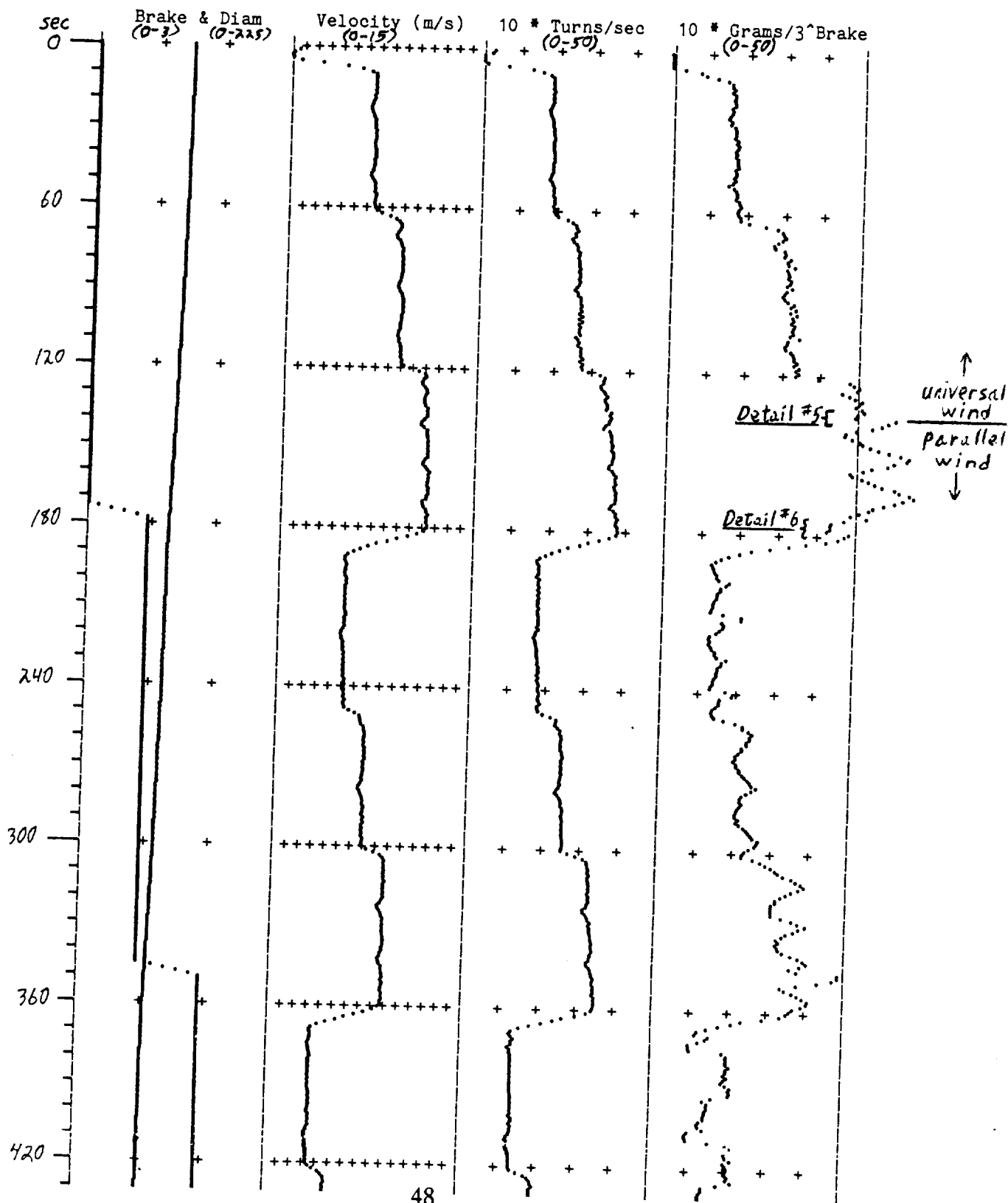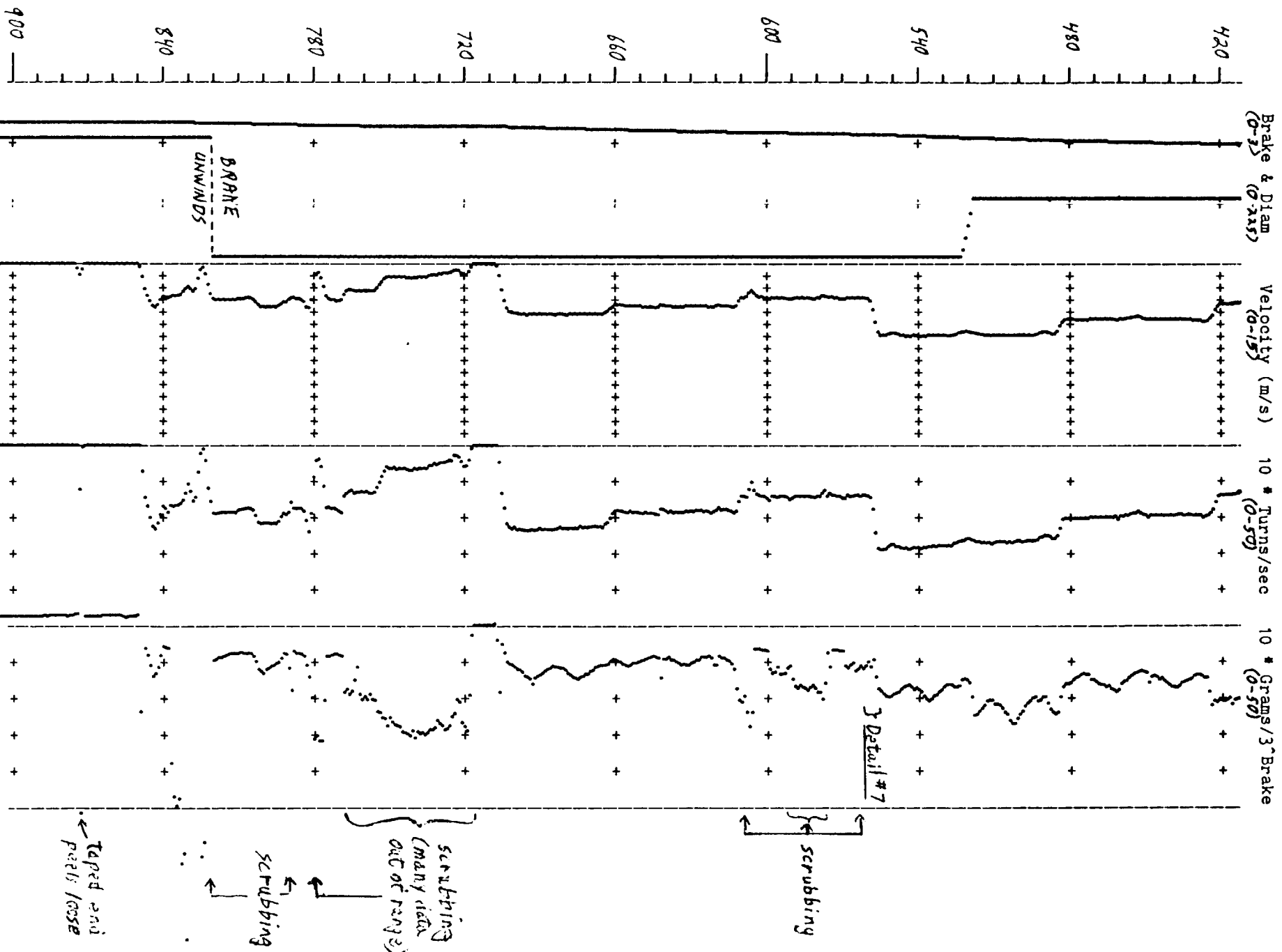by 3 for each BrakeTurn to keep the data on the page.


48

(Test #5)

Detail Plots

Below are 7 plots of 60-Hz tension data, plus two versions of a turn-count display. Each shows a six-second interval, during which typical or otherwise interesting waveforms occur. Each tension datapoint is the sum of five readings at 300 Hz. The tension was further smoothed by a "digital capacitor" having a 0.1 second time constant. The scale for each plot is different, and is listed below the plot. The plots show waveform well, but can be misleading if not used carefully. For example, in detail #5, the average tension in the parallel-wound second half of the plot is only 15% higher than in the universal-wound first half. The difference appears far larger because the plot only ranges from 46 to 64 grams.
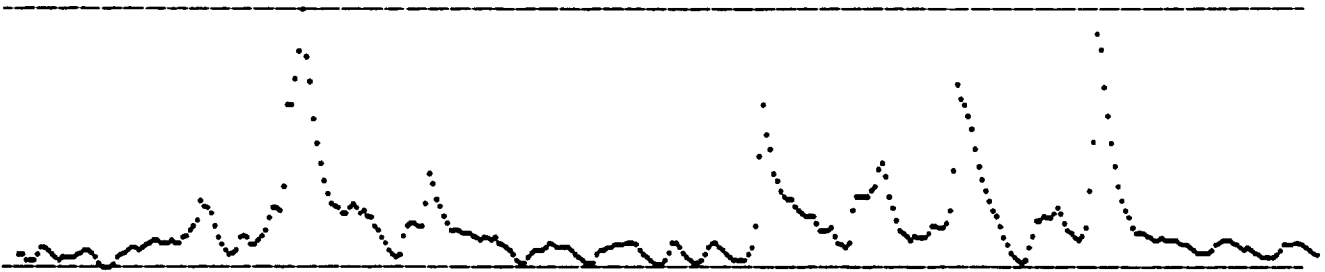
Detail #1. Typical early tension waveform at 0.7 m/s (Test 1, 24-30 sec)
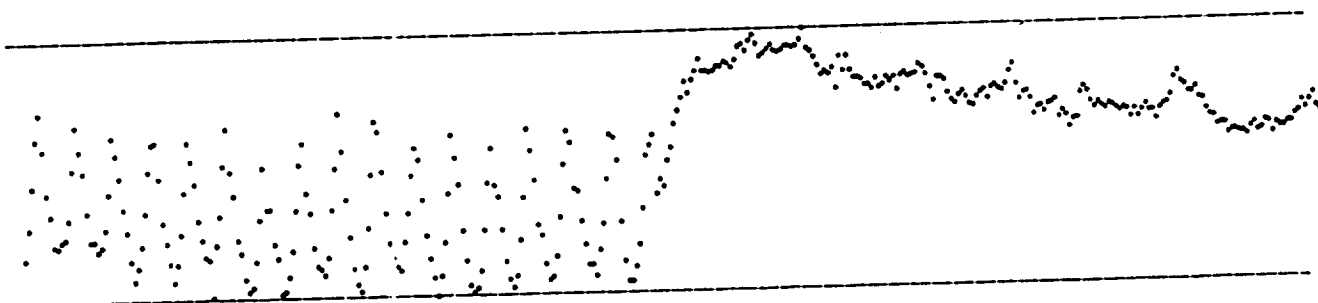Plot range: 0.7 to 8.8 grams; average value = 2.0 grams.

Detail #2. Typical early tension waveform at 1.5 m/s (Test 1, 204-210 sec)
Plot range: 0.2 to 5.7 grams; average value = 2.3 grams.
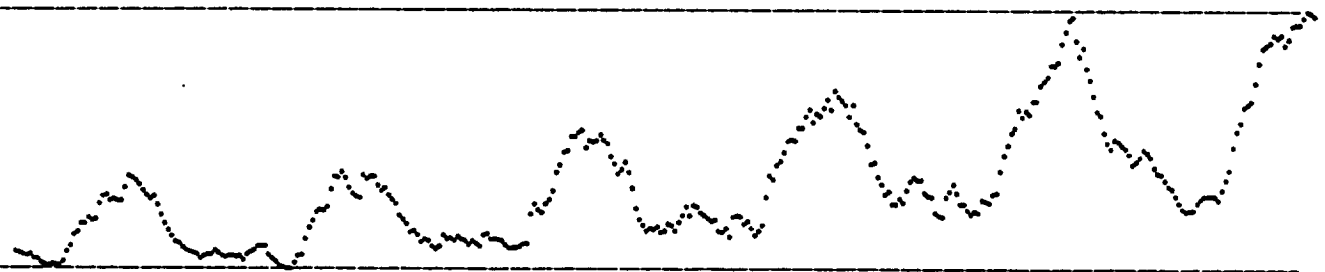
Detail #3. Effect of adding 1 turn brake at 1.9 m/s (Test 1, 281-287 sec)
Plot range: 0.6 to 23.5 grams; average value = 8.1 grams.

50

Detail #4. Typical early waveform with brake at 1.0 m/s (Test 1, 385-391 sec)
Plot range: 5.2 to 22.4 grams; average value = 12.5 grams.

Detail #5. Transition from universal to parallel wind at 11 m/s (Test 5, 134-140 sec)
Plot range: 46 to 64 grams; average value = 56 grams.
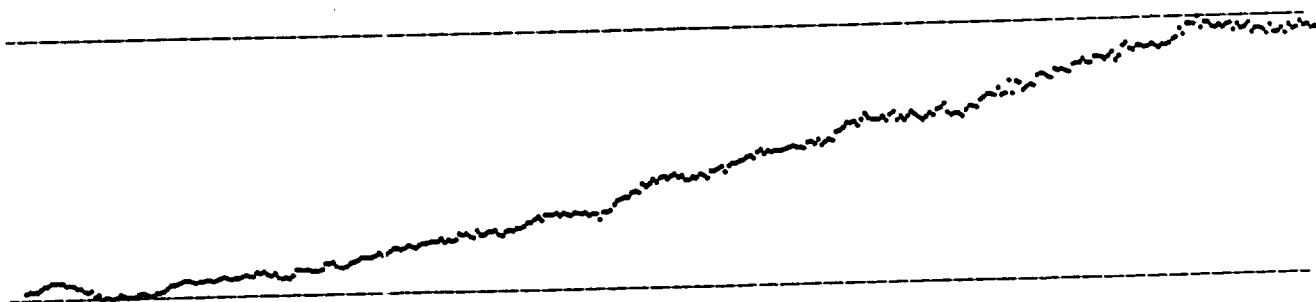
Detail #6. Effect of adding 1 turn brake at 11.4 m/s (Test 5, 174-180 sec)
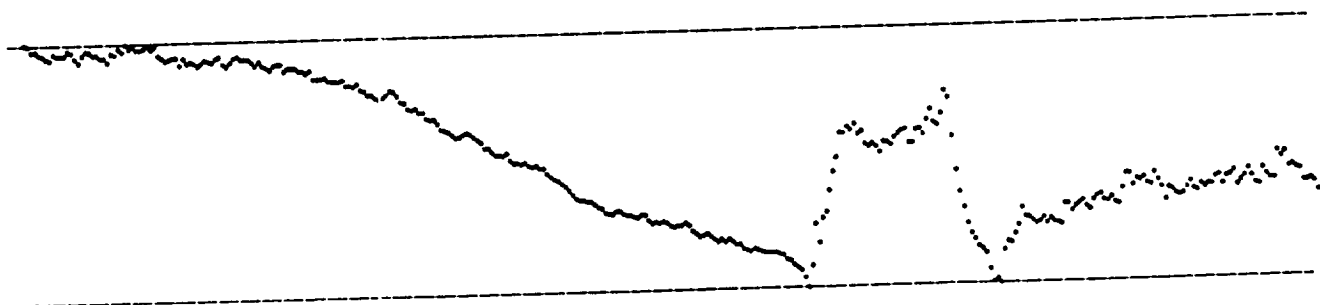Plot range: 53 to 140 grams; average value = 91 grams.

Detail #7. Transition to scrub mode at unwinding rate near 15 Hz (Test 5, 556-562 sec)
Plot range: 150 to 420 grams; average value = 293 grams.

Detail #8. Effect of Identifying a Spurious Count on Turn-Count Interval Pattern

Each line in the edit program display shows one axial cycle (four turns). "+" and "-" indicate counts believed real and spurious. Horizontal spacing indicates time from end of last cycle. Editing the circled count eliminates a discontinuity in the pattern.

Turn 1 of 4   Turn 2 of 4   Turn 3 of 4   Turn 4 of 4

←— Data from universal winding with 4 turns per axial cycle.

←— Note pattern change on this and following lines.

```
14993=PageStart; Test =4; Sec =    81 to    87; AvgMSPerLine =    330      ←—Display summary
PgUp,PgDown,FilePos,-,+,Arrows,ShowBlock,Turns/line,CountPos,Write,Quit,?←Prompt line
```

Note a tendency for spurious counts to recur near the same time in successive axial cycles.

←— Circled count was changed to "-". Now the same data shows a far more uniform pattern.

```
14993=PageStart; Test =4; Sec =    81 to    87; AvgMSPerLine =    334
PgUp,PgDown,FilePos,-,+,Arrows,ShowBlock,Turns/line,CountPos,Write,Quit,?
```

52

Appendix B. SEDS/STS Experiment Requirements Document

ERD
Functional Objectives

1. ACTIVATION

Step 1. Crew stows RMS and other deployable appendages

Step 2. Pilot orients Orbiter correctly--payload bay facing Earth, nose along velocity vector.

Step 3. Start split screen video recording with TV cameras pointed at deployer and endmass

Step 4. Turn on SEDS computer

2. DEPLOYMENT

Step 1. Wait for desired orbital location for deployment

Step 2. Deployer operator cuts endmass restraining bolts to initiate deployment

Step 3. Deployment proximity operations (approx. 5 min., during daylight): The three crewmembers carry out the following:

A. Pilot keeps Orbiter oriented horizontal, ready to initiate correct response to a jam or break

B. TV operator keeps one camera on endmass

C. Deployer operator monitors deployment

Step 4. Main deployment: The two crewmembers carry out the following:

A. Pilot keeps Orbiter oriented horizontal, ready to use thrusters in case of a tether break

B. Deployer operator monitors deployment

C. Turn on floodlights when daylight ends, to illuminate deployer and receding tether

Step 5. Braking: Same responsibilities as Step 4.

3. SWING AND RELEASE

   Step 1.   Swing: The two crewmembers carry out the
             following:

             A.   Pilot pitches Orbiter nose slowly towards
                  Earth to keep tether passing above nose at
                  correct angle

             B.   Deployer operator monitors tether status--
                  tether not slack or recoiling

   Step 2.   Deployer operator monitors automatic tether
             cut command to make sure tether release
             occurs at correct time

   Step 3.   Deployer operator, with help from pilot as needed,
             keeps tether in view until it recoils out of sight
             from orbiter (approx. 5 sec.)

   Step 4.   Deployer operator turns off SEDS computer

   Step 5.   If endmass re-entry will occur at night, camera is
             used at maximum magnification (zoom) to photograph
             the re-entry

4. DEACTIVATION

   Step 1.   After loss of visual contact, TV camera and video
             recorder are turned off, and the videotape is
             stowed.

FUNCTIONAL OBJECTIVE REQUIREMENTS SHEET

FUNCTIONAL OBJECTIVE REQUIREMENTS SHEET

EXPERIMENT NAME: ___SEDS___   F.O. NUMBER: ___1___

F.O. NAME: ___Activation___   PREREQUISITE: _____

NO. OF PERFORMANCES: MIN. ___1___ DES. ___1___   SEQUENCE: _____

REQUIRED TIME FRAME (MET): MIN. _any_ MAX. _any_   JOINT OPS. WITH: _____

STEP NUMBER			1	2	3	4	5	6
STEP DURATION (MINS:SECS)		MINIMUM	0	0				
		MAXIMUM	TBD	TBD				
		PREFERRED			2:00	3:00		
STEP DELAY (HRS:MINS)		MINIMUM						
		MAXIMUM						
		PREFERRED						
CREWMEN		NUMBER	TBD	1	1	1		
		PREFERRED						
TARGETS REQUIRED								
ATTITUDE REQUIRED				(A)	(A)	(A)		
INHIBITS: W= WATER, L= LIGHTS T= THRUSTER, A= ACCELERATIONS C= CREW MOTION					T	T		
AVERAGE POWER REQUIRED (KW)			0	0	0	.007		
EXPERIMENT COMPUTER	ECAS TASK NUMBER							
	NUMBER OF STL'S							
DATA	MBPS							
	ECIO (Y/N)							
	A= ANALOG, D= DIGITAL TV= VIDEO, V= VOICE C= COMMANDING	REAL TIME						
		NRT						
		RECORDED			TV	TV		
SPECIAL EQUIPMENT OR CONSTRAINTS								

STEP NO.	STEP DESCRIPTION
1	Crew stows all deployable appendages
2	Pilot orients Orbiter correctly
3	Start TV cameras and recording
4	Turn on SEDS computer
5	
6	

FUNCTIONAL OBJECTIVE REQUIREMENTS SHEET (Continued)

FUNCTIONAL OBJECTIVE REQUIREMENTS SHEET

EXPERIMENT NAME: ____SEDS____   F.O. NUMBER ____1____

F.O. NAME __Activation__   CONTINUED: PAGE __2__ OF __2__

COMMENTS

(A)   Orbiter should be oriented with payload bay facing the
      Earth, and nose aligned with the velocity vector.

FUNCTIONAL OBJECTIVE REQUIREMENTS SHEET

FUNCTIONAL OBJECTIVE REQUIREMENTS SHEET

EXPERIMENT NAME: ___SEDS___   F.O. NUMBER: __2__

F.O. NAME: ___Deployment___   PREREQUISITE: __FO-1__

NO. OF PERFORMANCES: MIN. __1__ DES. __1__   SEQUENCE: _____

REQUIRED TIME FRAME (MET): MIN. _____ MAX. _____   JOINT OPS. WITH: _____

STEP NUMBER		1	2	3	4	5	6
STEP DURATION (MINS:SECS)	MINIMUM						
	MAXIMUM						
	PREFERRED	5:00	0:00	5:00	75:00	5:30	
STEP DELAY (HRS:MINS)	MINIMUM						
	MAXIMUM						
	PREFERRED						
CREWMEN	NUMBER	3	3	3	2	2	
	PREFERRED						
TARGETS REQUIRED							
ATTITUDE REQUIRED		(A)	(A)	(A)	(A)	(A)	
INHIBITS: W=WATER, L=LIGHTS T=THRUSTER, A=ACCELERATIONS C=CREW MOTION			T (B)	T (B)	T (B)	T (B)	
AVERAGE POWER REQUIRED (KW)		.007	.007	.007	.007	.022	
EXPERIMENT COMPUTER	ECAS TASK NUMBER						
	NUMBER OF STL'S						
DATA	MBPS						
	ECIO (Y/N)						
A=ANALOG, D=DIGITAL TV=VIDEO, V=VOICE C=COMMANDING	REALTIME						
	NRT						
	RECORDED	TV	TV	TV	TV	TV	
SPECIAL EQUIPMENT OR CONSTRAINTS							

STEP NO.	STEP DESCRIPTION
1	Wait for correct orbit location
2	Start deployment
3	Deployment proximity operations
4	Main deployment
5	Braking
6	

FUNCTIONAL OBJECTIVE REQUIREMENTS SHEET (Continued)

FUNCTIONAL OBJECTIVE REQUIREMENTS SHEET

EXPERIMENT NAME: _____ SEDS _____   F.O. NUMBER _____ 2 _____

· F.O. NAME ___ Deployment ___   CONTINUED: PAGE __2__ OF __2__

COMMENTS

(A)   Orbiter should be oriented with payload bay facing the Earth, and nose aligned with the velocity vector.

(B) Thruster on upper side of Orbiter nose must be inhibited for attitude control, but available for use if tether breaks

FUNCTIONAL OBJECTIVE REQUIREMENTS SHEET

FUNCTIONAL OBJECTIVE REQUIREMENTS SHEET							
EXPERIMENT NAME: SEDS				F.O. NUMBER: 3			
F.O. NAME: Swing and release				PREREQUISITE: FO-2			
NO. OF PERFORMANCES: M N. 1 DES. 1				SEQUENCE:			
REQUIRED TIME FRAME (MET): MIN. _____ MAX. _____				JOINT OPS. W!TH:			

STEP NUMBER			1	2	3	4	5	6
STEP DURATION (MINS:SECS)		MINIMUM					0	
		MAXIMUM					TBD	
		PREFERRED	12:00	0:00	0:05	0:20	TBD	
STEP DELAY (HRS:MINS)		MINIMUM						
		MAXIMUM						
		PREFERRED					30:00	
CREWMEN		NUMBER	2	2	2	1	2	
		PREFERRED						
TARGETS REQUIRED							(B)	
ATTITUDE REQUIRED			(A)	(A)	(A)			
INHIBITS: W=WATER, L=LIGHTS T=THRUSTER, A=ACCELERATIONS C=CREW MOTION			T (C)	T (C)	T (C)			
AVERAGE POWER REQUIRED (KW)			.007	.007	.007	0	0	
EXPERIMENT COMPUTER	ECAS TASK NUMBER							
	NUMBER OF STL'S							
DATA	MBPS							
	ECIO (Y/N)							
	A=ANALOG, D=DIGITAL TV=VIDEO, V=VOICE C=COMMANDING	REAL TIME						
		NRT						
		RECORDED	TV	TV	TV		TV	
SPECIAL EQUIPMENT OR CONSTRAINTS								

STEP NO.	STEP DESCRIPTION
1	Swing
2	Tether is cut automatically
3	Camera follows recoiling tether
4	SEDS computer is turned off
5	(Optional) Re-entering endmass is videotaped.
6	

FUNCTIONAL OBJECTIVE REQUIREMENTS SHEET (Continued)

FUNCTIONAL OBJECTIVE REQUIREMENTS SHEET

EXPERIMENT NAME: ___SEDS___ F.O. NUMBER ___3___

F.O. NAME ___Swing and release___ CONTINUED: PAGE _2_ OF _2_

COMMENTS

(A) Orbiter orientation during the swing should keep
the tether passing over the nose thruster to allow
blowing the tether away from the Orbiter with thruster
exhaust if needed. The desired angle of the tether to
Orbiter nose-tail axis is about 30 to 40 degrees, depending
on the exact mounting location of the tether deployer in
the payload bay.

(B) If the optional endmass re-entry TV photography is
to be done, the Orbiter must be oriented correctly to
allow camera viewing

(C) Thruster on upper side of Orbiter nose must be inhibited
for attitude control, but available for use if tether
breaks

FUNCTIONAL OBJECTIVE REQUIREMENTS SHEET

EXPERIMENT NAME: _SEDS_   F.O. NUMBER: _4_

F.O. NAME: _Deactivation_   PREREQUISITE: _FO-3_

NO. OF PERFORMANCES: MIN. _1_ DES. _1_   SEQUENCE: _____

REQUIRED TIME FRAME (MET): MIN. _____ MAX. _____ JOINT OPS. WITH: _____

STEP NUMBER		1	2	3	4	5	6
STEP DURATION (MINS:SECS)	MINIMUM	1					
	MAXIMUM						
	PREFERRED	2:00					
STEP DELAY (HRS:MINS)	MINIMUM						
	MAXIMUM						
	PREFERRED						
CREWMEN	NUMBER	1					
	PREFERRED						
TARGETS REQUIRED							
ATTITUDE REQUIRED							
INHIBITS: W=WATER, L=LIGHTS T=THRUSTER, A=ACCELERATIONS C=CREW MOTION							
AVERAGE POWER REQUIRED (KW)		0					
EXPERIMENT COMPUTER	ECAS TASK NUMBER						
	NUMBER OF STL'S						
DATA	MBPS						
	ECIO (Y/N)						
	A=ANALOG, D=DIGITAL TV=VIDEO, V=VOICE C=COMMANDING REALTIME						
	NRT						
	RECORDED						
SPECIAL EQUIPMENT OR CONSTRAINTS							

STEP NO.	STEP DESCRIPTION
1	Turn off Tv and videorecorder, stow videotape
2	
3	
4	
5	
6	

Figure 1-1

SEDS Block Diagram

TABLE 1-1. EXPERIMENT FUNCTIONAL OBJECTIVES

FUNCTIONAL OBJECTIVE		EQUIPMENT REQUIRED	
NUMBER	TITLE	NUMBER	NOMENCLATURE
FO-1	Activation	1.	SEDS computer, brake, tether cutter, tether, and tether canister assembly
		2.	Endmass and endmass holder/ejector assembly
		3.	Orbiter monitor/command console
		4.	Standard Orbiter TV cameras (2), split screen monitor, and VCR
FO-2	Deployment	Same as FO-1	
FO-3	Swing and release	Same as FO-1	
FO-4	Deactivation	Same as FO-1	

INSTRUCTIONS FROM OPERATIONS AND INTEGRATION AGREEMENT (O&IA)

TABLE II-1. OPERATIONAL FUNCTIONAL FLOW

FO: _____1_____   FO TITLE: _____Activation_____
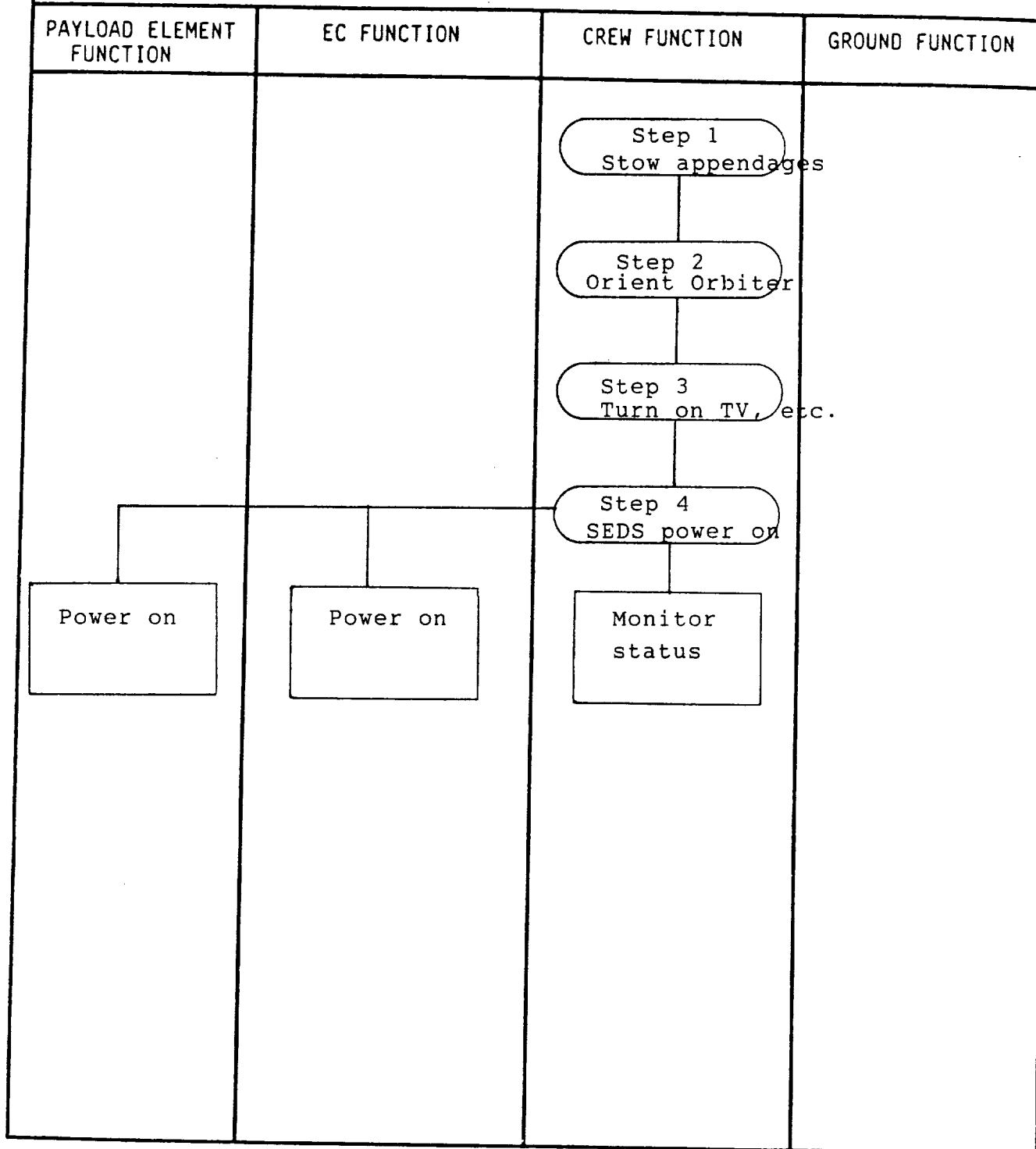
PAYLOAD ELEMENT FUNCTION	EC FUNCTION	CREW FUNCTION	GROUND FUNCTION
		Step 1 Stow appendages	
		Step 2 Orient Orbiter	
		Step 3 Turn on TV, etc.	
		Step 4 SEDS power on	
Power on	Power on	Monitor status	

INSTRUCTIONS FROM OPERATIONS AND INTEGRATION AGREEMENT (O&IA)

TABLE II-1. OPERATIONAL FUNCTIONAL FLOW

FO: 2   FO TITLE: Deployment

PAYLOAD ELEMENT FUNCTION	EC FUNCTION	CREW FUNCTION	GROUND FUNCTION
		Step 1 Wait for correct orbital position	
		Step 2 Start deployment	
Endmass released	Deployment datalogging		
		Step 3 Prox. deployment	
Normal deployment?	No	A	
Yes			
Tether continues deploying	Datalogging	Monitor deployment	
		Track endmass with TV camera	
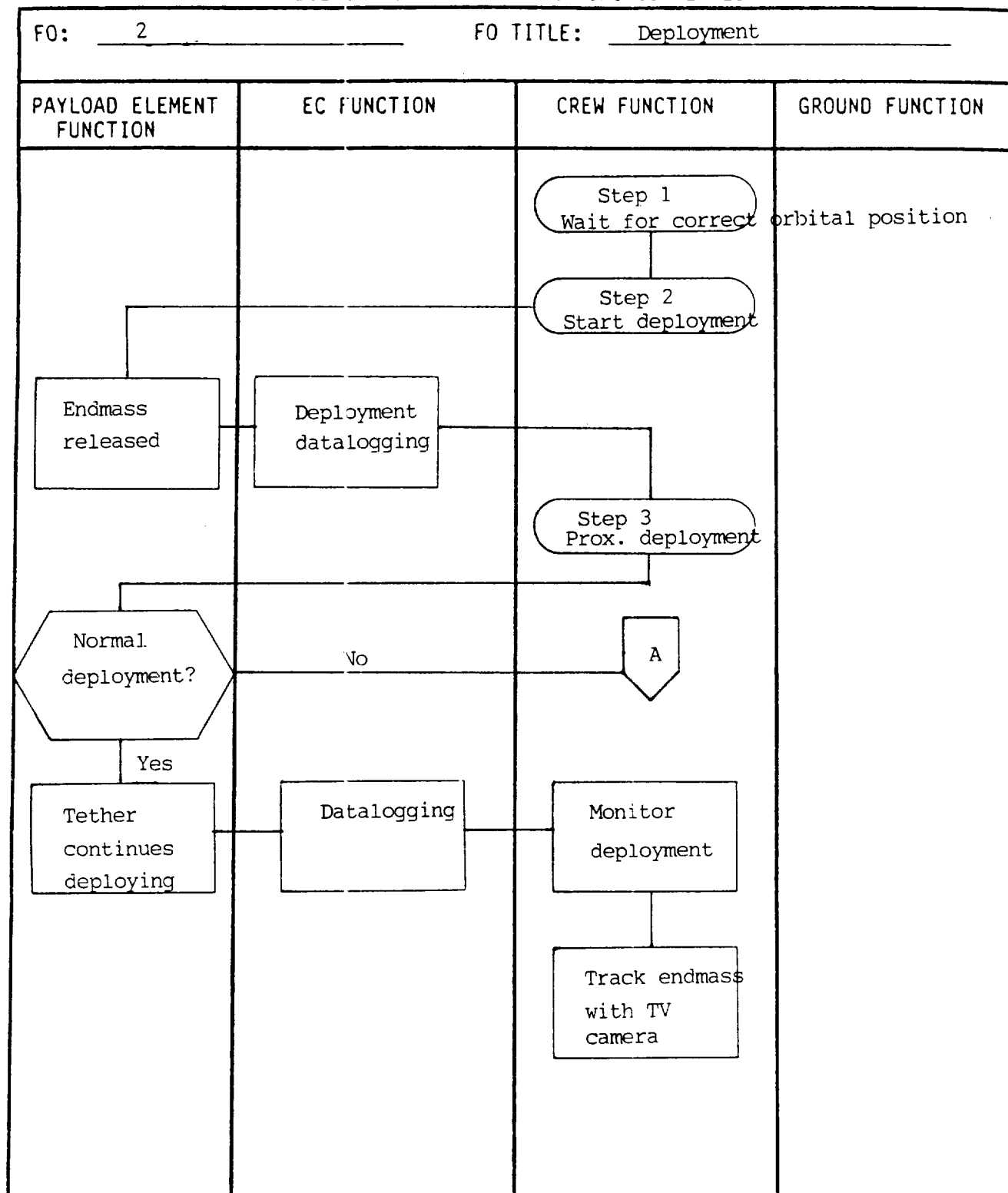
INSTRUCTIONS FROM OPERATIONS AND INTEGRATION AGREEMENT (O&IA)

TABLE II-1. OPERATIONAL FUNCTIONAL FLOW

FO: __2 (AFF)   Step 3__   FO TITLE: __Proximity deployment__

PAYLOAD ELEMENT FUNCTION	EC FUNCTION	CREW FUNCTION	GROUND FUNCTION

A

Tether break or payload recoil? — Payload recoil — Verify recoil (tether jam)

C

Tether is cut at deployer

Issue tether cut command

Payload less than 20 m. from Orbiter?   yes

no

Translate Orbiter sideways (Y axis) to avoid endmass

Translate sideways then forward to alter orbit

Terminate experiment when safe

<u>INSTRUCTIONS FROM OPERATIONS AND INTEGRATION AGREEMENT (O&IA)</u>

TABLE II-1. OPERATIONAL FUNCTIONAL FLOW

FO: _____2_____   FO TITLE: _____Deployment_____

PAYLOAD ELEMENT FUNCTION	EC FUNCTION	CREW FUNCTION	GROUND FUNCTION

Step 4
Main deployment

Normal deployment?

No

B

Yes

Tether continues deploying

Datalogging

Monitor deployment

Step 5
Braking

Normal braking?

No

B

Yes

Tether braking continues
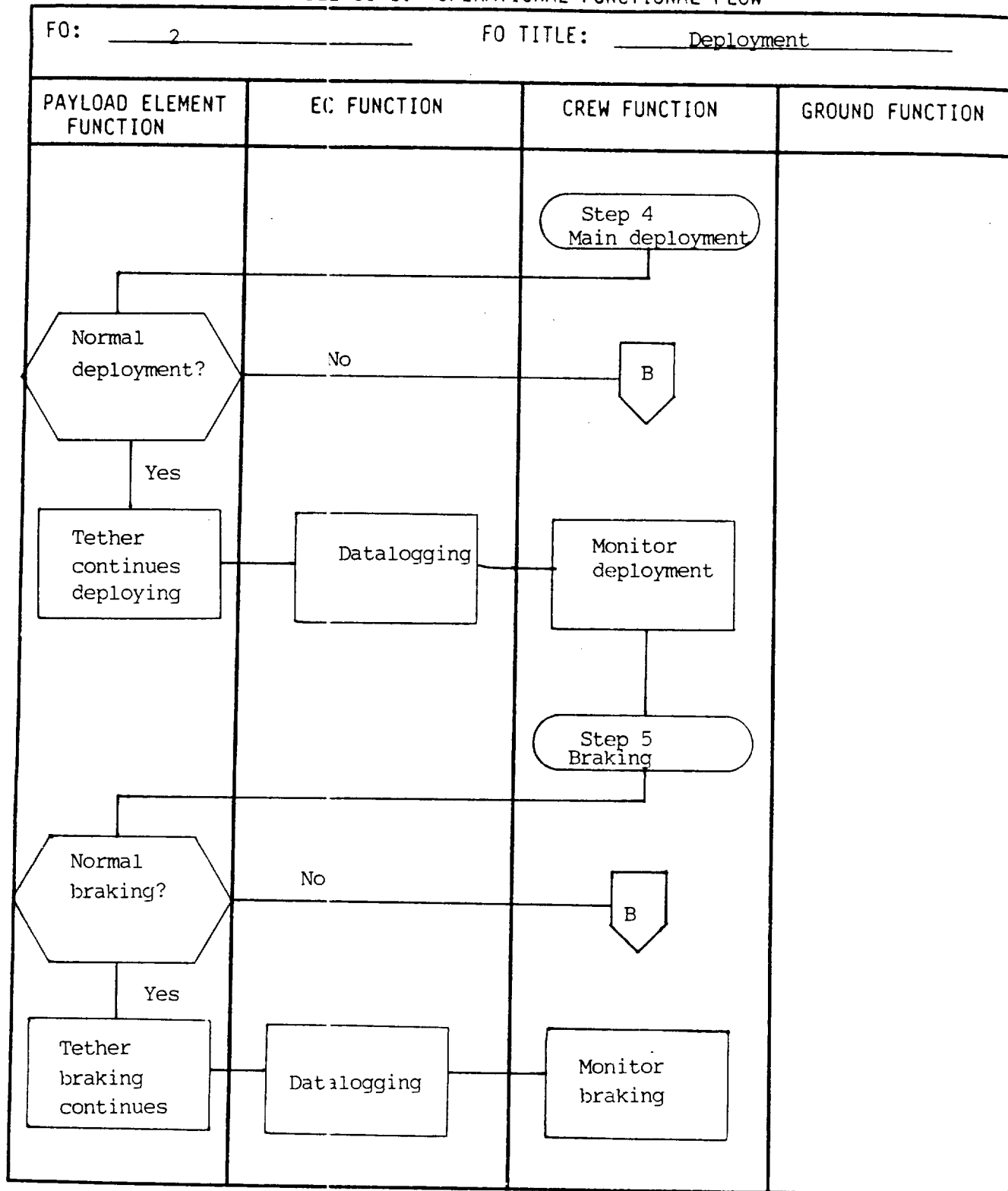
Datalogging

Monitor braking

INSTRUCTIONS FROM OPERATIONS AND INTEGRATION AGREEMENT (O&IA)

TABLE II-1.   OPERATIONAL FUNCTIONAL FLOW

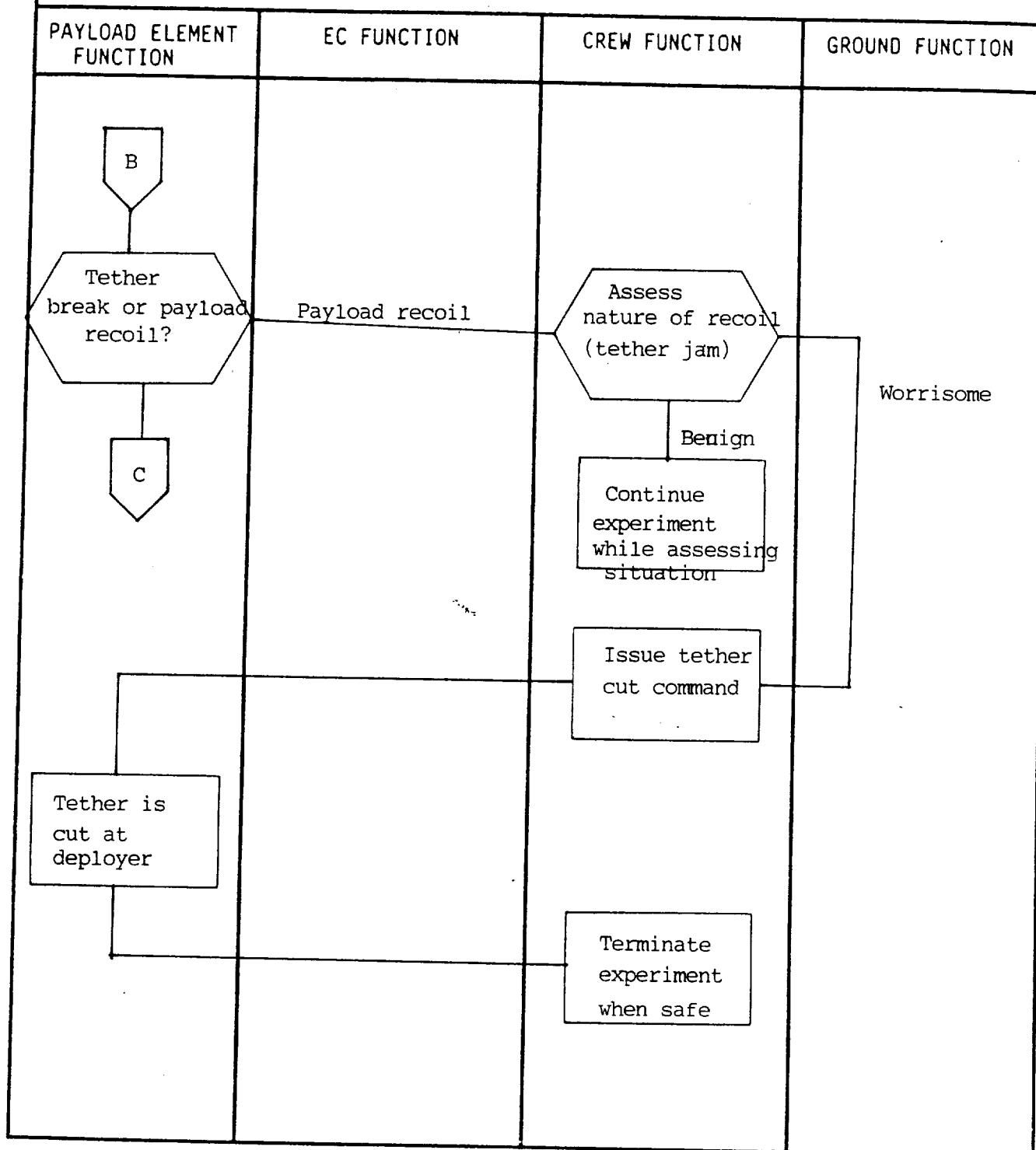FO: _2 (AFF) Step 4, 5_   FO TITLE: _Main deployment, braking_

PAYLOAD ELEMENT FUNCTION	EC FUNCTION	CREW FUNCTION	GROUND FUNCTION

B

Tether break or payload recoil?

C

Payload recoil

Assess nature of recoil (tether jam)

Worrisome

Benign

Continue experiment while assessing situation

Issue tether cut command

Tether is cut at deployer

Terminate experiment when safe

INSTRUCTIONS FROM OPERATIONS AND INTEGRATION AGREEMENT (O&IA)

TABLE II-1. OPERATIONAL FUNCTIONAL FLOW

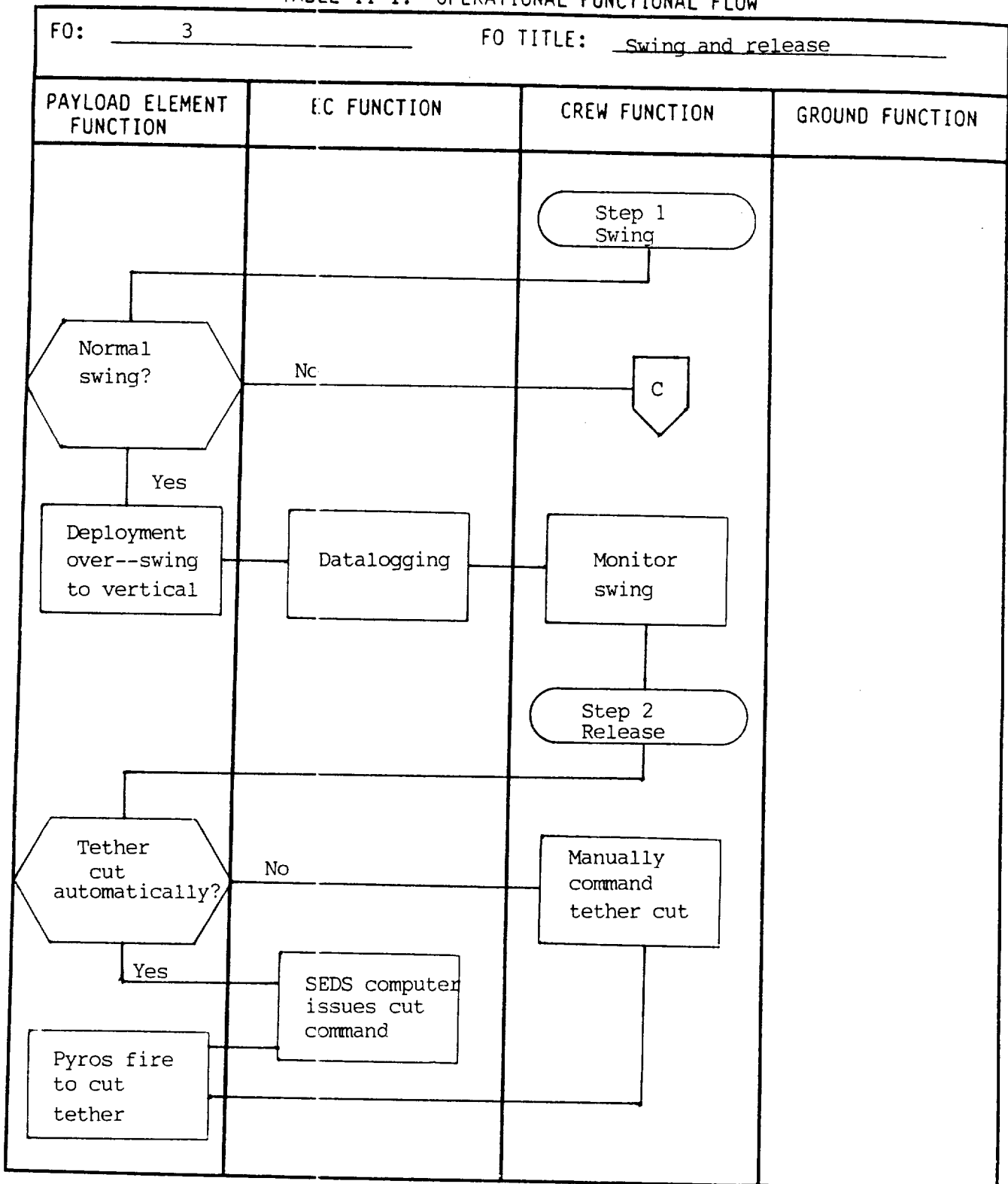FO: _____3_____   FO TITLE: _Swing and release_

PAYLOAD ELEMENT FUNCTION	EC FUNCTION	CREW FUNCTION	GROUND FUNCTION

INSTRUCTIONS FROM OPERATIONS AND INTEGRATION AGREEMENT (O&IA)

TABLE II-1. OPERATIONAL FUNCTIONAL FLOW

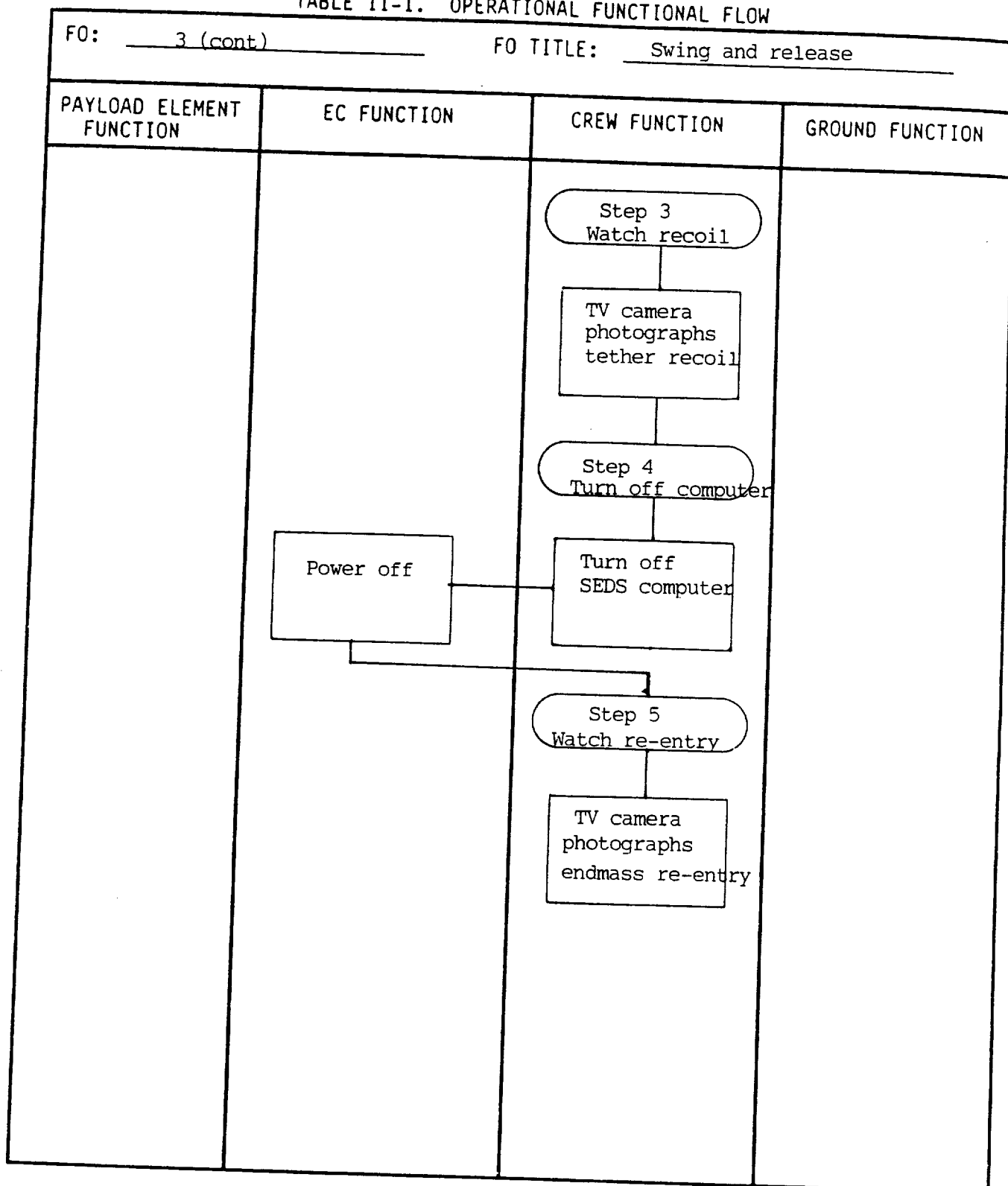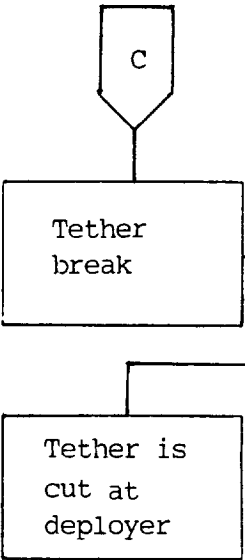FO: ___3 (cont)___   FO TITLE: ___Swing and release___

PAYLOAD ELEMENT FUNCTION	EC FUNCTION	CREW FUNCTION	GROUND FUNCTION
		Step 3 Watch recoil	
		TV camera photographs tether recoil	
		Step 4 Turn off computer	
	Power off	Turn off SEDS computer	
		Step 5 Watch re-entry	
		TV camera photographs endmass re-entry	

INSTRUCTIONS FROM OPERATIONS AND INTEGRATION AGREEMENT (O&IA)

TABLE II-1. OPERATIONAL FUNCTIONAL FLOW

FO: Alternate Functional Flow   FO TITLE: Tether Break

FO 2 and 3

PAYLOAD ELEMENT FUNCTION	EC FUNCTION	CREW FUNCTION	GROUND FUNCTION
C			
Tether break		Issue tether cut command	
Tether is cut at deployer		Blow recoiling tether away with upwards nose thruster	
		Terminate experiment when safe	

INSTRUCTIONS FROM OPERATIONS AND INTEGRATION AGREEMENT (O&IA)

TABLE II-1. OPERATIONAL FUNCTIONAL FLOW

FO: _____4_____   FO TITLE: Deactivation _____

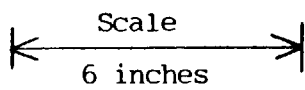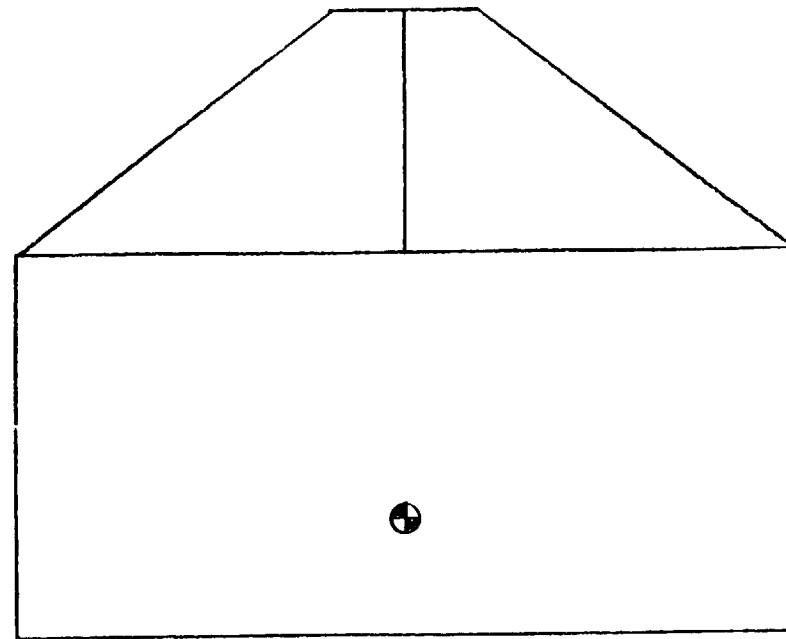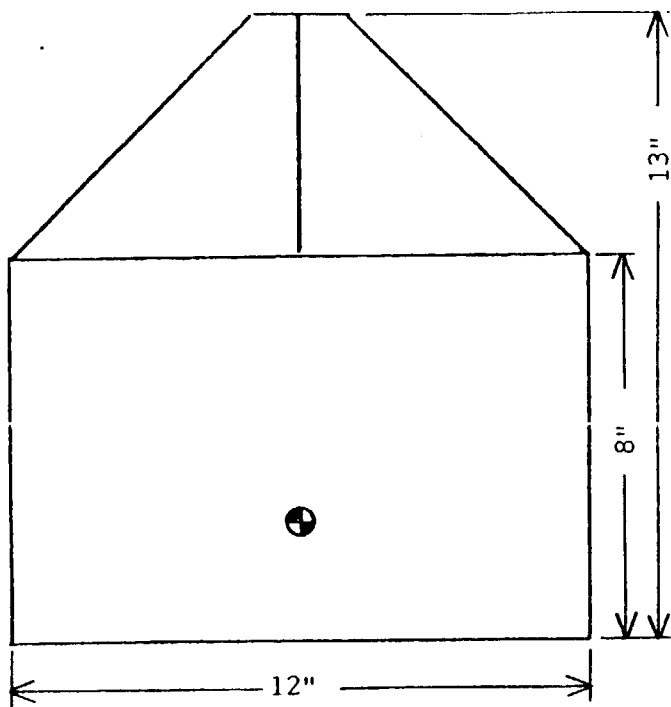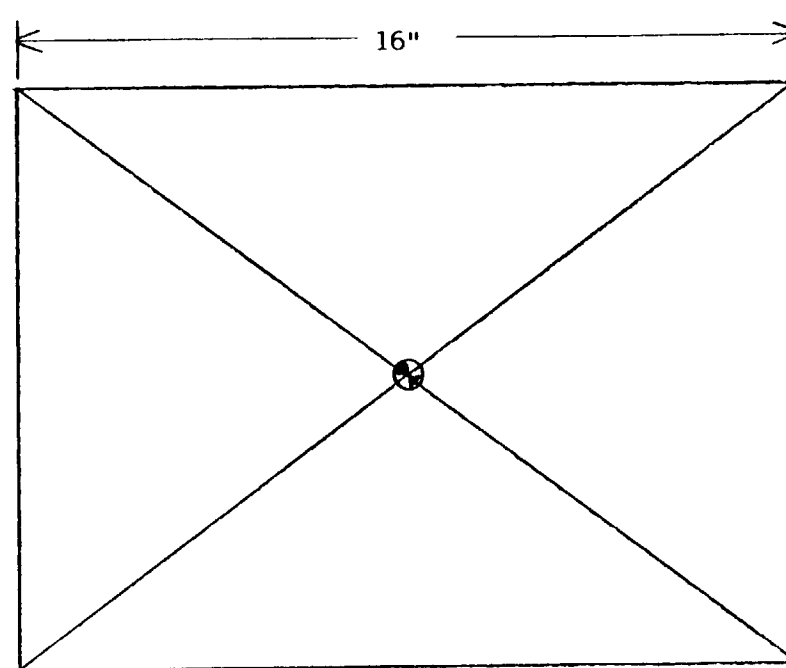| PAYLOAD ELEMENT FUNCTION	EC FUNCTION	CREW FUNCTION	GROUND FUNCTION
		Step 1 Stow equip.	

72

73

Scale

6 inches

Figure 2-1.
SEDS Endmass

50 lbs. total weight

13"

8"

12"
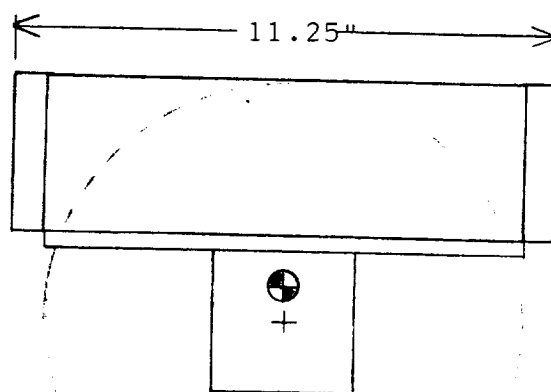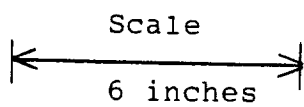
16"

22.5"

Scale

6 inches
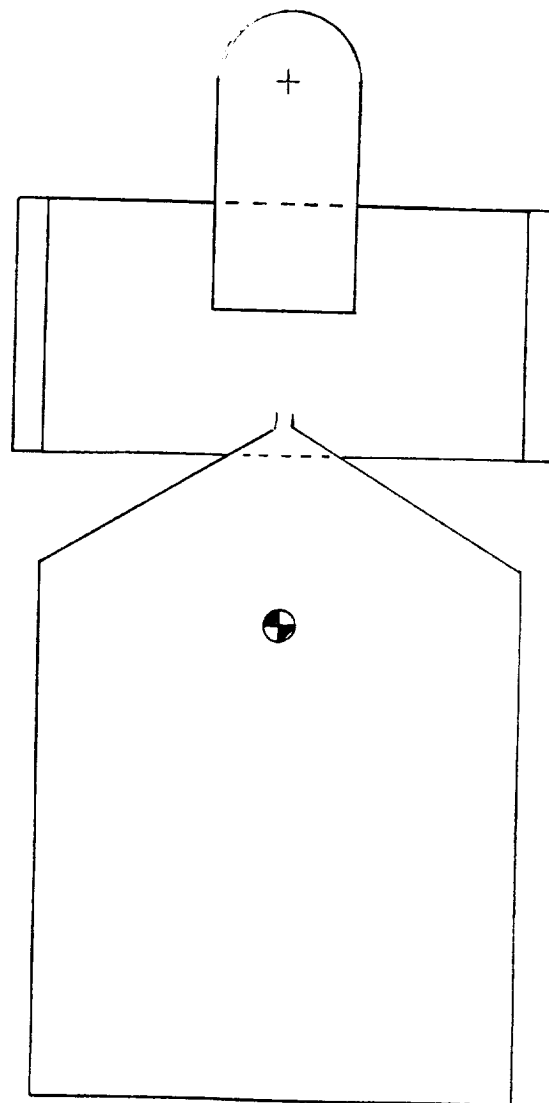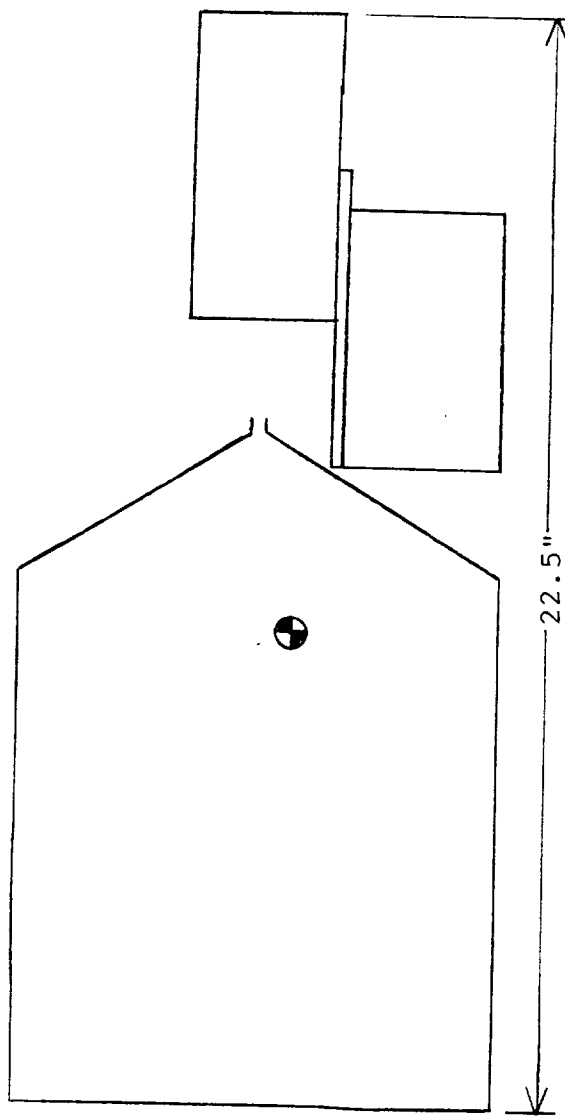
Figure 2-1.

SEDS Hardware Assembly

30 Lbs. total weight

11.25"

TABLE 3-1.   POINTING REQUIREMENTS (Sheet 1 of 2)

FO NUMBER	POINTING ACCURACY (*)	POINTING ERROR		STABILITY ERROR		STABILITY		POINTING KNOWLEDGE (*) (1)
		LOS (*)	ROLL (*)	LOS (*)	ROLL (*)	DURATION (min, sec)	RATE (*)/s	
1	5 deg. all axes							
2	Same							
3	Same							
4	As needed to photograph re-entering endmass ahead of and below Orbiter							Standard Orbiter pointing O.K.

(*) = deg, arc min, arc sec

(1) Not all experiments have both pointing accuracy and pointing knowledge requirements.

TABLE 3-1. POINTING REQUIREMENTS (Sheet 2 of 2)

FO NUMBER	TRACKING ERROR (*)	MAXIMUM SLEW RATE (*)/s	SETTLING TIME (m, s)	POINTING		FIELD OF VIEW	
				DIRECTION (2)	TIME (m, s)	INSTRUMENT (*)	UNOBSTRUCTED (*)
1				Earth	5 min.		As large as possible for all FO's
2				Earth	90 min.		
3 (Step 1)	5 deg.	0.1 deg/s		Tracking	12 min.		
3 (Step 5)	Desirable to photograph re-entering endmass ahead of and below Orbiter						

(*) = deg, arc min, arc sec   (2) Earth, Solar, Celestial

TABLE 3-2. ALIGNMENT/COALIGNMENT

DOES NOT APPLY

77

TABLE 4-1. DESIRED ORBIT CHARACTERISTICS

FUNC-TIONAL OBJEC-TIVE NUMBER	ORBIT ALTITUDE (km)			ORBIT INCLINATION (deg)			LAUNCH				SPECIAL REQUIRE-MENTS: ELLIPTICAL, MULTIPLE ALTITUDE, ETC.
	NOMINAL	MINIMUM	MAXIMUM	NOMINAL	MINIMUM	MAXIMUM	TIME OF DAY (GMT)		TIME OF YEAR		
							EARLIEST	LATEST	EARLIEST	LATEST	
All	296 circular	220 circ.	perigee 300 apogee any	28.5	any	any	any	any	any	any	See Note

NOTE: For eccentric orbits, perigee region must
be compatible with endmass re-entry location.

EX.

TABLE 4-2. EARTH AND CELESTIAL TARGET LIST AND VIEWING TIME REQUIREMENTS

DOES NOT APPLY

TABLES 4-3, 4-4. VIEWING REQUIREMENTS AND CONSTRAINTS

As written, neither table is relevant. However, the following constraints on solar illumination exist.

FO-2, Step 3. Proximity deployment operations should be done in sunlight.

FO-3, Step 5. Optional endmass re-entry photography must occur in darkness.

TABLE 4-5. VEHICLE MOTION AND g-LEVEL LIMITS

		SENSITIVITY LIMIT		EXPERIMENT GENERATED	
		OPERATING	NONOPERATING	OPERATING	NONOPERATING
1.	Rectilinear Acceleration (m/sec^2)	See Note	Any	All are	0
2.	Acceleration Resulting from Vehicle Rotation (m/sec^2)			very small Delta-V	
3.	Net Acceleration - not necessarily the sum of Items 1 and 2 above (m/sec^2)			less than 0.03 m/s	
4.	Angular Acceleration (rad/sec^2)				
5.	Angular Velocity (rad/sec)				
6.	On-Orbit Vibration (g^2/Hz)				

Note: Orbiter must maintain correct orientation relative to tether, with about a plus or minus 5 degree accuracy. Attitude motions must be small enough not to interfere with TV photography. Total translational Delta-V should be less than about 0.2 m/s, unless used for deployment or emergency maneuvers.

FIGURE 5-1. Total Power Profile

FO# 1

Step 4   SEDS power on

DC Power (Watts)

Time (minutes)
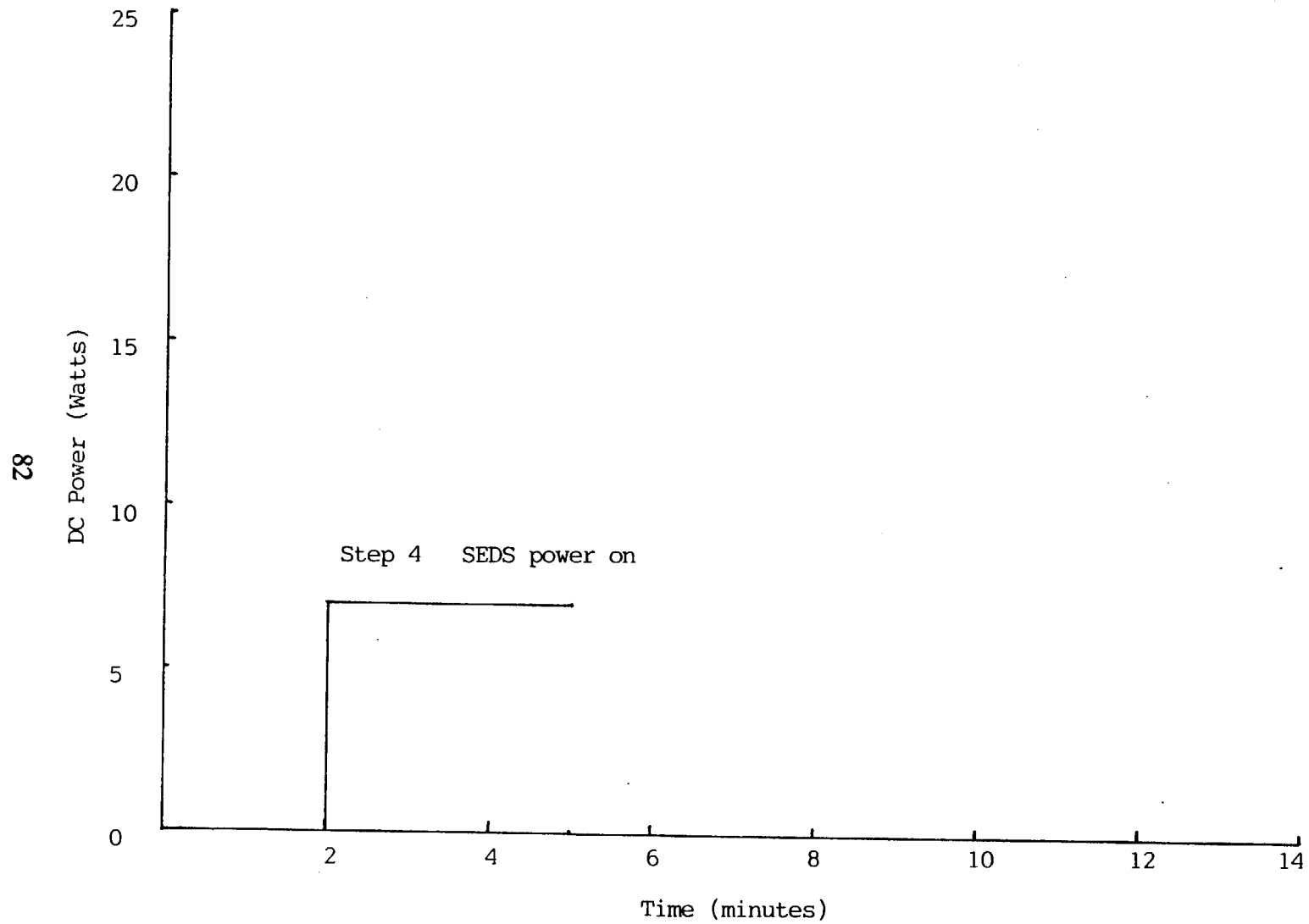
FIGURE 5-1.   Total Power Profile

FO# 2

FIGURE 5-1. Total Power Profile

FO# __3__

10 Amp spike for
tether cutter initiate
(2 NSI's)

All experiment
power off

DC Power (Watts)

Time (minutes)

84

FIGURE 5-1. Total Power Profile

FO# __4__

25 ⊢

20 ⊢

NONE

DC Power (Watts)   15 ⊢

10 ⊢

5

0

Time (minutes)
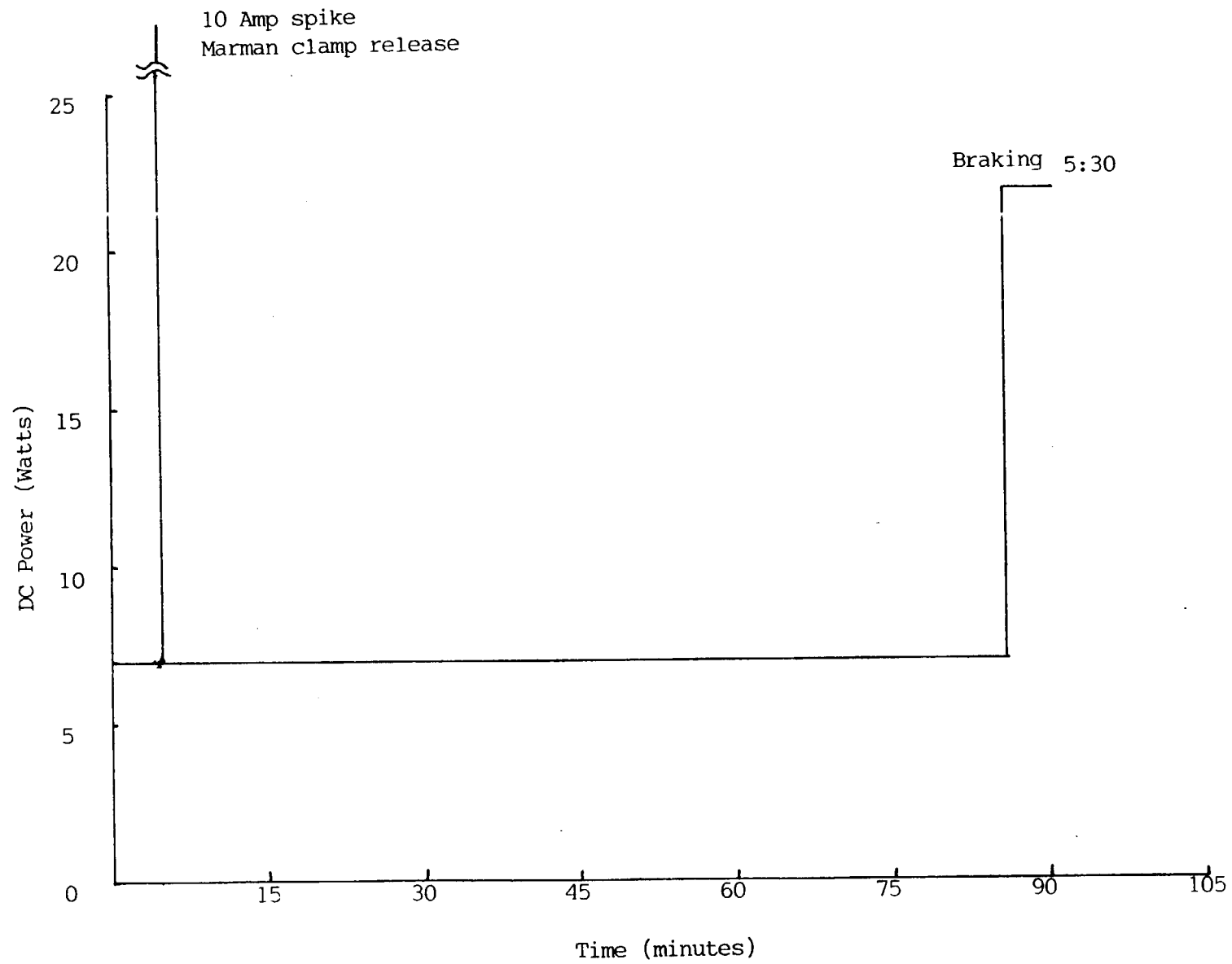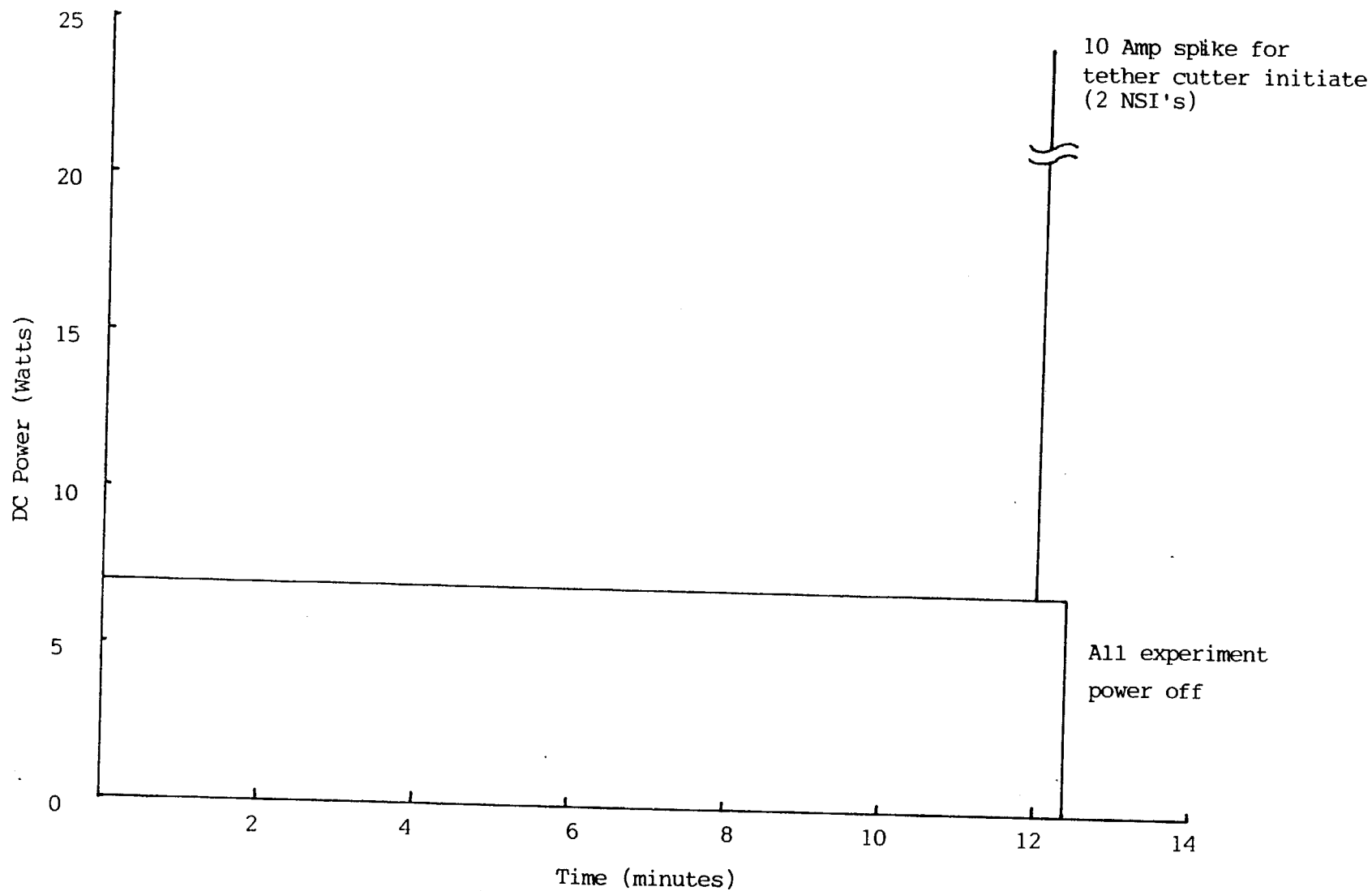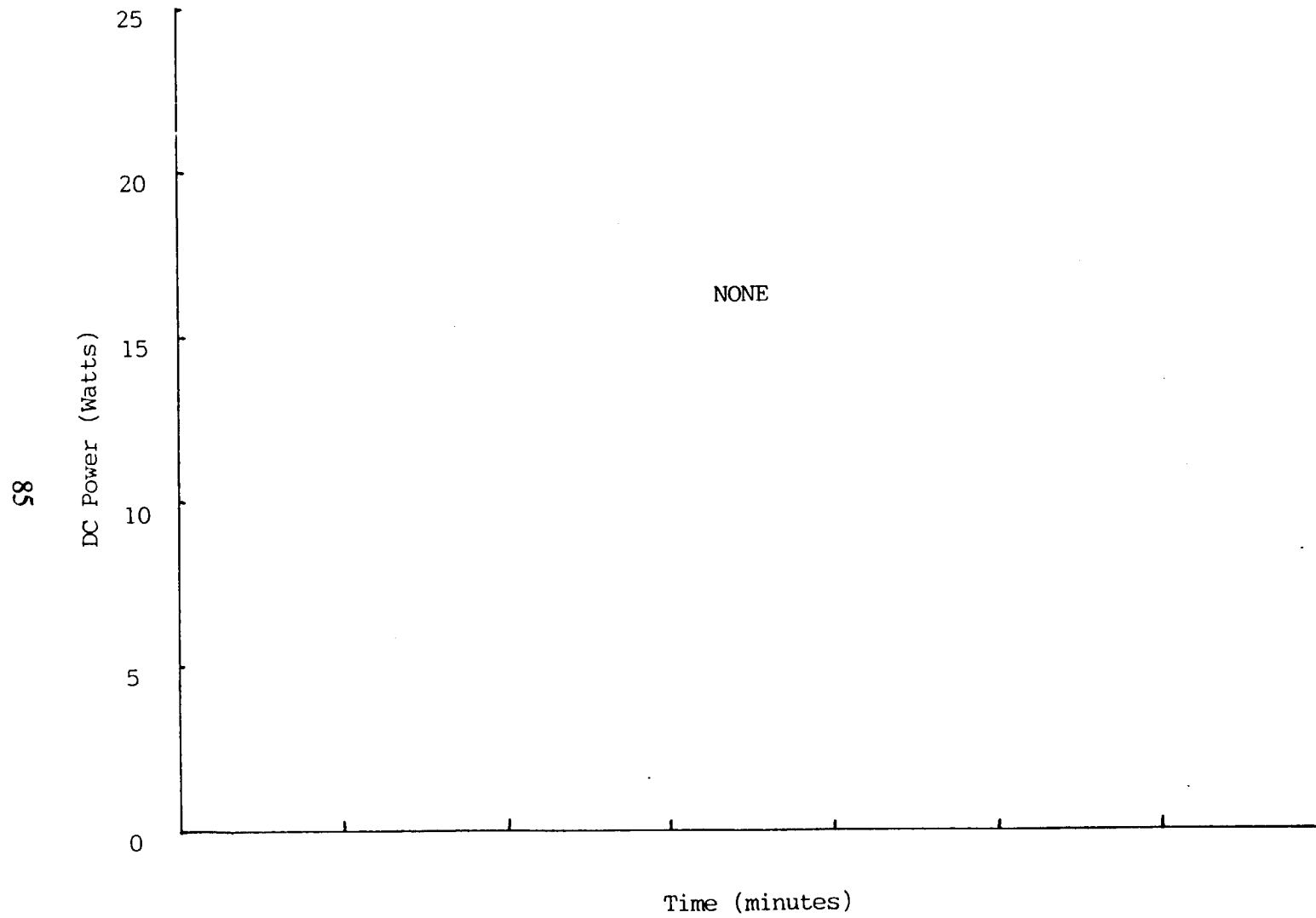
TABLE 6-1. MODULE EQUIPMENT THERMAL ACCOMMODATIONS

DOES NOT APPLY

NOT A SPACELAB MODULE PAYLOAD

TABLE 6-2. PALLET/AIRLOCK/MPESS EQUIPMENT ON-ORBIT THERMAL ACCOMMODATIONS

		ACCOMMODATIONS			CONSTRAINTS
FO NO(S).	ITEM NO(S).	COLD-PLATE	FREON LOOP	PASSIVE	
1	2	3	4	5	6
All	All	N/A	N/A	X	N/A

7. Data System Requirements

At present, the data system is based entirely on the stand-alone SEDS computer being developed for Delta secondary payload flights. However, as shown on the SEDS Block Diagram, Figure 1-1, a command link between the experiment and the crew must be established for the payload eject and the tether cut commands. In addition, some type of simple display of deployment data, such as tension and total deployed length, is probably desirable in the crew area. The formats for both the command and data display are yet to be determined.

8. FLIGHT SOFTWARE REQUIREMENTS

All software for the experiment, as presently defined, resides within the SEDS computer and is self-contained.

TABLE 9-1. EXPERIMENT/FACILITY REQUIREMENTS

(x) Experiment/Facility Preintegration

(   ) Experiment/Facility Preparation

(   ) Postmission Requirements

Description of Planned Activities: Verify SEDS computer is still
                                      functional

Total Floor Space Required Including Space for GSE __50__ Square Feet

Ceiling Height Required __X__ 10 ft ____ 15 ft ___ > 15 ft ____ Specify*

Overhead Crane Required _____ Yes _x_ No   Hook Height _____ Feet

Facility Power Required _____ 120 V, 1 φ, 60 Hz

                       _____ 208 V, 3 φ, 60 Hz

                       _____ Other*

Other Facility Support: Gases _____ GN2   Liquids _____*

                        _____ GHe   _____

                        _____ Other   _____

                Environment __x__ Standard _____ Other*

Hazardous Operations: _____ Yes _X_ No

Total Anticipated Use Time: __0.5__ Days

Other Facility Support Description:

* Define any nonstandard requirements

TABLE 9-1. EXPERIMENT/FACILITY REQUIREMENTS

(   ) Experiment/Facility Preintegration

(X) Experiment/Facility Preparation

(   ) Postmission Requirements

Description of Planned Activities: Installation of pyros:
                                            2 NSIs for tether cutter.

Total Floor Space Required Including Space for GSE __50 (approx)__ Square Feet

Ceiling Height Required __X__ 10 ft ____ 15 ft ___ > 15 ft ____ Specify*

Overhead Crane Required _____ Yes __X__ No   Hook Height _____ Feet

Facility Power Required _____ 120 V, 1 φ, 60 Hz

                          _____ 208 V, 3 φ, 60 Hz

                          _____ Other*

Other Facility Support: Gases _____ GN₂   Liquids _____*

                          _____ GHe   _____

                          _____ Other   _____

                  Environment __X__ Standard _____ Other*

Hazardous Operations: __X__ Yes _____ No

Total Anticipated Use Time: __0.5 (approx)__ Days

Other Facility Support Description:

* Define any nonstandard requirements

10.   MISSION OPERATIONS SUPPORT

PED/PI will be available for real-time consultation at an appropriate location.

No other requirements.

TABLE 11-2. TRAINING OBJECTIVES

TRAINING OBJECTIVE		TRAINEE	RESPONSIBILITY	SIMULATOR REQUIRED		COMMENTS
NO.	DESCRIPTION			YES/NO	DESCRIPTION	
1	Activation	Crew	PMM and PED/PI	No		
2	Deployment	Crew	PMM and PED/PI	Yes	All simulations until release of of endmass require full simulation of Orbiter, tether and endmass.	
3	Swing and release	Crew	PMM and PED/PI	Yes	Same	
4	Deactivation	Crew	PMM and PED/PI	No		
5	Tether break response	Crew	PMM and PED/PI	Yes	Same as above	Use of nose thruster to blow tether away
6	Proximity deployment payload recoil	Crew	PMM and PED/PI	Yes	Same	6 and 7 require cutting tether and Orbiter maneuvering
7	Main deployment payload recoil	Crew	PMM and PED/PI	Yes	Same	